



**RV Educational Institutions<sup>®</sup>**  
**RV College of Engineering<sup>®</sup>**

Autonomous  
Institution Affiliated  
to Visvesvaraya  
Technological  
University, Belagavi

Approved by AICTE,  
New Delhi, Accredited  
By NAAC, Bengaluru  
And NBA, New Delhi

## **DEPARTMENT OF MECHANICAL ENGINEERING**

### **NEUROREHABILITATION OF WRIST USING MANIPULANDUM**

#### **Submitted by**

**Amith R Achari**

**1RV16ME010**

**Nitesh Jha**

**1RV16ME071**

**Badrinath Nayak K**

**1RV16ME133**

#### **Under the guidance of**

**Dr. Ramesh S Sharma,**  
Professor,  
Department of Mechanical Engineering,  
RV College of Engineering

**In partial fulfilment for the award of degree  
of  
Bachelor of Engineering  
in  
Mechanical Engineering  
2019-2020**

# RV COLLEGE OF ENGINEERING<sup>®</sup>, BENGALURU-59

(Autonomous Institution Affiliated to VTU, Belagavi)

## DEPARTMENT OF MECHANICAL ENGINEERING



### CERTIFICATE

Certified that the major project work titled '*Neurorehabilitation of Wrist using Manipulandum*' is carried out by **Amith R Achari, (1RV16ME010), Nitesh Jha (1RV16ME071), and Badrinath Nayak K (1RV16ME133)** who are bonafide students of RV College of Engineering, Bengaluru, in partial fulfilment for the award of degree of **Bachelor of Engineering in Mechanical Engineering** of the Visvesvaraya Technological University, Belagavi during the year 2019-2020. It is certified that all corrections/suggestions indicated for the Internal Assessment have been incorporated in the major project report deposited in the departmental library. The major project report has been approved as it satisfies the academic requirements in respect of major project work (16MEP81) prescribed by the institution for the said degree.

Signature of Guide  
Dr. Ramesh S Sharma

Signature of Head of the Department  
Dr. Krishna M.

Signature of Principal  
Dr.K.N.Subramanya

External Viva

Name of Examiners

Signature with Date

1

2

**RV COLLEGE OF ENGINEERING<sup>®</sup>, BENGALURU-59**  
(Autonomous Institution Affiliated to VTU, Belagavi)

**DEPARTMENT OF MECHANICAL ENGINEERING**

**DECLARATION**

We, **Amith R Achari, Nitesh Jha, Badrinath Nayak K** students of eighth semester B.E., Mechanical Engineering, RV College of Engineering, Bengaluru, hereby declare that the major project titled '*Neurorehabilitation of Wrist using Manipulandum*' has been carried out by us and submitted in partial fulfilment for the award of degree of **Bachelor of Engineering** Mechanical Engineering during the year 2019-20.

Further we declare that the content of the dissertation has not been submitted previously by anybody for the award of any degree or diploma to any other university.

We also declare that any Intellectual Property Rights generated out of this project carried out at RVCE will be the property of RV College of Engineering, Bengaluru and we will be one of the authors of the same.

Place: Bengaluru

Date:

<b>Name</b>	<b>Signature</b>
1. AMITH R ACHARI (1RV16ME010)	
2. NITESH JHA (1RV16ME071)	
3. BADRINATH NAYAK K (1RV16ME133)	

## ACKNOWLEDGEMENT

The successful completion of this project work was made possible through valuable contribution of number of people. To say thank you to all of them is not even enough to express my gratitude.

We are indebted to our guide, **Dr. Ramesh S Sharma**, Professor, **Department of Mechanical Engineering** for his wholehearted support, suggestions and invaluable advice throughout our project work and also helped in the preparation of this thesis.

We also express our gratitude to the panel members, Department of Mechanical Engineering for their valuable comments and suggestions.

Our sincere thanks to **Dr. Krishna M.**, Professor and Head, Department of Mechanical Engineering, RVCE for his support and encouragement.

We would like to express our special gratitude and thanks to **Dr.Prem Kumar.B.N**, Associate Professor, Kempegowda Institute Of Physiotherapy, who willingly helped us out with his knowledge.

We express sincere gratitude to our beloved Principal, **Dr. K. N. Subramanya** for his appreciation towards this project work.

We thank all the **teaching staff and technical staff** of the Mechanical Engineering department, RVCE for their help.

Lastly, we take this opportunity to thank our **family** members and **friends** who provided all the backup support throughout the project work.

## ABSTRACT

Approximately 20,00,000 people suffer from Stroke each year, 50-70% of stroke survivors get back their functionalities post stroke while 30% are permanently disabled. In order to regain their functionalities neurological rehabilitation can be done to improve their motor skills using different exercises. In this context, the research mainly focuses on neurorehabilitation of wrist using a manipulandum, but very few devices which are patient centric and hence receiving an optimum therapy for recovery. The objectives of the work was to measure grip strength at various wrist positions and determine the competency level to devise suitable rehabilitation exercises and implementing resistance and assist as needed control provided by the manipulandum.

This single degree of freedom manipulandum simulates the human movement by providing either force or impedance at the end points. Further, with the implementation of machine learning, the evaluation parameters of the subjects are well off compared to that of the available data of healthy individuals for proper assessment and a competency level is determined for therapeutic exercises. The level of the exercises is varied by changing the resistive torque, frequency and the range of motion. The motor will provide assistance or resistance based on the competency of the subject. The modelling of the manipulandum is carried out in solidworks, finite element static analysis is done in Ansys, simulation is carried out in Matlab for PID controller tuning and this simulated value is used for position feedback control using PID to control position and torque control for therapeutic exercises.

The results obtained are compared with that of the outcome from the test subjects, the measuring metrics being the grip strength, range of motion and precision. The grip strength was increased from 24.3N to 28.6N, increasing the range of motion by 8.5% for flexion and extension of a wrist with a precision of 88.3%. The future work of the project aims to implement a multi Degree of Freedom manipulandum not only specific to wrist for flexion and extension but also for other two degrees of freedom and an extension to the forearm as well.

## TABLE OF CONTENTS

	Page No
<b>Acknowledgement</b>	<b>iv</b>
<b>Abstract</b>	<b>v</b>
<b>List of Tables</b>	<b>xi</b>
<b>List of Figures</b>	<b>xii</b>
<b>Chapter 1</b>	<b>1</b>
<b>1. Introduction</b>	<b>2</b>
1.1 Motivation	2
1.2 Background	3
1.3 Problem Definition	3
1.4 Literature Review	4
1.4.1 Therapy and assessment	4
1.4.2 Neurorehabilitation using a manipulandum	4
1.5 Literature Gap	8
1.6 Research Objectives	8
1.7 Outline of thesis	9
<b>Chapter 2</b>	<b>11</b>
<b>2. Design of manipulandum</b>	<b>12</b>
2.1 Kinematic analysis	12
2.2 Force analysis	17
2.3 Design of compliant revolute joint	22
<b>Chapter 3</b>	<b>24</b>
<b>3. Project Objectives and Detailed Methodology</b>	<b>25</b>
3.1 Detailed Objectives	25
3.2 Flowchart	26
3.3 Methodology	27

<b>Chapter 4</b>	<b>28</b>
<b>4. Development of manipulandum</b>	<b>29</b>
4.1 Manipulandum	29
4.2 Material properties	29
4.3 Prerequisites of machining	30
4.4 Feed and specifications of the prototyping machine	31
4.5 Main frame	32
4.6 Material properties of Aluminium 6061 T6 series	33
4.7 Prerequisites of machining	34
4.8 Fabrication of main frame	34
4.9 Drawings	37
4.9.1 Manipulandum body	37
4.9.2 Main frame	38
4.9.3 Finger grip	39
4.10 Importance	40
4.11 Applications	40
<b>Chapter 5</b>	<b>41</b>
<b>5. Motor skills and its control</b>	<b>42</b>
5.1 Motor skills	42
5.2 Selection of motor	42
5.3 Comparison of servo and stepper motor	42
5.3.1 Advantages of servo over stepper motor	42
5.3.2 Disadvantages of servo over stepper motor	43
5.4 Specifications of RMCS- 2251	43
5.5 Base motor specifications	43
5.6 Encoder and drive specifications	44
5.7 System modelling	45
5.8 Estimation of motor parameters	45
5.9 System equations	47
5.10 Transfer function	47
5.11 Design requirement	47

5.12	Mathematical modelling of position feedback with PID controller	49
5.13	Proportional control	50
5.14	Proportional derivative control	51
5.15	Proportional integral control	52
5.16	Proportional derivative control	53
5.17	Controller selection	54
5.18	Control of servo motor	55
5.19	Voltage regulation and power supply	55
5.20	Load cell	56
<b>Chapter 6</b>		<b>60</b>
<b>6. Implementation of machine learning</b>		<b>61</b>
6.1 Stages in applying machine learning		61
6.1.1 Collection of data		62
6.1.2 Selection of parameters		62
6.1.3 Selection of learning method		63
6.1.4 Selection of training and test data		63
6.1.5 Evaluation		64
6.2 Data preparation and preprocessing		64
6.3 Logistic regression		66
6.4 Support vector machine		69
6.5 K- nearest neighbours		72
6.6 Decision trees		73
<b>Chapter 7</b>		<b>77</b>
<b>7. Finite element simulation</b>		<b>78</b>
7.1 Material specification		78
7.2 Meshing process		79
7.2.1 Specify global mesh settings		79
7.2.2 Insert local mesh settings		79
7.2.3 Preview and generate mesh		80
7.2.4 Mesh quality		81
7.3 Mesh metrics		81
7.3.1 Element quality		81



7.3.2	Aspect ratio	82
7.3.3	Skewness	82
7.4	Approximate boundary conditions	83
7.5	Estimation of parameters	84
7.6	Gripper	86
7.7	Support structure	86
<b>Chapter 8</b>		<b>87</b>
<b>8. Results and discussions</b>		<b>88</b>
8.1	Structure analysis	88
8.1.1	Comparison of numerical results and finite element methods results	88
8.2	PID Controller	92
8.3	Evaluation of machine learning models	93
8.3.1	Logistic regression	93
8.3.2	Decision trees	95
8.3.3	Support Vector Machines	96
8.3.4	K- nearest neighbours	97
8.4	Comparing the models	99
8.5	Neurorehabilitation	100
<b>Chapter 9</b>		<b>103</b>
<b>9. Conclusion and future scope</b>		<b>104</b>
9.1	Conclusion	104
9.2	Scope for future work	105
<b>References</b>		<b>106</b>
<b>Appendix</b>		<b>109</b>

## List of Tables

<b>Table No</b>	<b>Description</b>	<b>Page No</b>
2.1	Degree of Freedom For various Joints	13
4.1	Material Properties Of ABS	29
4.2	Specifications of the 3D printing machine	31
4.3	Aluminium 6061-T6 Properties	33
5.1	Performance Data of the Motor	44
5.2	Comparison of types of controllers	54
7.1	Statistics of the Mesh	80
7.2	Element Quality	81
7.3	Aspect Ratio	82
7.5	Skewness Mesh Matrix Table	83
8.1	Results of Equivalent stress	88
8.2	Deformation comparison	89
8.3	The tuned values of P, PD, PI, PID controller	93
8.4	Logistic Regression Confusion Matrix	93
8.5	Logistic regression performance metrics	94
8.6	Decision Tree Confusion Matrix	95
8.7	Decision tree performance metrics	95
8.8	SVM Confusion Matrix	96
8.9	SVM performance metrics	96
8.10	K-Nearest Neighbour Matrix	97
8.11	KNN performance metrics	98
8.12	Comparison Of all the ML models	99
8.13	Grip Strength of Affected Arm and Unaffected arm of Pre and Post Rehabilitation	101

## List of Figures

Figure No	Description	Page No
2.1	Schematic of the Revolute Joint Mechanism	14
2.2	Instantaneous Centre Method	16
2.3	Type 1 Loading condition	17
2.4	Type 2 Loading Condition	19
3.1	Flowchart of Methodology	26
4.1	Model of the Manipulandum	32
4.2	Laser Cut pieces of main frame	34
4.3	Fully Fabricated Main Frame	35
4.4	Mechanical Assembly of the Model	36
4.5	Final Setup of the Model	36
4.6	CAD Drawing of the body of the manipulandum	37
4.7	CAD drawing of the Main Frame	38
4.8	CAD drawing of finger Grip	39
5.1	Electrical Representation of DC servo motor	45
5.2	Closed loop control system using a controller	49
5.3	The open loop response and closed loop response of the plant without the controller can be found out once we know the transfer function of the plant.	49
5.4	Step response of a closed loop transfer using a Proportional Controller	50
5.5	Step response of a closed loop transfer using a Proportional Derivative Controller	51
5.6	Step response of a closed loop transfer using a Proportional Integral Controller	52
5.7	Step response of a closed loop transfer using a Proportional Integral Derivative Controller	53
5.8	Step Response of a general Transfer Function	54
5.9	Wheatstone Circuit	56
5.10	Loading Condition of Load cell	57
5.11	CAD model Of Load Cell	58
5.12	Load Cell Interface with Arduino	58
5.13	Calibration Flow Chart	59
6.1	Flow diagram for machine learning	61
6.2	Representation of K-fold cross validation with k=5	64
6.3	Logistic regression curve	66
6.4	Output of MATLAB implementation of Logistic regression in 6-fold cross validation	68
6.5	Problems in logistic regression, decision boundary	69
6.6	SVM boundary shown with support vectors	69

6.7	Results of Python implementation of SVM using RBF kernel	71
6.8	Results of MATLAB implementation of KNN with k=3 with 6-fold cross validation	73
6.9	Decision tree with x1,x2 attributes	74
6.10	Results of ID3 algorithm implementation	76
7.1	Material data of Acrylonitrile Butadiene Styrene (ABS)	78
7.2	Material data of Aluminium 6061-T6	79
7.3	Global Mesh Settings	79
7.4	Local Mesh Settings	80
7.5	Mesh on the assembly	80
7.6	Graph of Element quality Mesh metric vs the number of elements	81
7.7	Graph of Aspect ratio Mesh metric vs the number of elements	82
7.8	Skewness mesh Metric Spectrum	83
7.9	Graph of Skewness Mesh metric vs the number of elements	83
7.10	Boundary conditions on the assembly	84
7.11	Maximum Principal Stress on the assembly and Maximum Principal Elastic Strain on the assembly	84
7.12	Factor of Safety of the assembly	85
7.13	Total Deformation of the structure	85
7.14	Equivalent Stress on the gripper and Factor of Safety of the gripper	86
7.15	Equivalent Stress on the support structure and Factor of Safety of the support structure	86
8.1	Structural Analysis of the Body OF the Manipulandum	89
8.2	FEM analysis for Deformation	90
8.3	FOS determination from the FEM package	91
8.4	Response of closed loop transfer function without controller, PD, PI, PID	92
8.5	Graph of Grip Strength vs Absolute number of days	101
8.6	Representation of grip strength and ROM of Pre vs Post Rehabilitation	102

# ***CHAPTER-1***

## ***INTRODUCTION***

# CHAPTER 1

## Introduction

### 1.1 Motivation

Approximately 780,000 people suffer from stroke in the US. Even though majority number of people survive, they do so with a permanent disability. Greater than 11 lakh adults reported restraints in their day to day activities caused due to stroke. 50% - 70% of stroke survivors get back their functionalities post stroke. Still 30% are disabled permanently, in which 20% require professional care for 3 months post stroke [1]. The chances of stroke doubles after every decade after the age of 55 years, this group is specifically prone to prone to suffer from cerebrovascular accident. It was found out that the estimated stroke cost around 3% of the total national health expenditure which is approximately \$30 billion in the US[2].

Recovery from stroke imposes both physical and psychological challenges, so to cope up with the challenges faced post stroke neurorehabilitation becomes critical. The physical and psychological consequences of stroke may lead to difficulties like anxiety and depression; there are a limited number of studies which discuss the types of problems faced by those who have experienced a stroke. Wood-Dauphinee et al examined the performance of traditional care versus a disciplinary team in a randomized controlled trial for male and female patients and compared the performance measures, this was tested for motor performance and functional abilities [3]. The total time spent on rehabilitation varies significantly between institutions, countries and units. Lincoln et al. (1996) stated that only 25% of the total time was engaged for rehabilitation purpose. De Weerd et al.(2000) quantified the duration of time spent on therapeutic or remedial activities using behavioural mapping for two units, one in Switzerland and the other in Belgium. There was a direct relationship between activity and stroke severity, however only 11% of their active day walking was performed by mild stroke patients [4]. There are different types of issues being faced by patients like some form of communication deficit ranging from not able to speak to slurring of speech. The extent of participant's speech rehabilitation that they were not able to give enough time to cater to their physical needs, and most of the times ignored. There was dissatisfaction caused because of issues like shared rooms, delay in emergency departments and insensitive caretaking [5]. The pace of rehabilitation is also necessary so that the affected don't stress themselves from

overly optimistic expectations. Rehabilitation is important so that participants can adapt to a new way of life, involving how to do things, relearning abilities and commitment towards neurorehabilitation process. Traditionally stroke rehabilitation has not been so advancing nonetheless the development of technology based on robotics and different rehabilitation methods show that this is developing. There is potential for easier deployment, scope for application in a wide range of motor impairment while also being highly reliable [1].

## **1.2 Background**

The success of a rehabilitation program depends on the initial assessment of the impairment, and evaluation of the conditions of a patient that can affect the motor skills during the progress of the rehabilitation program. Human sensori-motor system is capable to learn by experience and practice. There are broadly two types of motor learning: skill acquisition to maximize function and adaptation in executing tasks [6]. Motor adaptation refers to the ability of the individual to adapt to external disturbances and their errors to accurately accomplish determined motions by eliminating any discrepancies that may occur in the motion. Studies have proven that best results are obtained when the tasks are done in one continuous session. Skill learning refers to “ability to reach an environmental goal with maximum certainty and minimum expenditure of energy and time”. A patient with high speed of motion might not qualify as an improved skill, as the accuracy is critical in evaluation of skill. The speed-accuracy trade-off function is an accurate measure of the skill, i.e. ability to maintain reasonable speed in executing tasks at a moderate pace.

It was proven that the rehabilitation process should begin within a month of the stroke, or as soon as post-surgery casts are removed, to utilize the neuroplasticity during this period. The motor learning was very quick in the initial phase, which gradually slowed down by the six-month mark. However, there was still marginal improvements till as long as a year.

## **1.3 Problem Definition**

As the pace and extent of recovery after cerebrovascular accidents such as stroke is contingent upon the engagement in the rehabilitation process, the exercises must be made accessible to patients more often to cater to their needs. Moreover, there is a need for continuous assessment to monitor their progress in the rehabilitation programs which can accurately give them feedback as to how their programs are to be modified for fastest recovery.

## 1.4 Literature Survey

Fugl-Meyer Assessment [7], is a popular clinical assessment procedure which gives an index based on performance of a stroke patient. However, due to only three levels of scoring, most patients get intermediate scoring and thus, does not accurately distinguish the intermediate performers. Motricity index [8] is another measure where scores are given for manual muscle test for shoulder abduction, elbow and pinch grip, and a cumulative UE score is generated. Grip strength and pinch strength [9] is also proven to indicate the motor performance. Action Research Arm Test (ARAT) [8] is a test used to evaluate functional performance. It assesses gross motor skill, grip, grasp, and pinch on a 4-point scale.

Margaret Rood provided the origin of the exercises to enhance the neuromuscular function and achieve motor control [10]. She also provided maneuvers such as stretching, joint positioning, and resistance which could help in the rehabilitation of the affected. These methods have shown only modest, and sometimes delayed effects, and are best used as a complimentary procedure in addition to other rehabilitation methods. Functional Electrical Stimulation (FES) is an alternative to the conventional rehabilitation [11]. The stimulation can lead to activation of muscles which enhances motor performance. The results of studies in control groups showed that the FES group had better performance growth over a period of time. However, the intensity of the stimulation, impact on quality of life and the time before the rehabilitation program began after the stroke, and any detrimental effects of FES in the group were unaccounted for. The size of the test group was a major factor, as the numbers were too less to generalize on properties of the electrical stimulation.

Acupuncture is treatment originated from ancient Chinese medicine, which involves application of fine needles over the body as a therapy.[12] A randomized control trial group treated with Acupuncture was compared to the results of conventional treatment with the baseline data. The subjects were of 24-95 years old and had a stroke in the last 1 month-8.5 years. Measures included Barthel index, Instrumental activities of daily living (IADL) scale, and Physical self-maintenance scale (PSMS). While acupuncture was beneficial for increasing dependency (activities of daily living), it showed no advantage over acupuncture in neurological impairments like motor skills, cognition ability.

Exercise therapy [13], or functional exercise is the rehabilitation of the muscle, joints and the sensory system. The joint damage could cause loss of motion in the wrist and fingers. The



immobility of the muscles can lead to muscle disuse atrophy, which is reversible. Hand exercises can be done with instruments with contractions through pulleys. To regain the sensory skills, exercises can be performed to execute tasks first with vision feedback, and then with the vision occluded. This would give the patient a sense of touch and improve the tactile feedback.

Occupational therapy is the rehabilitation of the impairment to execute a particular task(s) essential for the daily life, for example, labor, cognition activity. This follows execution of meaningful and purposeful tasks, where the difficulty level of tasks can be used to improve performance. To devise occupational therapy, the function should be evaluated, followed by the check for functional damage in the hand [13]. Different existing therapeutic techniques have been discussed in the following text [14].

Robotics therapy is also useful in the task of rehabilitation. Because of its ability to provide functional therapy that was not only reproducible but could also be provided at high-intensity, they may be used more often by therapists in rehabilitation programs [15]. It was found out that after a period 12 weeks of robot assisted therapy there was no considerable development of motor function compared to traditional care however after 36 weeks of rehab there was considerable improvement (Fugl-Meyer score of about 2.9 points). It is evident to indicate a potential role in the future of robotic assisted therapy in stroke rehabilitation, while much is left to explore in this field [15].

There have been different trials explored in the application of techniques where in cortical stimulation is performed in a non-invasive manner for the advancement of neuro-plasticity and rehab post-stroke. In repetitive transcranial magnetic stimulation, there is induction of electric current by a magnetic field in the cortex. This is done to either increase or decrease different parameters using high or low frequencies respectively. A small pilot study showed the improvement in upper limb function using rTMS combined with intensive occupational therapy. This method of rehabilitation was found to be safe, well tolerated and has a potential for further therapeutic option for rehabilitation of strokes but still needs a lot of research and hence not yet recommended for use in rehabilitation [15].

A novel curative approach for advancement of the recovery is the Stem Cell Therapy; this has enormous potential for rehabilitation. This can be achieved by repair of infarcted portion of brain by augmenting neuroprotection and different mechanisms for repair. This therapy reduces cerebral inflammation after stroke by promoting revascularization post stroke. This

therapy needs advance research and more randomized studies further we may see stem cell therapy in application for rehabilitation [15].

Mirror therapy (MT) was used for stroke rehabilitation until recent years, but there have been no clear outcomes in the pilot studies performed. In this technique the affected is asked to observe the unaffected limb in a mirror as he/she performs different exercises. The perception of a functional limb from the visual feedback in the mirror was found to be beneficial[15].

### **Neurorehabilitation using a manipulandum**

Neurorehabilitation is a medical process aiding recovery from a nervous system injury. Wrist based neurorehabilitation involves repetitive tasks, varied exercises for the proper functioning of the wrist and overcome the damage as a result of nervous injury. These interactive exercises improve the muscle strength of the individual and coordinate the movement of the muscles gradually in subjects with neurological impairments [16]. This type of training serves to improve the patient performance in a particular task and not to those which are encountered in day to day activities [17]. Progressive trends in the field of rehabilitation show a combination of conventional and innovative technologies which includes manipulandum, virtual reality and robotic platforms. The inclination towards technology based has increased in the past decade [18] [19]. The manipulandum acts as a guide to motor simulation, in turn an effective tool in understanding and acquisition of motor skills of the individual [20] [21] [22]. Certain studies prove that performing the rehabilitation tasks in an interactive environment for cases involving the expensive traditional rehabilitation [23], and can be a basic part of telerehabilitation for upper limb after stroke [24].

The manipulandum is a device used to manoeuvre something with ease, and to determine the motor skills. The device may comprise of multiple linkages or grip which enables to test, assess and thereby manipulate the motor skills. Consequently, the human response can also be measured and change accordingly to perform the required tasks. A manipulandum can serve as a device to study the kinematics. Along with the kinematics the device also performs the task assessing the biomechanical forces and moments developed by the human on it and ease the surrounding interaction.[25] The independent path of movement of the manipulandum may vary depending on the application, consisting of one degree of motion to a complex three degree of freedom. With respect to wrist manipulation, the major independent path of the wrist are ulnar and radial deviations, extension and flexion, and supination and pronation.

The mode of manipulation involves the impedance control of motor that is coupled with the grip through a torque arm. Most of the strategies used to control the device incorporate the variables such as the target position, the wrist angle position. The impedance control of the motor seeks an advantage over the rest where in the parameters that are accountable are force and velocity which is most suitable for the optimal facilitation

An ideal manipulandum assessing the human movement should provide the required output at any point for a given range of motion of the wrist. Meaning the device should be capable of providing impedance from zero to infinity.[26] Studies have proven that a cylindrical grip has a major contribution to the activity of the forearm muscles. For enhanced tasks involving the forearm grip, the shape of a cylinder provides enough space for placement of fingers and the palm. Care was taken such that the wrist muscles contribute for the movement of the manipulandum and that of the finger muscles are least. The design of the manipulandum should not cause considerable fatigue to individual muscles and assess the required parameters. [27]

Machine learning models have been used previously in assessing motor skills in rehabilitation. Machine learning refers to “the ability of a computer to make decisions on tasks without being explicitly programmed” using data known as ‘training data’. Machine learning is extremely useful in cases where conventional algorithms are infeasible. There are two broad types of learning: Supervised and unsupervised learning In supervised learning, the dataset used for training is labeled, meaning that the output and input is defined, and the algorithms develops a mathematical function which can accurately map the input data to the desired output with minimum generalization error. In unsupervised type of learning, the training data contains only the inputs and no desired output. The algorithms tried to find structure in the data and classify them accordingly.

Bochniewicz et al [28], conducted study on stroke patients to develop methods to assess the impact of a rehabilitation program by classification of movement as functional or non-functional use. They used videotaping to obtain baseline data and sensors mounted on subjects to record input variables such as acceleration and velocity. They used Random Forest classifier, which is a collection of multiple decision trees. The Random Forest model was able to classify correctly upto 94.8% in inter-subject testing of control subjects and 91.53% in intra-subject testing.

Yu et al[29] proposed a framework to remotely assess the upper limb function on the Fugl Meyer scale. They used two accelerometers and seven flex sensors to capture the movements of the wrist and elbow. They implemented the Relief algorithm to select most optimal features. Sensor inputs were denoised before being used for feature extraction, which was then followed by the SVM algorithm. The model showed that the quantitative FMA predictor could accurately give the actual FMA score in the clinical scale.

## **1.5 Literature Gap**

- i) In most of the past studies, the data was recorded for specific age group of patients and they focused on one type of grip, which could have led to incorrect interpretation of grip strength data set.
- ii) The input parameters were not all recorded simultaneously, and the result in successive evaluations were used to assess motor performance. This might have led to inability to capture the interlinking of the evaluated parameters.
- iii) Rehabilitation exercises devised was a generalized one, and not patient-centric. Such rehabilitation programs would lead to engagement in exercises which are either easier than his/her ability, or are difficult for the patient to overcome. Hence the patient would not receive optimum therapy for recovery.

## **1.6 Research Objectives**

The objective of the project was to develop neurorehabilitation for wrist using a manipulandum. This could record patient grip at various wrist positions, using which, patient competency was determined by comparing data between healthy individuals and patients. For rehabilitation, an adaptive algorithms was incorporated to devise suitable rehabilitation exercises. Implementation of variable resistance for manipulation, and assist-as-needed control was also done.

## **1.7 Outline of the thesis**

The thesis comprises of seven chapters following this chapter.

### **Chapter 1: Introduction:**

Basic concepts of motor skills were explained. Literature survey is done to evaluate existing rehabilitation therapies. Through the literature survey, potential areas for improvement are identified and thus the objectives of or project are formulated.

### **Chapter 2: Design of the manipulandum**

The kinematic analysis of the mechanism using various methods such as Graphical and Instantaneous Center method is presented here. This is followed by the force analysis which together form the basis of the manipulandum. Procedure for design of revolute joint and calculations are explained. Material selection, and various components for functioning is discussed along with mention of prerequisites for fabrication.

### **Chapter 3: Project objectives and detailed methodology**

Objectives are explained in detail along with the flowchart depicting the working of project that is required for integration of the components. Steps required for sub-tasks are explained.

### **Chapter 4: Development of the manipulandum**

The assembly of the manipulandum is shown in this chapter. CAD drawings of parts are shown, followed by an explanation of integration of the entire model with the usage of load cell in the assembly.

### **Chapter 5: Motor and its control**

Motor skills and its importance is briefly discussed. The parameters involved in selection of motor is explained along with performance parameters. Mathematical modelling of various controllers are performed with their response characteristics. Selection of controller is then discussed followed by load cell working, circuit connections and calibration.

## **Chapter 6: Use of Machine Learning**

Scope of application of Machine learning is discussed. Features required for training are then identified through inputs from the manipulandum. Data preparation methods are mentioned for enhancing performance of algorithms. Algorithms suitable for the purpose are identified and evaluation strategies are discussed. Implementation of various algorithms are done.

## **Chapter 7: Finite Element Analysis**

Selection of appropriate mesh is discussed in the chapter. Suitable boundary conditions are explained, followed by selection of loading conditions that occur in the functioning of manipulandum. Simulation is done and the various parameters are estimated.

## **Chapter 8: Results and discussion**

All domains of the project are taken into account to discuss the implementation details and also compare the results for the overall functioning of manipulandum.

## ***CHAPTER-2***

### ***DESIGN OF MANIPULANDUM***

## CHAPTER 2

### Design of Manipulandum

#### 2.1 Kinematic Analysis

Kinematics of the mechanism involves the study of the relative motion of its links. The key thing is to analyse the number of independent paths of motion of the links followed by the velocity and acceleration component of the links. Further the design also involves the study of the combined effects inertia forces due to both mass and its motion on itself is included.

The governing equation for determining the number of degrees of freedom involves is given by Gruebler's Criterion. The equation is as follows

$$F=3(N-1)-2L-H$$

Where ,

F - Mobility Of the Mechanism

N - Number of Links in the Mechanism (including the frame)

L – Number of Joints with Single Degree of Freedom (Lower Pair)

H – Number of Joints with Two Degree of Freedom (Higher Pair)

The Calculation is as follows with the set of known variables

$$N=2; L=1; H=0$$

With two links and one joint of single degree of freedom the Gruebler's Criterion happens to be

$$F=3(2-1)-(2*1)-0$$

$$F=1$$

The above value states that the mechanism results with a single degree of freedom.

The number of degrees of freedom for different joint is stated in the table 1. It specifies the nature of motion and corresponding degrees of freedom for a specific joint.



**Table 2.1 Degree of Freedom For Various Joints**

Type Of Joint	Nature of Motion	Degrees of Freedom
Hinges (Revolute)	Pure rolling	1
Slider (Prismatic)	Pure Sliding	1
Cylindrical, Cam, Gear, Ball Bearing	Rolling And Sliding	2
Rolling Contact	Pure Rolling	1
Spherical		3

From Table 2.1 and the results that we obtained, implies the mechanism is simple revolute joint with one degree of freedom. The mechanism is a hinge of rolling nature of motion.

The number of degrees of freedom accounts for the kind of rehabilitation that the subjects can undergo. This result determines the kind of rehabilitation done for subjects, implies to say one kind of motion of wrist, which is either of flexion and extension or pronation and supination or radial or ulnar deviation of the wrist, but not all three at a time.

The velocity and acceleration component of the links are essential to know the evaluation parameters at various positions of the manipulandum. The corresponding analysis can be carried out in many ways. They include

1. Velocity and Acceleration Analysis Using Graphical Methods
2. Velocity and Acceleration Analysis Using Instantaneous Centre Method
3. Velocity and Acceleration Analysis Using Analytical Method

The mechanism is a simple revolute joint, as a matter of fact the analysis is carried out using the graphical methods and instantaneous centre method, as the measurement of the length of the links is quite accurate than the angle measurement in real. Further the range of motion is to be known for analytical method, which is dependent on further calculations based on the above analysis results.

The principle of the method of analysis is as follows

**Graphical Method:** The method depicts that velocity of a link is length of the link times the angular velocity. Moreover, the velocity of the link relative to the fixed link is always zero. Further, acceleration is rate of change of velocity. Mathematically it implies the square times the velocity by the length of the link gives the acceleration of the link.

**Instantaneous Centre Method:** An instant centre is a point on one body about which some other body is rotating either permanently or at the instant end. The number of instant centre for a given mechanism is obtained by the equation

$$N = (n*(n-1))/2$$

Where, N= Number of instant Centre.

n= Number of Links Or Bodies.

### Graphical Method Analysis

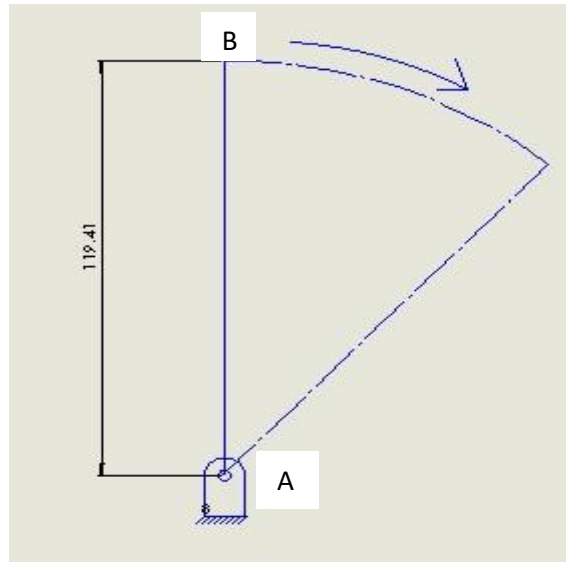


**Fig 2.1 Schematic of the Revolute Joint Mechanism**

The schematic of the simple revolute mechanism of the manipulandum is shown in the Fig 2.1 above. The link A is the fixed link, while AB the pivot link which pivots about centre A.

The direction of rotation is specified by an arrow mark. The length of the link is 119.40mm. The length of the link is obtained based on the condition of the grip measurement and articulation required for movement of the wrist. This is the optimal length so as to avoid interference with the main frame and allow easy motor skill test of the wrist.

The replica of the same is drafted in solidworks and the dimensions are obtained.

Calculations:

Length Of The Link AB =119.41mm

The angular velocity of the link is given by  $\omega=2*\pi*N/60$

Where N is the rpm of the motor selected, with the required steps to be of 1/80, the corresponding rotation per minute is 10.

On substitution we have

$$\omega=1.046\text{rad/s}$$

With the angular velocity of the link known, with the help of graphical method the velocity of the link can be determined

$$V_{AB}=AB* \omega$$

$$V_{AB}=119.41*1.046 \quad (\text{On Substitution})$$

$$V_{AB}=124.982\text{mm/s}$$

$$V_{AB}=0.124982\text{m/s}$$

The velocity is found to be 0.124982m/s for the constant speed of 10 rpm.

The acceleration is just the rate of change of velocity.

As a motor of constant rotation per minute is used the tangential component of the acceleration does not exist and only the normal component of the acceleration is to be determined.

$$a_n= V_{AB}^2/AB;$$

$$a_n= 124.982^2/119.41$$

$$a_n=130.814\text{mm/s}^2$$

The acceleration of the link is  $.130814\text{m/s}^2$ .

The velocity and acceleration enable to know the motor shaft position at every instant of time.

### **Instantaneous Centre Method:**

The number of instantaneous centres for a mechanism is determined by the equation

$$N = (n*(n-1))/2$$

$$n=2$$

$$N=1$$

Thus there is one instantaneous centre for the given mechanism at lies exactly at the centre of the fixed link. The Fig 2.2 describes the instant centre for the simple revolute mechanism.  $I_{AB}$  is the instant centre and lies at the centre of the fixed link. AB being the total length of the moving link.

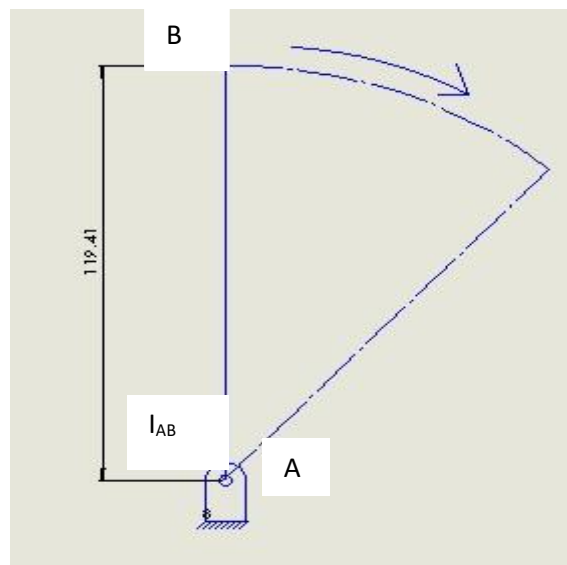


**Fig 2.2 Instantaneous centre method**

The velocity is determined by the following equation

$$V_{AB} = \omega * I_{AB} * AB$$

$$V_{AB} = 1.046 * 1 * 119.41$$

$$V_{AB} = 124.982\text{mm/s}$$

Thus, the results obtained from both the graphical method and instantaneous centre methods are in line with each other

## 2.2 Force Analysis

The ideology of the analysis is the body of the manipulandum is a curved beam, which is more ergonomic and quite effective for measurement of the evaluation parameters. The first design involved a simple soda bottle as the body, but due to inefficacy of the sensor to adapt to the grip, the model was redesigned. With the suggestion from the physiotherapist and existing manipulandum, the design was modelled in the form of a curved beam. This enabled a better integration of all the sensors and is good in load bearing.

The constraints of the model are as follows:

- Fixed Beam
- Distance Between the upper and lower fixed end = 170mm
- Distance between the frame and the gauge = 90mm
- Distance between the swivel and the grip centre = 70mm

The loading conditions are determined from the book, “The Biomechanics of Kinesiology”, which gave us the maximum probable torque and force that is applied by an average healthy individual on a manipulandum.

### Loading Conditions

- Force on to the frame = 150-300N
- Maximum Torque on the frame = 8Nm

Case 1:

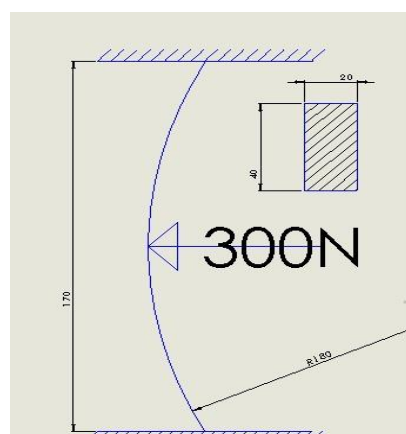


**Fig 2.3 Type 1 Loading Condition**

The case is assuming the beam to be a closed curved beam. As that is the best assumption to derive the results of the type of loading shown in the Fig 2.3. The load is acting along the radius of the closed beam. The cross section of the beam is shown by the shaded portion.

Force on the curved beam is 300N.

Inner Radius of the Curved Beam  $R_i$ ,

$$R_i = 166.375 \text{ mm}$$

Outer Radius of The Curved Beam  $R_o$ ,

$$R_o = 186.4156 \text{ mm}$$

Radius of the Curved Beam  $R$  (Centroidal Axis),

$$R = 176 \text{ mm}$$

e- Eccentricity of the curved beam is given by  $= R - (h / \log(R_o / R_i))$

$$e = 176 - (20 / \ln(186 / 166));$$

$$e = 176 - 175.81$$

$$e = 0.18955 \text{ mm}$$

$$A - \text{Area of the cross section} = b * h = 20 * 40 = 800 \text{ mm}^2$$

Distance of load line from the centroidal axis is 176mm

Bending Moment  $= F * R$

$$= 300 * 176$$

$$= 52800 \text{ Nmm}$$

The key is to determine the stress on the curved beam, which makes way for the selection of the material for the beam.

To Determine the Stress:

Stress on the inner fiber is given by  $\sigma_{Ri} = -(F/A) - (M * C_i / A * e * R_i)$

Where  $F$ - Load Applied

A- Cross Sectional Area

M- Bending Moment

$C_i$ - Distance Between the centroidal axis and the inner fiber

$R_i$ - Radius of the Inner fiber

e- Eccentricity

$$\sigma_{Ri} = -0.375 - 20.576$$

$$\sigma_{Ri} = -20.9519 \text{ MPa}$$

The stress on the inner fiber is 20.9519 MPa and compressive in nature. Hence the sign is negative.

Similarly the stress on the outer fiber is

$$\text{Stress on the outer fiber is } \sigma_{Ro} = -(F/A) + (M \cdot C_o / A \cdot e \cdot R_o)$$

$$\sigma_{Ro} = 18.7 \text{ MPa.}$$

The stress on the inner fiber is 18.7 MPa and is tensile in nature. Hence the sign is positive.

Case 2:

Load line at a distance from the centroidal axis

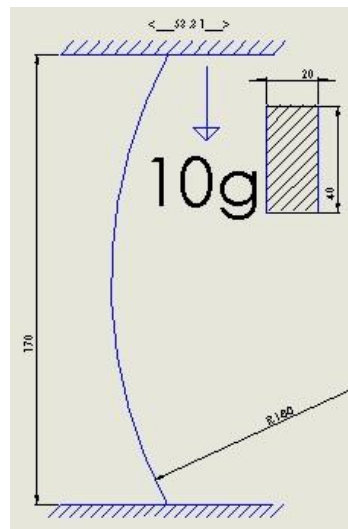


**Fig 2.4 Type 2 Loading Conditions**

The Fig 2.4 describes the load line acting at a distance from the centroidal axis of the curved beam. The direction of loading is vertical and the cross section of the curve beam is hatched.

The load in this case is applied at a distance of 53.31mm from the centroidal axis.

Radius of the curved beam  $R_n$ ,

$$R_n = 175.81 \text{ mm}$$

$C_i$ - Distance Between the centroidal axis and the inner fiber

$$C_i = 9.81 \text{ mm}$$

$C_o$ - Distance Between the centroidal axis and the Outer fiber

$$C_o = 10.19 \text{ mm}$$

R-Distance of the load line = 63.31mm

Bending Moment =  $F \cdot R$

$$= 100 \cdot 63.31$$

$$= 6331.1 \text{ Nmm}$$

Stress on the inner fiber  $\sigma_{Ri} = -(F/A) - (M \cdot C_i / A \cdot e \cdot R_i)$

Where F- Load Applied

A- Cross Sectional Area

M- Bending Moment

$C_i$ - Distance Between the centroidal axis and the inner fiber

$R_i$ - Radius Of the Inner Fiber

e- Eccentricity

$$\sigma_{Ri} = -2.4829 \text{ MPa.}$$

The stress in the inner fiber under this loading condition was found out to be 2.48MPa and compressive in nature.



## Deflection Analysis

Governing equations for the deflections both horizontally and vertically are as follows

### Horizontal Deflection

$$\delta_H = F(3\pi - 8)R^2 / (12EI)$$

where F- force under consideration

E- Modulus of elasticity

I –moment of Inertia

R- Radius of the curved beam

For Acrylonitrile Butadiene Styrene (ABS)

$$E = 1.6 \text{ GPa}$$

$$I = 26666.66 \times 10^{-12} \text{ mm}^4$$

$$R = 176 \text{ mm}$$

$$\delta_H = 0.0886 \text{ mm}$$

### Vertical Deflection

$$\delta_V = (\pi PR^3) / (2EI)$$

$$\delta_V = 1.176 \text{ mm}$$

Thus both horizontal and vertical deflections are well within the safe region and further the material Acrylonitrile Butadiene Styrene (ABS) can be used to fabricate the manipulandum.

Maximum Shear Stress is

$$\tau_{\max} = 0.5 \times 20.9519$$

$$\tau_{\max} = 10.475 \text{ MPa.}$$

## 2.3 Design of the compliant revolute joint

The role of the compliant revolute joint is mainly to produce a pure rolling action. Of all the existing revolute joints, considerable of them are notch type joints, having the axis drift along which the rib of the joint is drafted. The usual trend of the joint is the main frame along with a swivel, whose swivel axis is defined by a rib or a body. As this rib is susceptible to continuous motion, it is necessary to design them for high stiffness and a large range of motion.

The governing equations or the design is as follows

$$\text{Bending Stiffness } k_{11} (F_x/d_x) = k_{22} (F_y/d_y) = (24 \cdot E \cdot I)/L^3$$

where E- Modulus of elasticity =1.4GPa

$$I = \text{Moment Of inertia} = 26666.66 \cdot 10^{-12} \text{mm}^4$$

$$L - \text{Length of the Rib} = 170 \text{mm}$$

$$k_{11} = k_{22} = 6.057 \text{N/mm}$$

$$\text{Axial Stiffness } k_{33} (F_z/d_z) = (2 \cdot A \cdot E)/L$$

Where A- area of the cross section =800mm<sup>2</sup>

$$E - \text{Modulus of elasticity} = 1.4 \text{GPa}$$

$$L - \text{Length of the Rib} = 170 \text{mm}$$

$$k_{33} = 437.64 \text{N/mm}$$

$$\text{Bending /Rotational stiffness } k_{44} (M_x/\theta_x) = k_{55} (M_y/\theta_y) = (8 \cdot E \cdot I)/L$$

$$k_{44} = k_{55} = 58,352.795 \text{Nmm/rad}$$

$$\text{Torsional Stiffness } k_{66} (M_z/\theta_z) = \{(w/t) - .373\} \cdot ((4 \cdot G \cdot t^4)/3 \cdot L)$$

Where G- Shear Modulus

t- rib thickness

$$k_{66} = 9247.11 \text{Nmm/rad}$$

Knowing all the stiffness values, the range of motion can be determined for the maximum application of torque and force.

The torque stress relationship for a compliant Revolute joint is given by

$$\tau_{\max} = T/Q$$

where T- Torque Applied

Q-Polar Moment Of Inertia

$$T = 10.475 \times 79450$$

$$T = 832240.54 \text{ N } \Theta$$

But we know that  $T = k_{\Theta} \Theta$

From which the positive value of range of motion is  $\Theta = 90^{\circ}$

Hence the model is satisfying the rehabilitation requirements

***CHAPTER-3***  
***PROJECT OBJECTIVES AND DETAILED***  
***METHODOLOGY***

## CHAPTER 3

### Project Objectives and Detailed Methodology

#### 3.1 Detailed objectives

- A manipulandum is to be developed which consists of a grip that can swing about a motor axis. Using wrist flexion/extension, the patient range of motion is to be recorded using encoder readings.
- The grip also has to measure grip strength using a load cell so that patients can record their grip strengths at angles in steps throughout their range of motion.
- Motor coordination is to be measured as the patient tries to coordinate wrist motion with a pre-programmed marker which moves randomly about the same axis as the grip.
- A machine learning model has to be deployed and trained to classify the patients either as healthy or as impaired, in which case the degree of impairment is also determined.
- Suitable therapies are determined according to degree of impairment. These therapies have to differ from each other in terms of torque impedance of motor that has to be overcome in order to move the grip, or even the speed and randomness with which the marker which has to be followed, moves.
- Assist-as-needed control of servo motor also has to be programmed to implement passive motion in case of inability to move wrist.

### 3.2 Flowchart

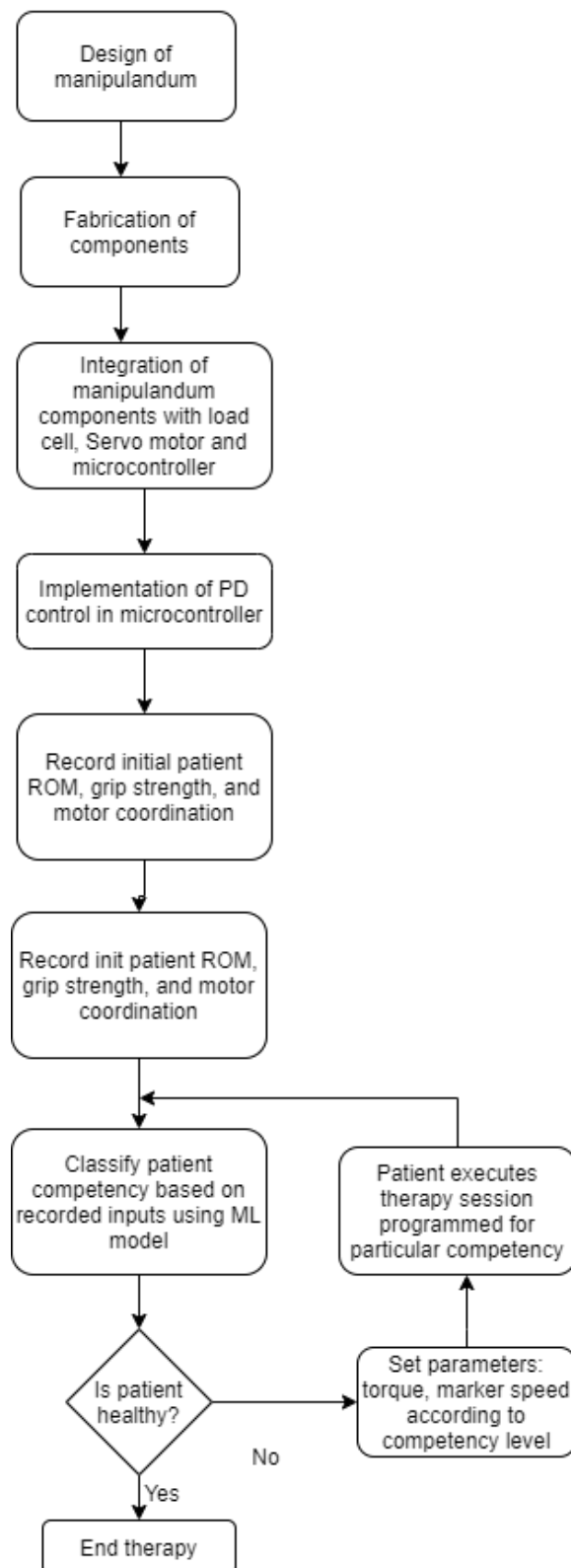


**Fig 3.1 Flowchart of Methodology**

### 3.3 Methodology

Fig 3.1 shows the flow of steps in the project. Design of the manipulandum involves kinematic analysis considering two links: base and swing arm. Velocity and acceleration are calculated for the given RPM of motor to be used. Force analysis is then performed for horizontal and vertical loading conditions. Components of the manipulandum include frame, slotted disc, grip assembly. These are fabricated as explained in Chapter 4. The components are to be integrated with actuators and sensors to fulfil the functions of passive-assisted motion and grip sensing respectively. For this, a DC servo motor and load cell is used. A micro controller is used for calibration and taking input from the load cell. When the grip cannot be rotated by the patient, passive motion is imparted using servo motor that is controlled using a PD control algorithm. Proportional and derivative constants are fed to the micro controller for having position and speed control.

The diagnosis phase begins with initializing variables of torque with base values. Range of motion is first determined using extreme readings of encoders of servo motor. Then, a marker moves in arcs about the axis of grip assembly. Patient is asked to coordinate his/her wrist motion with the marker motion. Then, curve similarity index is calculated between the two motions and accuracy is determined. Third factor of diagnosis is grip strength at various angles of wrist position. The force vs. Angle curve is used to determine grip quality index. This completes the diagnosis phase with three quantities: range of motion, motor coordination and grip strength.

A machine learning model is trained using data from many patients for classification of patients using these inputs. The classification is multi-class, i.e. patients are classified as healthy or impaired with different degrees of impairment. Appropriate exercises are also determined which would be suitable for patients with degree 1 disability, degree 2 disability, and so on. These exercises are translated in terms of impedance to wrist motion and randomness and speed of marker.

Post-diagnosis, appropriate therapy parameters are set according to the classification and patient undergoes one session of therapy. Parameters used for classification are again sampled from the therapy session and again used for classification. If there is a change in classification result, the therapy parameters are modified accordingly. This is repeated till the motion parameters are sufficiently high to be classified as 'healthy'. At this stage, the therapy is ended.

## ***CHAPTER-4***

### ***DEVELOPMENT OF MANIPULANDUM***



## CHAPTER 4

### Development of Manipulandum

#### 4.1 Manipulandum

The device manipulandum as stated earlier is used to test the motor skills of an individual. It might comprise of many degrees of freedom starting from a simple one degree of freedom to complex twelve degree of freedom. The design calculations referred to above are for one degree of freedom. Our manipulandum test the motor skills of the subjects for their motion of wrist which is flexion and extension. Our design is motivated by the existing jamar dynamometers. The existing manipulandum are not ergonomic and the kinematics of the device failed to meet all the requirement of the rehabilitation exercises.

Further, after having several literature reviews, it is to be seen that most of the components are of aluminium. Having known the load acting on the manipulandum and force calculations done, the material considered is Acrylonitrile Butadiene Styrene (ABS) for the main body of the manipulandum. The procedure of fabrication is rapid prototyping (3-D printing), as the required contours are made easily. The design is perfectly fabricated to exact dimension with least error and high precision make it ergonomic to with high level of tolerance. Further the number of working hours of fabrication is reduced compared to traditional machining, which is a computer numerically controlled machines to fabricate the aluminium billet.

#### 4.2 Material Properties

The material properties of the material Acrylonitrile Butadiene Styrene (ABS) is given in Table 4.1.

**Table 4.1 Material Properties of ABS**

Property	Value
Ultimate Strength	40MPa
Density	1.04g/cm <sup>3</sup>
Coefficient of Thermal Expansion	90µm/m- <sup>0</sup> C
Maximum Service temperature	98 <sup>0</sup> C

Extruder temperature	220-250 <sup>0</sup> C
Specific Heat Capacity	1.393-1.92J/kg <sup>0</sup> C
Tensile Strength	27.6-55.2MPa
Elongation	.015-1% Strain
Vickers Hardness	54.9-158MPa
Young's Modulus	1.19-2.9GPa
CO <sub>2</sub> Footprint	91-102kg/kg

As the device is subjected high number of working hours and a considerable amount of heat is experienced due to repeated motion, the properties such as maximum service temperature play a vital role. With 6-8 hours of working per day the maximum heat generated is 54-58<sup>0</sup>C. Hence it is quite evident that the material is well off within the working range. Further to have a greener project the carbon footprint is taken into consideration which makes it very a relative less polluting agent and the material is recyclable as well. Thus the project adds the value for a greener project.

The material is further impact resistant relative to other rapid prototyping materials and highly resistant to heat. Further the printability of the material on a scale of 1-10, is awarded 8, which makes it more reliable. The durability of ABS is very high which accounts for the longevity and efficiency.

### 4.3 Prerequisites of Machining

There are certain prerequisites for rapid prototyping of Acrylonitrile Butadiene Styrene (ABS). They are as follows

- The material should be in filament form in order to feed it to the machine.
- The machining has to be performed on a heated bed
- The bed temperature has to be maintained between 95-110<sup>0</sup>C
- The recommended build surface is Kapton tape or ABS slurry.
- An enclosure is recommended to avoid any interference of foreign materials while rapid prototyping, so as to avoid any warping, void or any other kind of damage.

- To avoid any water or moisture content in the extruder opening or in the material or in the bed on which printing happens. The moisture content may result in reduced stiffness of the structure making way for air holes and causing warpage within few duty cycles of the structure.

#### 4.4 Feed and Specifications of the Rapid Prototyping Machine

The machine is a desktop 3D printing machine by SHINING 3D. The technical specifications of the machine are stated in Table 4.2.

**Table 4.2 Specifications of the 3D printing machine**

Specification	Value
Print Envelope	400*400*350mm
Layer Thickness	0.15-0.8mm (adjustable)
Printer Head Diameter	0.4mm,0.6mm,0.8mm,1mm
Axis Running speed	40mm/s
Print Speed	10-100cm <sup>3</sup> /h
Highest Temperature Recommended For printer Head	240 <sup>0</sup> C
Position Accuracy	0.01mm(XY)0.01mm(Z)
Consumable Materials	ABS, PLA, Carbon Fiber PETG.
Data Input	USB connection
Data Import Format	STL
Type Of Fill	Hollow, Semi Solid, Solid.

With the specifications known, the parameters were set for our model fabrications. The type of fill was set to solid fill as of the model was 19hours. The material was preheated to a temperature of 40-45<sup>0</sup>C to enable easy flow of material into the printer nozzle. The layer thickness was set to 0.6mm, as anything less than that would make the printability of the structure difficult causing the slipping of layers as soon as they get annealed. The print speed was set at 75cm<sup>3</sup>/h totalling to 19 work hours. The working bed temperature was set at 98<sup>0</sup>C, and is of ABS slurry. The bed was also treated with a releasing agent so as to retain the

component without any burrs. The material was procured in its filament form and was fed into the machine. Having imported the STL file of the model on to the machine, the fabrication was set. After inspection of all the pre-set conditions, the process of printing is started. Fig 4.1 gives the isometric view of the manipulandum body that is to be rapid prototyped.

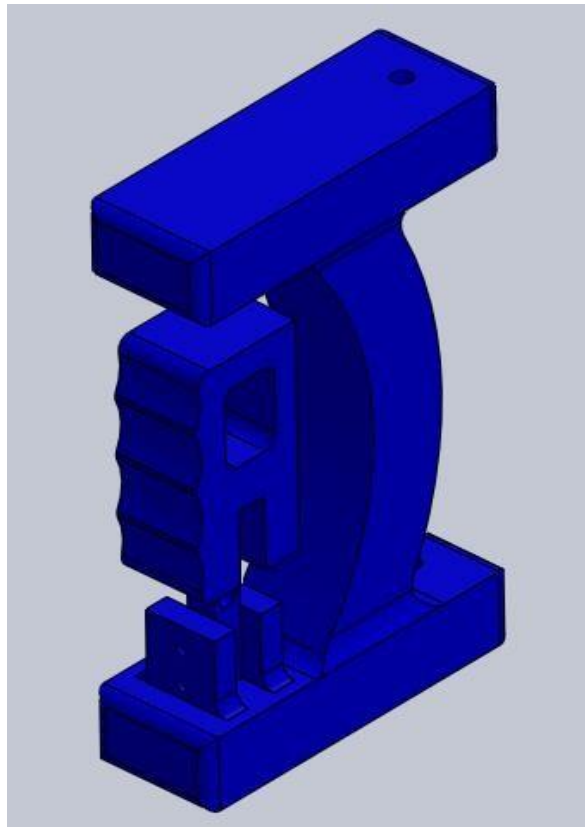


**Fig 4.1 Model of Manipulandum**

## **4.5 Main Frame**

The main frame is the supporting structure of the manipulandum, which houses the body, motor and other auxiliaries. It is a rectangle frame that encloses the body and acts as the primary fixed link, while the body is the secondary moving link. The two links are connected in a manner such that it is a revolute joint, having pure rolling motion between the two links. The body of the manipulandum serves as the rib between the upper and lower end of the main frame, making it a compliant revolute joint. The axis of the revolute joint is such that the axis of the motor shaft and that of the centre of the two links are along the same line.

As the main frame just has to bear the nominal forces, the material selected for frame is Aluminium 6061T6 series.

## 4.6 Material Properties of Aluminium 6061T6 series

The properties of Aluminium 6061T6 series is stated in the Table 4.3 below.

**Table 4.3 Aluminium 6061T6 properties**

Property	Value
Density	2.7g/cc
Ultimate Tensile Strength	310MPa
Tensile Yield Strength	276MPa
Modulus of Elasticity	68.9GPa
Poisson's Ratio	0.33
Shear Strength	207MPa
Fatigue Strength	96.5MPa

The machinability and weldability properties of the Aluminium 6061T6 properties make it more reliable than any other series of the same metal. T6 implies the type of heat treatment the metal underwent. The metal is solution heat treated and aged artificially. The composition involves aluminium, chromium, copper, iron and few parts of manganese, magnesium, silicon and rest involves residuals.

The property that accounts for the choice of material is mainly density, strength and machinability index. The availability of the metal in a sheet form also adds a key factor to choose the material. As the material is in sheet form, the mode of fabrication is high precision laser cutting.

## 4.7 Prerequisites of Machining

Laser cutting involves the principle of high energy (laser) concentrated at a point making the metal to melt and evaporate. It is quite essential to prepare the surface of the metal to undergo process of cutting.

- The surface of the metal has to be cleaned and ensure no dust exists on it.
- The material should possess completely flat profile.
- The thickness of the material should be uniform.

## 4.8 Fabrication of Main frame

The material is procured in sheet form with a thickness of 6mm. The surface of the material is then prepared as per the prerequisites of the fabrication. The fabrication of laser cutting happened in one pass. The feed was set at 0.5mm/s. The total time elapsed between start and end of fabrication is 84minutes with tolerance of 0.001mm.

The laser cut components were then filed to remove the burrs generated at the sides of the component. All the components were re-checked for their dimension along with the original orientation. Fig 4.2 gives the top views of the laser cut pieces of the parts of the main frame.

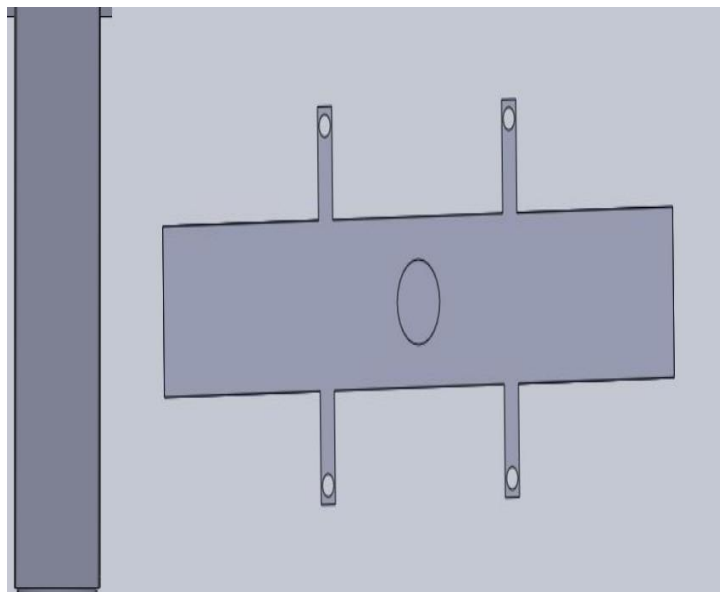


**Fig 4.2 Laser Cut Pieces of Main Frame**

The pieces were to be combined to form a rectangle so as to house the body. The joining process was done by welding. The choice of joint opted out for the process was lap joint. The

joint was positioned in such a manner all the joints formed the corner of the rectangle. All the pieces were aligned with the help of right-angle reference and a bead of weld was welded so as to keep it intact. Further after all the corners were beaded, the seam welding was done to finish the process of permanent joint. During the process of beading the holes in the component were inserted with corresponding bolt so as to avoid the shrink or increase in the diameter of the hole. The type of welding used was Tungsten Inert Gas Welding (TIG) to remove the oxide layer formed during the metal puddle formed. The polarity of the electrode was positive while that of the base metal is negative. This enables a cleaner surface to weld, as the current flows from the negative terminal to that of the positive will take away any oxides. Thus the fresh surface of the metal is exposed to weld. The frame once welded was allowed to cool under atmospheric condition without any external aid, as any external coolant might disturb the weld life of the frame. Fig 4.3 shows the isometric view of fully fabricated main frame. Fig 4.4 and 4.5 gives shows the isometric view of the setup without and with the modelled hand respectively.

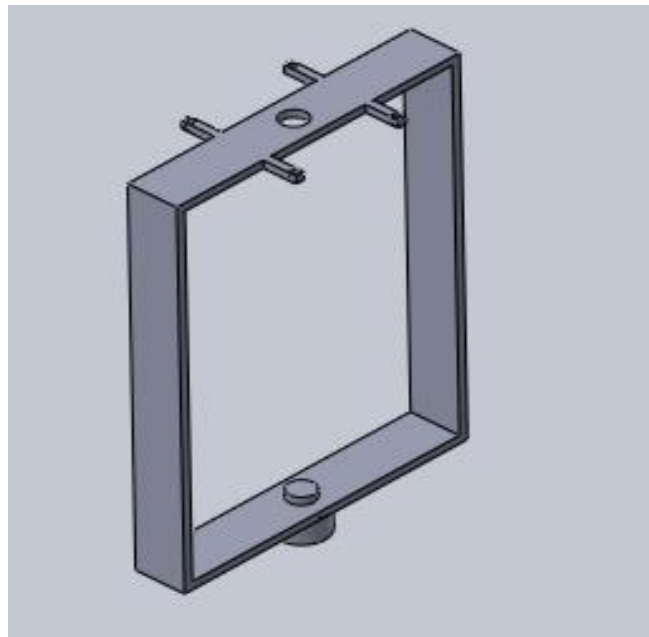


**Fig 4.3 Final Assembly of Main Frame**

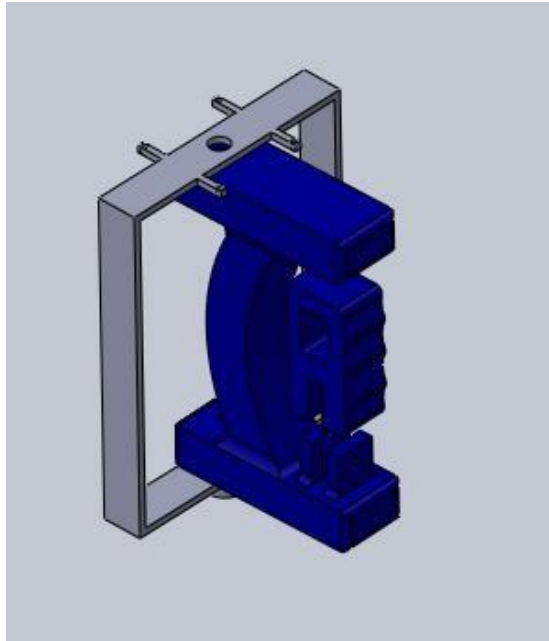


**Fig 4.4 Mechanical Assembly of the Manipulandum**

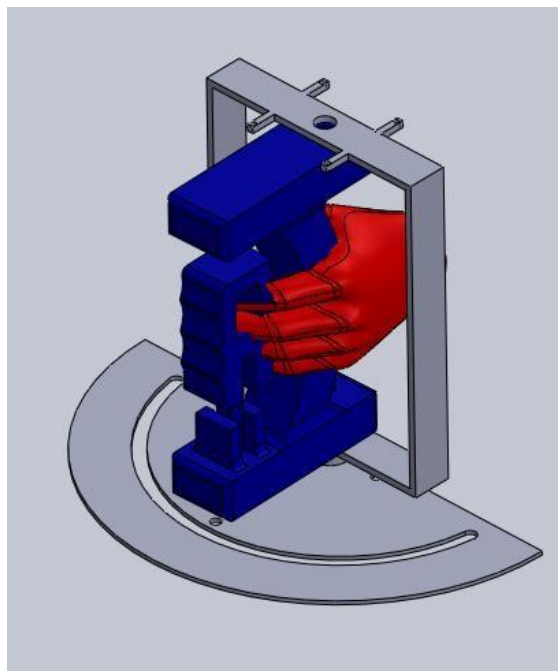


**Figure 4.5 Final Setup of the model**



## 4.9 Drawings

### 4.9.1 Manipulandum Body (1)

The body of the manipulandum is the moving link of the mechanism. It serves as a rib between the two ends of the fixed link (Main frame). The CAD drawing of the body is shown below Fig 4.6 having all three views in first angle projection.

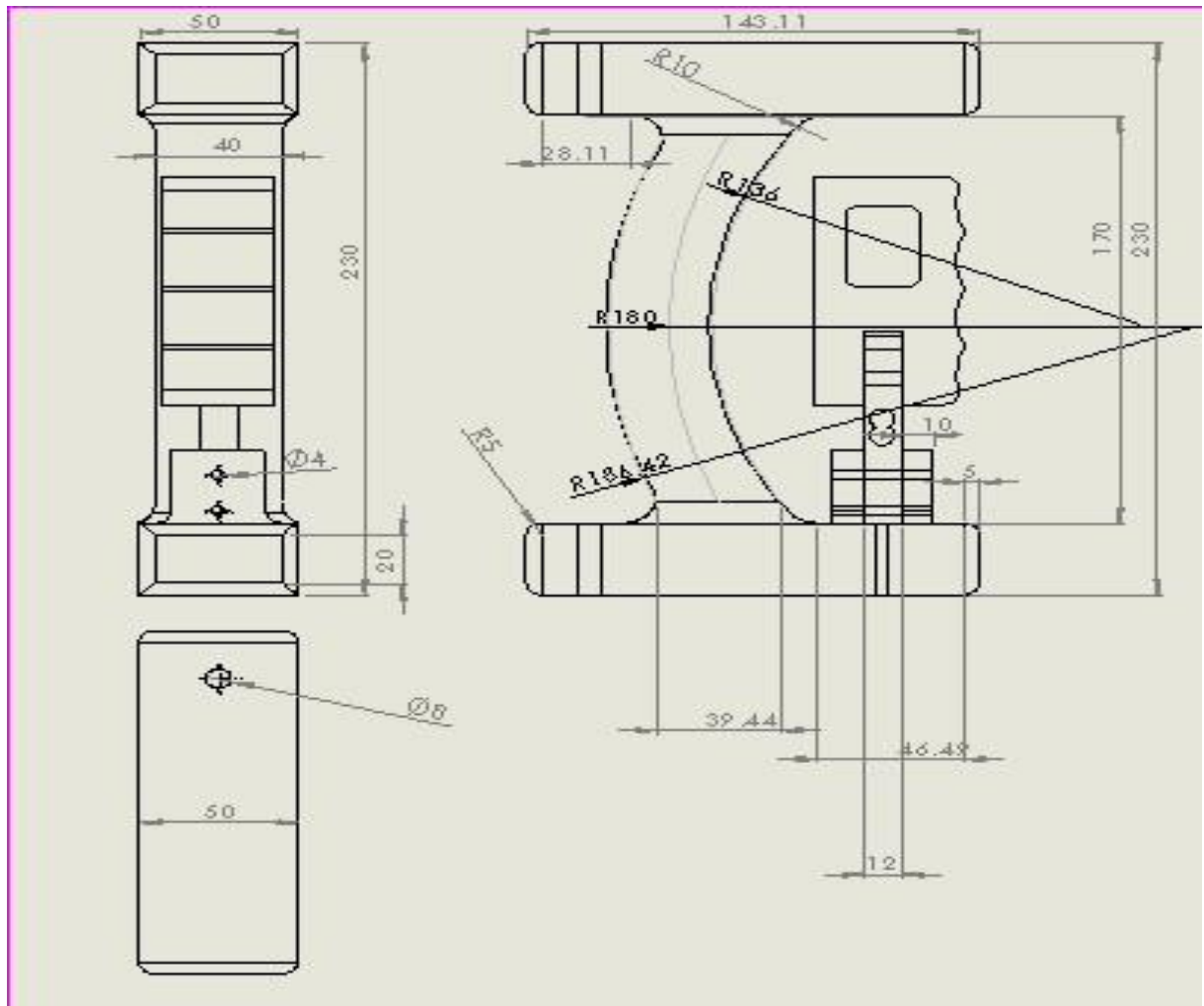


**Fig 4.6 CAD drawing of the body of the manipulandum**

### 4.9.2 Main frame

The main frame is fixed link of the manipulandum. It is a rectangular enclosure that houses the body and also holds the motor that drives the mechanism. The integration of the main frame and body is in such a manner that the relative motion is pure rolling, thus making the mechanism a simple revolute joint. The CAD drawing of the main frame is shown below in the Fig 4.7 having all the views in the first angle projection.

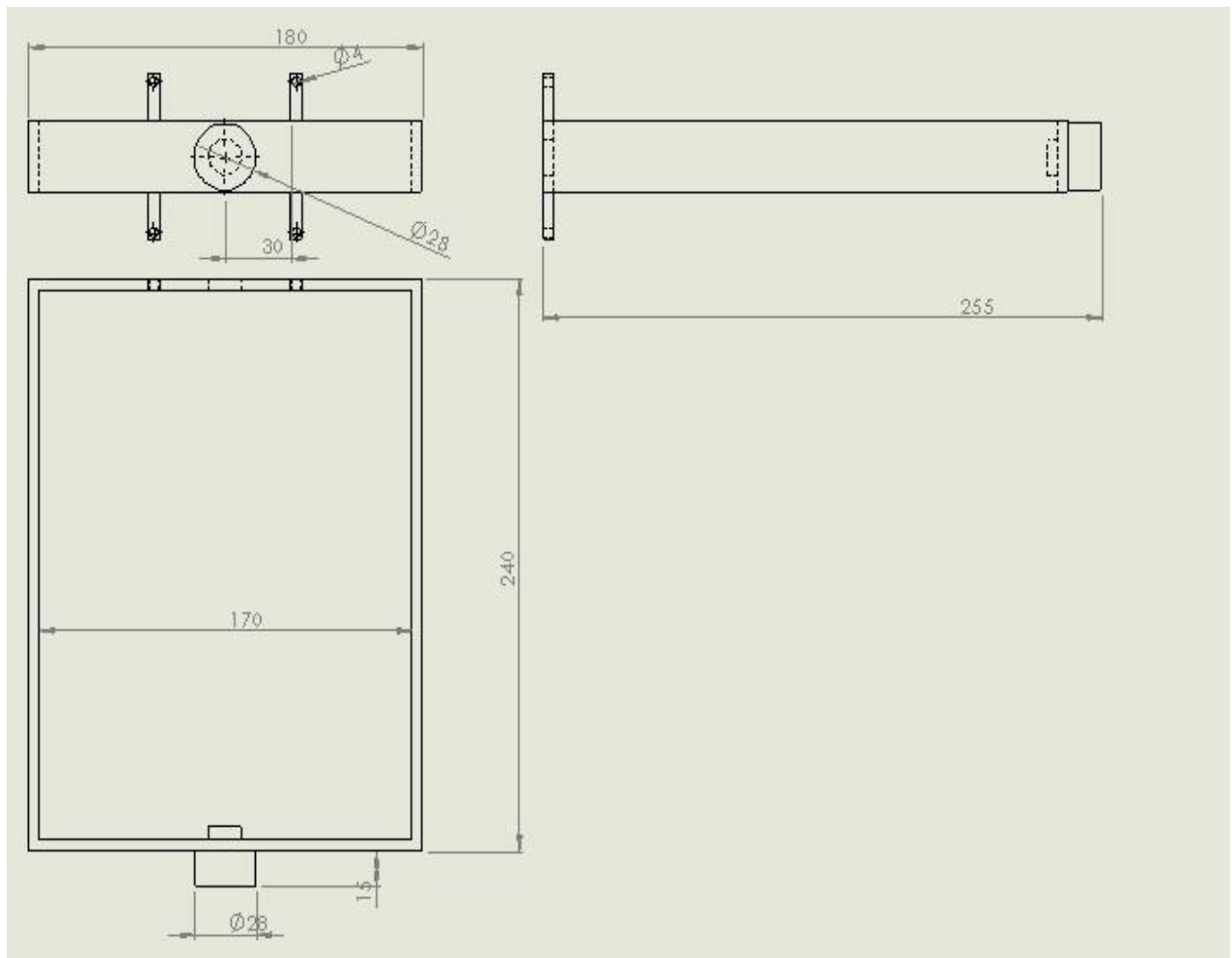


**Fig 4.7 CAD drawing of the main frame.**

### 4.9.3 Finger Grip

The finger grip is the part of the manipulandum to have the subject wrist their fingers on it, enabling the measurement of evaluation parameters. The finger grip in turn is integrated with the load cell to measure the grip strength of the individual subjects. The CAD drawing of the finger grip is as shown in Fig 4.8.

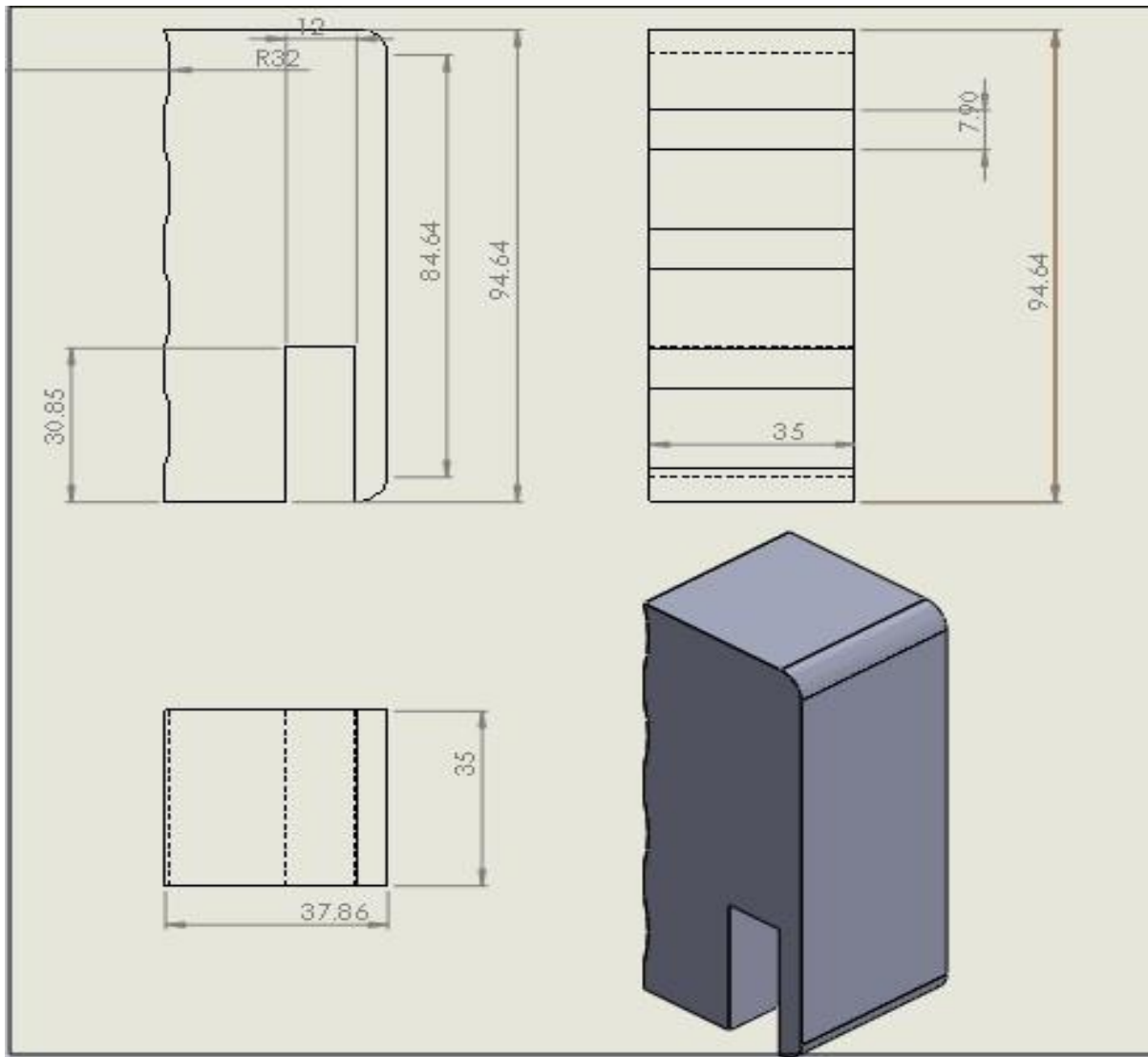


**Fig 4.8 CAD drawing of finger Grip**

#### **4.10 Importance**

The impairment of wrist, forearm is very common these days. It becomes very important for them to undergo rehabilitation. They can be advised to have rehabilitation exercises, without avoiding professional intervention. So a single degree of manipulandum is developed to provide the required them to perform the exercises in a designated manner.

#### **4.11 Applications**

The applications of manipulandum not only limits to testing of motor skills, but can be used as a rehabilitation device. The number of independent paths described for the manipulandum can be very wide, making a scope if interest of rehabilitation device not only upper limb but also to other locomotory organs of the human body. Apart from the rehabilitation device, it serves as the purpose of diagnostic and measurement tool for various evaluation parameters. Further as a part of motor parameter testing, manipulandum are used too.

## ***CHAPTER-5***

### ***MOTOR SKILLS AND ITS CONTROL***

## **CHAPTER 5**

### **Motor Skills and Its Control**

#### **5.1 Motor Skills**

Motor Skill is the ability to perform a predetermined task with maximum certainty. The one with high motor skill can perform activities with higher precision, accuracy, by the usage of least energy with maximum success rate. There are majorly two types of motor skills namely, Gross motor skills and Fine motor skills. Gross motor skills involve the use of large muscles for activities like walking, crawling, running and balancing. Most of the gross motor skill learning happens during the childhood. Fine motor skills make use of small muscle groups involving wrist, fingers, hands, feet. Generally, these motor skills are precise in nature. These motor skills can be impaired because of reasons like injury, stroke, illness, cerebral palsy.

These motor skills can be mathematically modelled using optimal control theories, now in this study we are considering the motor skill of a wrist involving the flexion and extension. In order to promote rehabilitation of this motor skill, a passive motion is provided by the motor to the stroke patient reducing the spasticity and muscle stiffness improving the mobility. This passive motion is applied in such a way that it takes your joint through the full range of extension and flexion.

#### **5.2 Selection of Motor**

For better efficiency and productivity of motion control applications, selection of motor is very important. In our project the motor selection was narrowed down to either a servo motor or a stepper motor because of the need to control torque and position simultaneously. There were different parameters considered while making a comparison between a servo motor and a stepper motor like torque, efficiency, speed, integration, control complexity.

##### **5.3.1 Advantage of servo motor over stepper motor**

- For better position control, use of servo motor is suited because servo can handle loads which are mostly inertial instead of friction.
- Higher power output, when compared with a similar motor size and weight stepper motor.

- For low speed and higher smoothness use of DC servo motor is recommended.
- The control method, is a closed loop, which means it has a feedback mechanism, so the accuracy and resolution depends on the encoder.
- Servomotor has higher efficiency when compared with stepper motor.
- Servomotors have better Torque to Inertia ratio; hence it has better acceleration.

### **5.3.2 Disadvantages of servo motor over stepper motor**

- More expensive compared to stepper motors
- Cannot work with open loop controls, a closed feedback is essential
- Require tuning for closed loop parameters for stabilizing the closed loop.
- Life of servo motors is usually lesser compared to stepper, so servicing is required.

Hence considering the above parameters, servo motor was selected for our requirement of better position control, higher torque, lower speeds and higher controllability for therapeutic exercises like passive assistance and resistance needs the control of both position and force.

For actuation servo motor selected required for our application needed a higher torque value of above 80kg-cm, and having speeds lesser than 15rpm, so a RMCS-2251 DC servo motor was selected, which is a 10rpm high torque motor of 120kg-cm and having a encoder which integrates 0.2deg resolution optical encoder. This motor is suited because it works well for slow speeds and a closed loop PID controller can adjust the torque values.

### **5.4 Specifications of RMCS-2251**

- 10RPM 12V DC motors with Metal Gearbox and Metal Gears
- Gearbox diameter 37 mm.
- Shaft dimensions: 3.175 X 15.0 mm
- 180gm weight and 120kgcm torque

### **5.5 Base Motor Specifications**

- Dimensions:29.0 X 47.0 mm
- Shaft Diameter:3.175mm
- Input Voltage:12.0 V DC

- No Load Speed: 17034rpm
- No Load Current:0.80A
- Stall Torque:176.86mNm
- Stall Current:176.86A
- Maximum Output Power:79.00W
- Maximum Efficiency: 62%
- Operating Temperature: -40 to 85 °C
- Range Storage Temperature Range: -40 to 100 °C

**Table 5.1 Performance data of the Motor****Performance Data:**

	No Load	Stall	Maximum Efficiency	Maximum Power
Current (A)	0.80	176.86	5.04	16.18
Efficiency (%)	-	-	62	39
Output Power (W)	-	-	37.47	79.00
Speed (rpm)	17034	-	14689	8517
Torque (mNm)	-	176.86	24.35	88.43

The Performance data of the base servo motor without the encoder is shown in Table 5.1 for No Load, Stall, Maximum Efficiency and Maximum power condition

## 5.6 Encoder and drive specifications

- Direct replacement for 50W stepper motor and drive
- Zero-backlash DC servo performance
- 0.2deg resolution optical encoder integrated on motor output shaft
- High-Current DC Servo motor driver integrated with the motor
- Fixed stepping of 1800 steps per rotation on output shaft
- Industrial Grade Aluminium housing for motor and drive
- 2.5V, 3.3V and 5V compatible PULSE and DIRECTION inputs with 2-wire opto-isolated interface



## 5.7 System Modelling

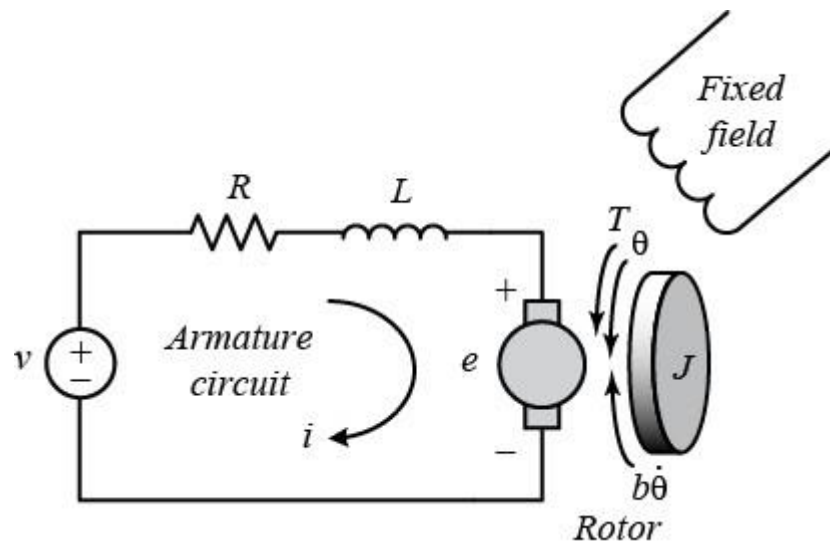


Fig 5.1 Electrical Representation of DC servo motor

The actuator for our project is a DC servo motor, which is controlled using position feedback, in which the input to the system is voltage source(V) applied to the motor's armature, and position of the shaft(theta) being the output as shown in Fig 5.1. The assumption made is that the shaft and rotor are rigid. This is a viscous friction model, implying friction torque to be proportional to shaft angular velocity.

- (J) Moment of inertia of the rotor  $2.2917\text{E-}5 \text{ kg.m}^2$
- (B) Motor viscous friction constant  $1.5836\text{E-}5 \text{ N.m.s}$
- (Kb) Electromotive force constant  $0.004831 \text{ V/rad/sec}$
- (Kt) Motor torque constant  $0.004831 \text{ N-m/Amp}$
- (R) Electric resistance  $0.0678 \text{ Ohm}$
- (L) Electric inductance  $2.75\text{E-}6 \text{ H}$

## 5.8 Estimation of motor parameters

Given:

Mass(m)=109g

Radius (R)=14.5mm

Current ( $i_a$ ) = 5.04 A

Torque (T) = 24.25 Nm<sup>2</sup>

Efficiency( $\eta$ ) = 0.62

Output Power(P) = 37.47 W

1) Torque constant and electromotive force constant:

$$T = K_T i_a \quad (K_t = \text{Torque constant})$$

$$\begin{aligned} K_T &= T / i_a \\ &= 24.85 / 5.04 \\ &= 0.004831 \text{ Nm/A} \end{aligned}$$

$$K_b = K_T \quad (K_b = \text{Electromotive force constant})$$

2) Moment of Inertia:

$$\begin{aligned} J &= (mR^2)/2 \\ &= ((109 \times 10^{-3}) \times 8 \times (14.5 \times 10^{-3})^2)/2 \\ &= 2.2917 \times 10^{-5} \text{ kgm}^2 \end{aligned}$$

3) Armature Resistance

$$\text{Output power (W)} = \eta * \text{input power}$$

$$O/P = \eta * I/P = \eta * VI \quad (\eta = 0.62)$$

$$37.47 = 0.62 * V * 5.04$$

$$V = 12 \text{ V (applied voltage)}$$

$$\text{Stall current } (i_s) = 176.86 \text{ A} = V/R_T = 12/R_T$$

$$R_T = 0.0678 \text{ ohm}$$

4) Motor constant

$$K_m = K_T / \sqrt{R_T} = 0.004831 / \sqrt{0.0678}$$

$$K_m = 0.018472 \text{ N-m}/\sqrt{\text{W}}$$

5) Motor Viscous friction coefficient (B) =  $K_T * i / W$

$$W = 2\pi N/60$$

$$B = (0.004831 * 5.04 * 60) / (2 * \pi * 14689)$$

$$B = 1.5836 \times 10^{-5} \text{ N-m-s}$$

## 5.9 System Equations

For a DC servo motor the torque is directly proportional to both armature current and the strength of the magnetic field. So, a motor can be either armature controlled or field controlled. In our case we will assume that the magnetic field is constant and only armature current is responsible for motor torque, and are proportional by a constant factor of  $K_t$ .

$$T = K_t i$$

The back emf  $e$  is proportional to the angular velocity of the shaft by a constant factor of  $K_b$

$$e = K_b \dot{\theta}$$

The back emf constant  $K_b$  and motor torque constant  $K_t$  are equal, therefore we will use  $K$  to represent both the motor torque and electromotive force constant.

Applying Newton's 2<sup>nd</sup> law and Kirchoff's voltage law.

$$\begin{aligned} J\ddot{\theta} + b\dot{\theta} &= Ki \\ L\frac{di}{dt} + Ri &= V - K\dot{\theta} \end{aligned}$$

## 5.10 Transfer Function

Applying the Laplace transform, we can express the equations in terms of Laplace variable  $s$ .

$$\begin{aligned} s(Js + b)\Theta(s) &= KI(s) \\ (Ls + R)I(s) &= V(s) - Ks\Theta(s) \end{aligned}$$

From the above equations we arrive at an open-loop transfer function by eliminating  $I(s)$ , where the input is voltage and output is rotational speed.

$$P(s) = \frac{\dot{\Theta}(s)}{V(s)} = \frac{K}{(Js + b)(Ls + R) + K^2} \quad \left[ \frac{\text{rad/sec}}{V} \right]$$

But we are more concerned about the position as the output, hence by integrating the speed we obtain position as the output; hence the transfer function has to be divided by  $s$ .

$$\frac{\Theta(s)}{V(s)} = \frac{K}{s((Js + b)(Ls + R) + K^2)} \quad \left[ \frac{\text{rad}}{V} \right]$$

```
P_motor =  
  
          0.004831  
-----  
6.302e-11 s^3 + 1.554e-06 s^2 + 2.441e-05 s  
Open-Loop time transfer function.  
  
sys_cl =  
  
          0.004831  
-----  
6.302e-11 s^3 + 1.554e-06 s^2 + 2.441e-05 s + 0.004831  
Closed loop transfer function.
```

## 5.11 Design Requirements

The objective of developing a control system is to have a stable and efficient control of the motor. The primary purpose is to serve the following requirements

- The required transient response is achieved
- Ensuring the steady state error as minimal as possible
- The stability of the system
- The response of the motor to the external disturbance is to be minimized

The simulation was carried out for a unit step input  $r(t)$ , with the output motor having following transient parameters in order for the motor position of the system to be very precise, achieving the final position in the least time.

- Settling time less than 40 milliseconds
- Overshoot less than 16%
- No steady-state error
- No steady state error due to a disturbance

## 5.12 Mathematical Modelling of Position feedback with PID controller

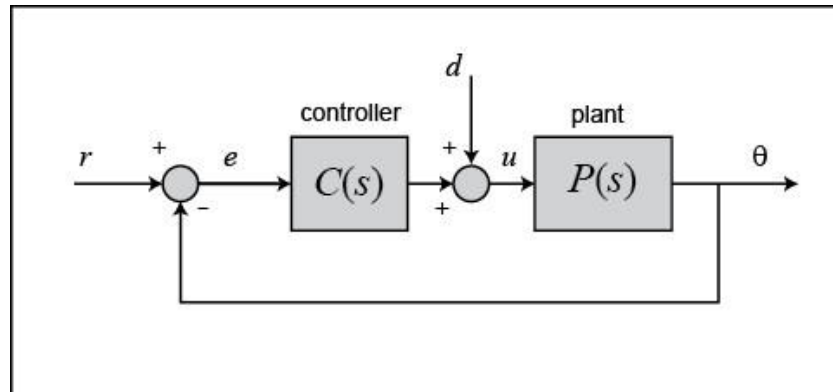


**Fig 5.2 Closed loop control system using a controller**

A DC servo motor can be controlled using a position feedback and the error can be compensated by using a PID controller involving proportional, integral and derivative actions as shown in Figure 5.2.

$$u(t) = K_p e(t) + K_i \int e(t) dt + K_d \frac{de}{dt}$$

$$K_p + \frac{K_i}{s} + K_d s = \frac{K_d s^2 + K_p s + K_i}{s}$$

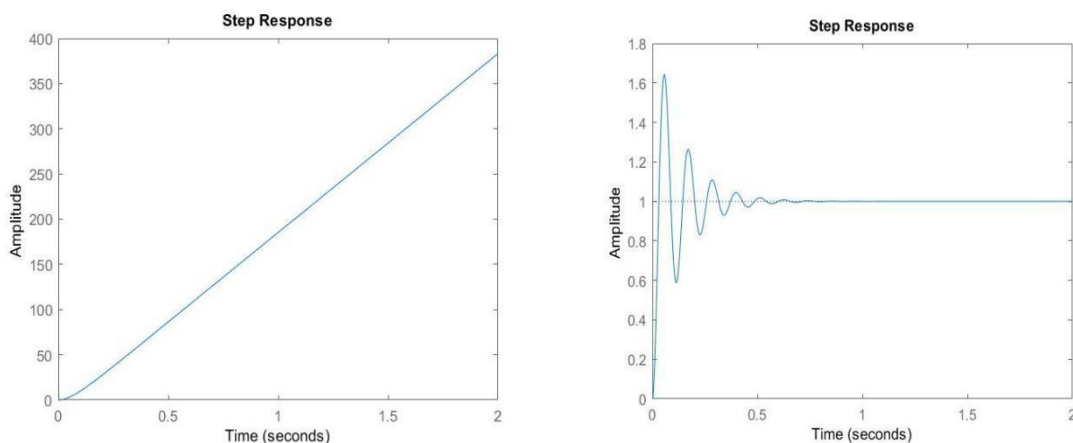


**Fig 5.3 The open loop response and closed loop response of the plant without the controller can be found out once we know the transfer function of the plant.**

It is clear from Fig 5.3 that the open loop response is not even stable, and analyzing the closed loop response, by adding a feedback the system has stabilized. So different controllers have been compared in order to reduce settle time, and to achieve zero steady state error in the presence of a step disturbance.

### 5.13 Proportional Control

Proportional action improves the response time and also reduces the steady-state error, but the value of overshoot increases as seen in Fig 5.4, which means the system becomes less stable. The transfer function of the motor is coupled with P controller along with unity feedback.

$$C = K_p = 0.168$$

$$T = \frac{0.0008121}{6.302e-11 s^3 + 1.554e-06 s^2 + 2.441e-05 s + 0.0008121}$$

```
Kp = 0.1681;
C = pid(Kp)
T = feedback(C*P_motor,1)
t = 0:0.01:2;
step(T,t)
```

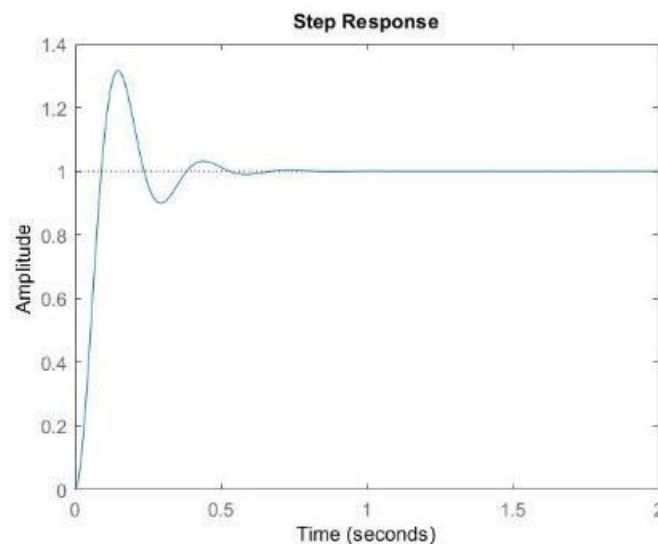


**Fig 5.4 Step response of a closed loop transfer using a Proportional Controller**

## 5.14 Proportional Derivative Control

Derivative control improves damping, similar to that of velocity feedback, making it more stable by basically having lesser overshoot as seen in Fig 5.5, while keeping the speed of response the same. But the disadvantage of having a derivative control is that it amplifies high-frequency noise and disturbances. Practical use of pure derivative control is not possible using analog hardware.

The transfer function of the motor is coupled with PD controller along with unity feedback.

$$C = K_p + K_d * s \quad \text{with } K_p = 0.168, K_d = 0.0093$$

$$T = \frac{4.491e-05 s + 0.0008121}{6.302e-11 s^3 + 1.554e-06 s^2 + 6.932e-05 s + 0.0008121}$$

```
Kp = 0.1681;
Kd = 0.009296;
C = pid(Kp,0,Kd)
T = feedback(C*P_motor,1);
stepinfo(T)
```

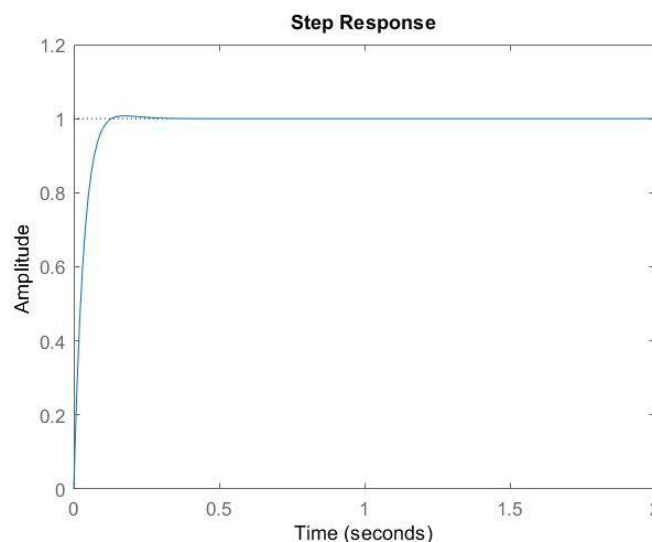


**Fig 5.5 Step response of a closed loop transfer using a Proportional Derivative Controller**

## 5.15 Proportional Integral Control

It is clear from Fig 5.6 that Integral control reduces the steady-state error, usually the error tends to zero, but at the same time it degrades the system's stability and the speed of response. The transfer function of the motor is coupled with PD controller along with unity feedback.

$$C = \frac{1}{K_p + K_i * \frac{1}{s}} \quad \text{with } K_p = 0.168, K_i = 0.676$$

$$T = \frac{0.0008121 s + 0.003266}{6.302e-11 s^4 + 1.554e-06 s^3 + 2.441e-05 s^2 + 0.0008121 s + 0.003266}$$

```
Kp = 0.1681;
Ki = 0.676;
C = pid(Kp,Ki)
T = feedback(C*P_motor,1)
t = 0:0.01:2;
step(T,t)
```

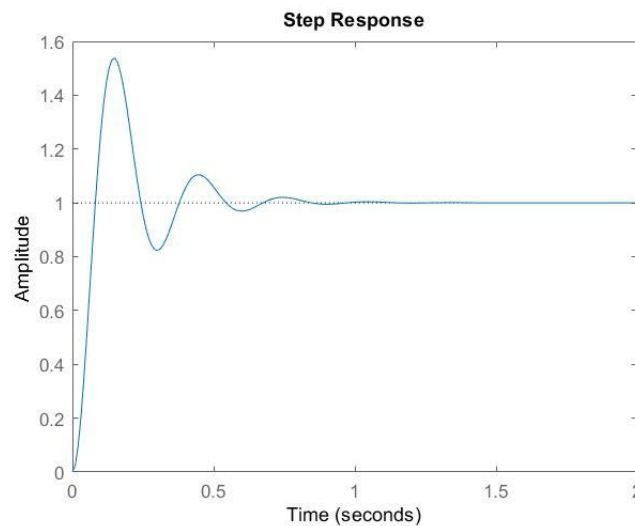


**Fig 5.6 Step response of a closed loop transfer using a Proportional Integral Controller**



## 5.16 Proportional Integral Derivative Control

PID control reduces the rise time, while tending to have a steady state error of zero. It also reduces the overshoot and settling time.

The transfer function of the motor is coupled with PID controller along with unity feedback.

$$C = K_p + K_i * \frac{1}{s} + K_d * s$$

with  $K_p = 0.168$ ,  $K_i = 0.676$ ,  $K_d = 0.0093$

$$T = \frac{4.491e-05 s^2 + 0.0008121 s + 0.003266}{6.302e-11 s^4 + 1.554e-06 s^3 + 6.932e-05 s^2 + 0.0008121 s + 0.003266}$$

```
Kp = 0.1681;
Ki = 0.676;
Kd = 0.009296;
C = pid(Kp,Ki,Kd)
T = feedback(C*P_motor,1)
t = 0:0.01:2;
step(T,t)
```

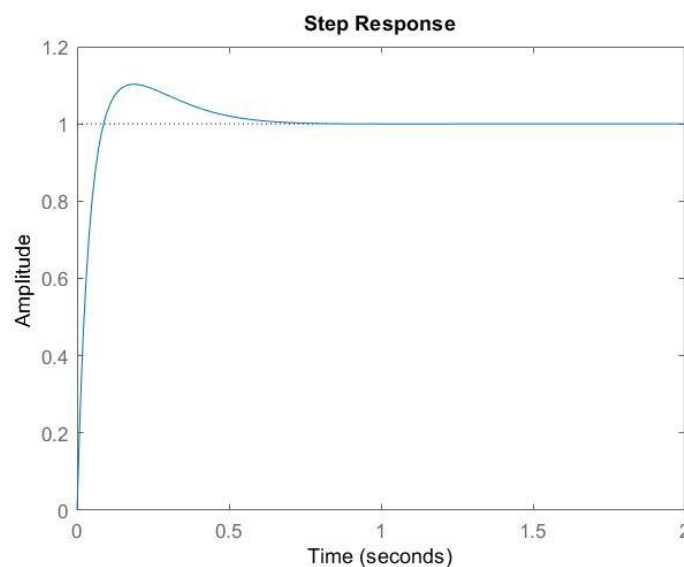


**Fig 5.7 Step response of a closed loop transfer using a Proportional Integral Derivative Controller**

## 5.17 Controller Selection

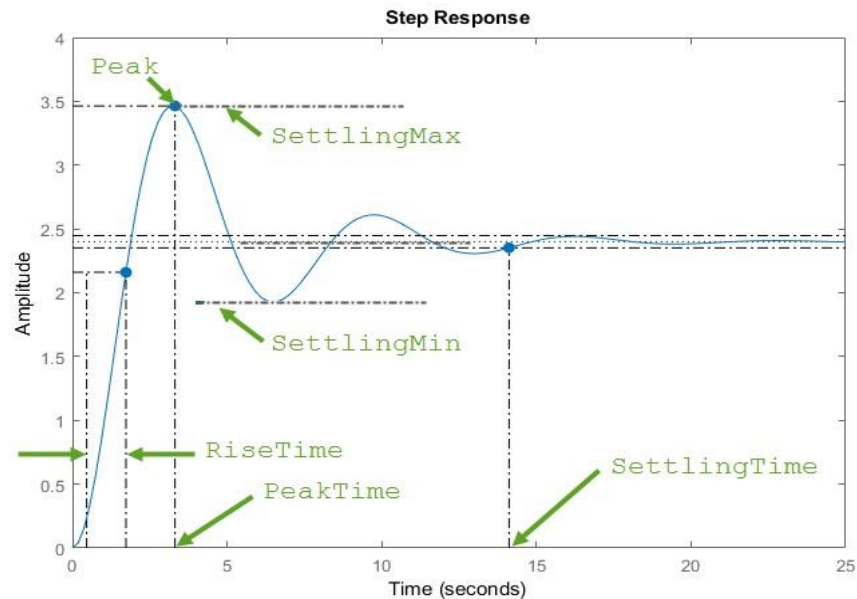


**Fig 5.8 Step Response of a general Transfer Function**

From Figure 5.8, the time taken for the response to rise from 10% to 90% of the steady-state response is the *Rise Time*. *Settling Time* is the time it takes for the error between the response and the steady-state response to reach with 2% of the steady-state response. The maximum amount by which the response overshoots the steady-state value, which being the first peak is called the *Overshoot* and is often written as a percentage of the steady-state value. The absolute maximum of the response is known as the *Peak* and the time taken to reach peak is *Peak Time*.

**Table 5.2 Comparison of types of controllers**

Performance	Motor with unity feedback	Motor with PD controller	Motor with PID controller
Rise Time	0.0209	0.0668	0.0601
Settling Time	0.4699	0.1046	0.5023
Settling Min	0.589	0.9063	0.9132
Settling Max	1.6414	1.0075	1.1025
Overshoot	64.1401	0.7472	10.2548
Undershoot	0	0	0
Peak	1.6414	1.0075	1.1025
Peak Time	0.0563	0.1732	0.1859

From the Table 5.2 it is clear that the system with a PD controller is better than any of the other controllers used namely P, PI, PID. The response of the motor without any controller was ruled out because of very high overshoot characteristics leading to high inaccuracies for position control. The response of the closed loop transfer function with the PD controller gave the result of a slightly higher rise time compared to PID control, but all other parameters were better in the case of a PD controller than a PID controller; hence a PD controller was used for a position feedback control.

### **5.18 Control of Servo motor**

The DC servo motor can achieve precise position control using Arduino along with a driver involving the PID calculations. The DC geared motor is connected with shaft of encoder, making it a closed loop; this encoder is connected with Arduino on interrupt pins. Then angle setpoints are sent to the Arduino and this runs the motor meanwhile the encoder sends the real time position feedback to Arduino as per the calculations done. So when the encoder pulse matches with the required position, the Arduino stops the DC motor at that position, and all of it is PID controlled meaning there is a smooth and a clean motion.

For our optical encoder there is fixed stepping of 1800 steps per rotation on output shaft, which means 1800 transition pulse for 360 degree revolution, so for a motion of 45 degree, the  $1800/360 \times 45 = 225$  pulse from encoder tells it to move 45 degrees, which means that the resolution of the optical encoder connected to output shaft is 0.2deg per pulse.

### **5.19 Voltage Regulation and Power Supply**

There are mainly three kinds of power supply

- Unregulated
- Linear Regulated
- Switching

Unregulated powers supply has its output voltage varying based on the main voltage. The linear regulated drops the main voltage to a much lesser one and further the rectifiers filter to make it a DC component.

The switching mode power supply deals with switching regulator to change the main input voltage to desired characteristics. Further the output can be of a regulated DC or an

unregulated AC as well. It has multiple insulated output ports. The efficiency of switching is so high making it more reliable when compared to other power supply. The unique feature that stands out in it is the inbuilt potentiometer which enables to control the required voltage at the output, thus making it a multipurpose power supply. The key reason to use switch mode power supply is that a controlled and a desired output can be obtained. Moreover, the circuit elements are well protected from any sort of disturbance.

## 5.20 Load cell

We have used a parallel beam load cell for measuring the grip strength.

This load cell is based on the wheatstone circuit.as shown in Fig 5.9. It has the following terminals

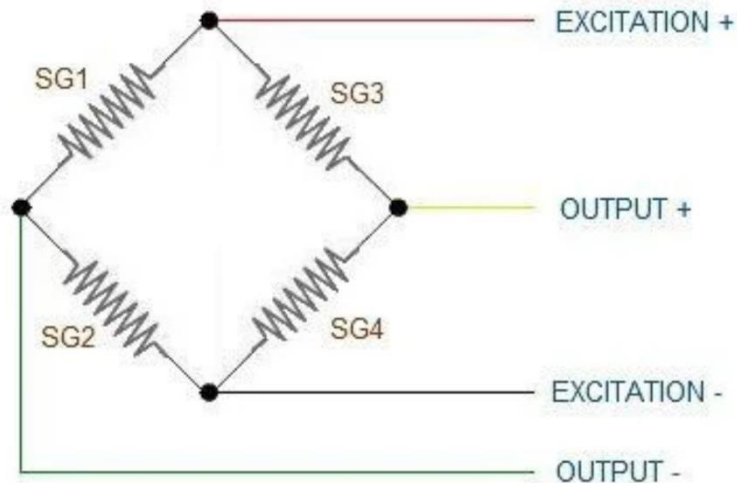


**Fig 5.9 Wheatstone Circuit**

E+ : Excitation+/VCC is red: E+

E- : Excitation-/ground is black: E-

A+ : Output+/Amplifier+ is yellow: A+

A- : Output-/Amplifier- is green

The reliability of the arrangement is contingent on how loads are applied on it. The load cell is provided 4 mounting holes, two on each end. Testing of a cell is done in perfect conditions.

Ideally, the application of load must be such that the one end is fixed on a rigid support. Then, the other end is loaded through the mounting holes. The direction of the load must be perpendicular such that it is in pure bending as shown in Figure 5.10.

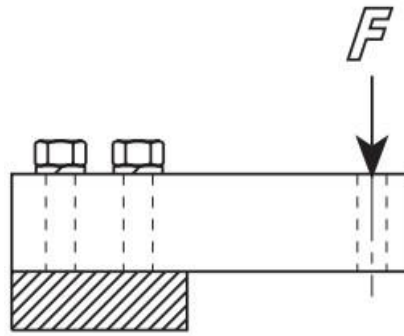


**Fig 5.10 Loading Condition of load cell**

Even after calibration (see next section), load cells might give erroneous results due to incorrect loading conditions. These can be categorized as follows:

- **Angular loading:** In this type of loading, a force is applied on the load cell through the holes provided for loading. However, they are applied at an angle to the axis of cell. This results in splitting of total load into horizontal and vertical components. The vertical component is the only component to which the load cell will respond, as it puts the beam in pure bending. The horizontal component has no effect on the load cell reading, hence decreasing the intensity.
- **Eccentric loading:** In this loading, although the load is vertical, it is at an offset to the mounting hole. However, if the loading point is constant along the load cell and does not alter every time, then calibrating the load cell with such loading effectively compensates for this error. But if there is horizontal translation of the load, a non linearity is induced. There are also chances of retention of effects of loading. Therefore, it leads to erroneous results.

This assembly puts the load cell in cantilever loading condition which would give most accurate readings, which can be seen in Fig 5.11.

The electrical resistance is changed as loads are applied on the load cell. However, for this change to be recorded, there is a requirement of amplification of this signal. For this purpose, an HX711 module is used. HX711 is a 24 bit analog-to-digital converter which amplifies the signal, which is sent to the microcontroller.

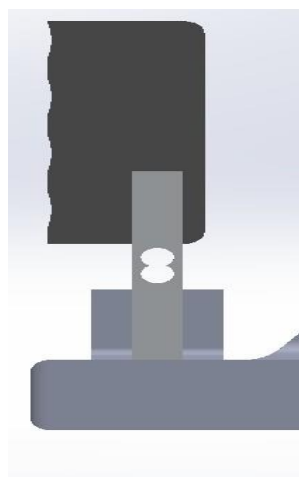


**Fig 5.11 CAD model of load cell**

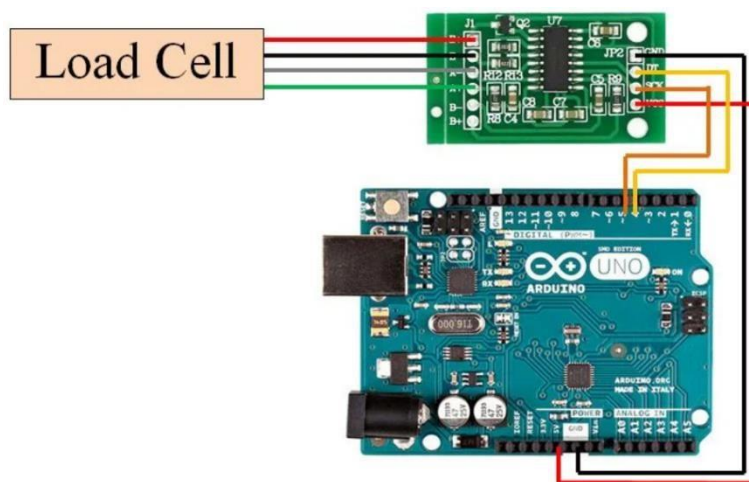


**Fig 5.12 Load Cell Interface with Arduino**

The interfacing with Arduino Uno with HX711 amplifier is shown in Fig 5.12. The HX711 module can be powered with a 2.7V - 5V source. Hence, the Arduino Uno can be used for this purpose and is used to obtain the grip strength values from the Communication with the HX711 module can be established with the help of a driver. It is installed in the system and added to the existing libraries. Calibration of the load cell is performed to scale the inputs to Arduino in terms of force (N). For this, we required a number of known weights which are used for adjusting the calibration factor. The methodology for calibration is as follows:

Calibration factor is increased in steps of 10 till readings are in the tolerable limit of actual values. This is an iterative process as shown in the flow chart, Fig 5.13.

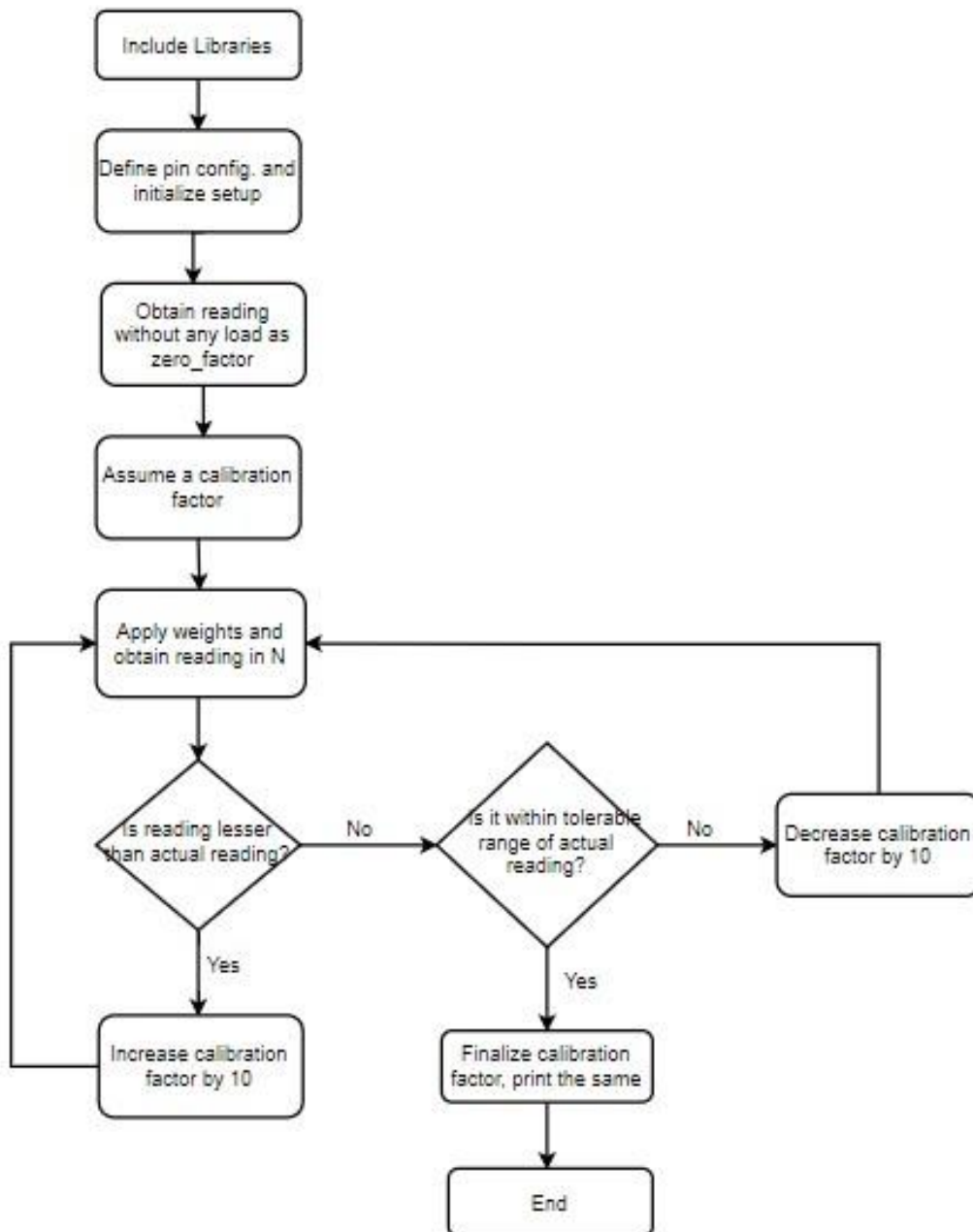


**Fig 5.13 Calibration Flow chart**

## ***CHAPTER-6***

### ***IMPLEMENTATION OF MACHINE LEARNING***



## CHAPTER 6

### Implementation of Machine Learning

Diagnosis of a patient in medical science is a type of classification. Another look at the process of diagnosis reveals how befitting it is to machine learning implementation. Patients undergoing a test give out the test report to the physician(model) and the patient is classified as healthy or impaired (to what extent). The rehabilitation of wrist for patients post-CVA or post-surgery involves repetitive exercises to recover the adequate wrist action for activities of daily living. Execution of these is critical to ensure a positive recovery, which could otherwise lead to no effect- or worse- even detrimental. The advantages of a self operated device are three fold: (1) Useful in cases of inaccessibility (2) Continuous monitoring and feedback (3) Adaptive difficulty based on performance

#### 6.1 Stages in applying machine learning

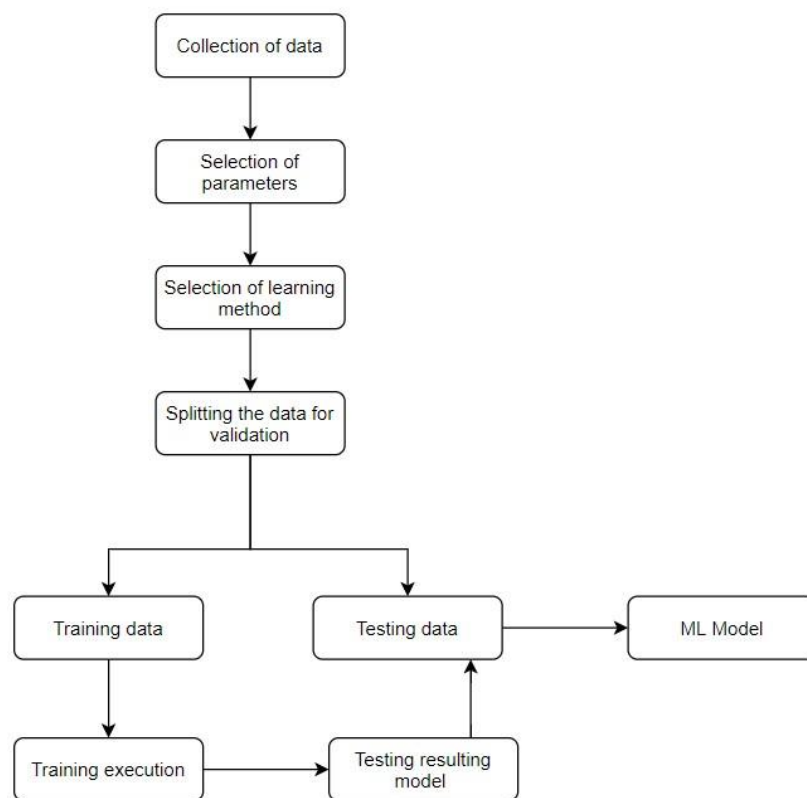


**Fig 6.1 Flow diagram for machine learning**

Fig 6.1 depicts the stages of creating and training a machine learning model. This is explained in detail in the following subsections.

### **6.1.1 Collection of data:**

Accurate diagnosis is subject to selection of collection of data set from both healthy and impaired individuals, comprising of various parameters. The size of data set helps in developing a more robust model, and thus be more reliable. Allgower & Hermsdorfer [30] recorded various factors, and studied nine parameters in 22 patients for their fine motor skills, and concluded that the grip force scaling, speed of motion, and motor coordination were the three major factors to help differentiate between healthy and impaired individuals.

Our experimental setup consists of components that will give the observations when put to use. The strain gauge provides the grip force values. The handle grip at the end of torque arm is rotated by the individual end-to-end. Being connected to servo motor, the encoder readings are recorded for determining Range Of Motion (ROM). Encoder readings in continuous motion are used to determine the speed of motion. In the diagnosis stage, a marker is moved randomly and the user tries to coordinate his/her hand movement with the marker. These accuracy with which this is done (error) is also recorded. Thus we have:

- Range of Motion
- Speed of motion
- Motor coordination parameter (MSE of error)

These data then become the differentiating measure between healthy and impaired individuals.

### **6.1.2 Selection of parameters**

Flexion and extension refer to the movement of the wrist in sagittal plane. Radial and Ulnar deviation are movements of wrist in the frontal plane. The maximum values for these parameters achievable by an individual is of importance. Also, a person might only be able to move the wrist by a certain amount by himself/herself, but this reading can also be increased if he/she is supported externally. These values correspond to the active (unassisted) and passive (assisted) readings of the motion. Moreover, side of dominant hand and age are also an important factor.

### 6.1.3 Selection of learning method:

Machine learning algorithms are broadly classified into the following paradigms:

- Supervised learning
- Unsupervised learning
- Reinforcement learning

The task of determining the condition of a person based on various input features is an example of classification. The features and the feature type are as follows:

1. Age: Continuous variable
2. Range of motion in sagittal plane (flexion range+ extension range): Continuous variable
3. Range of motion in frontal plane (radial deviation range + ulnar deviation range): Continuous variable
4. Dominant side: Categorical variable
5. Gender: Categorical variable

Here, the output of a system would be binary- Healthy or Impaired.

There are the following algorithms that work best for binary classification consisting of combination of continuous and categorical variables:

- a. Logistic regression
- b. K-nearest neighbour
- c. Support Vector Machine
- d. Decision Tree

### 6.1.4 Selection of training data and test data:

The entire data set is not used for training. Instead a part of it is kept for testing the learned model and validating the model. This can be performed by simply dividing data set into training set and testing set. However, this resulted in variation in the model accuracy. Thus, the problem can be solved using a technique called cross validation, in which the input data

set is divided into 'k' equal folds, or parts, and the training is iteratively given to the model such with k-1 folds and one is held back for testing, such that each fold has been used for testing once. Fig 6.2 shows 5-fold cross validation with a different portion of data set being used as test data in every iteration.



**Fig 6.2 Representation of K-fold cross validation with k=5**

### 6.1.5 Evaluation

To give an objective evaluation of the learning model, the metric most commonly used is the accuracy of classification. This is expressed as a percentage:

$$\text{Accuracy} = \frac{\text{No. Of correct classification}}{\text{No. Of total classifications}} * 100\%$$

No. Of total classifications

When the number of classes is imbalanced, the accuracy might not give a complete representation of the classifier ability. In such cases, TPR, True Positive Rate is another measure which evaluates the percentage of the correctly classified inputs:

$$\text{TPR} = \frac{\text{Total no. Of correct positive classifications}}{\text{Total no. Of positives in output}} * 100\%$$

Total no. Of positives in output

## 6.2 Data preparation and preprocessing

In the data set, it is important to consider the number of features and the samples available for training. In our data set, we had 11 variables in which six were angle- of range-of-motion terms. Greater number of features poses the following problems:

- a) A greater number of data samples are required to accurately capture the structure of the input space.
- b) The greater the number of features, greater is the risk of over-fitting, which means that the model essentially memorizes the input samples rather than capturing the structure in the data. This can lead to poor generalization on unseen data.
- c) It can lead to capturing the noise in the data.

To avoid these, the dimensionality of the data set can be reduced by merging dependent variables together. In complex cases, algorithms like PCA can be used to obtain principal components of data through merging them in a linear manner.

For the problem consisting of Active/Passive flexion and extension, a better representation is the total range of the flexion/extension motion. Thus, the two variables are simply added to generate a new variable.

$$S\_flex\_ext = \max(\text{flexion}) + \max(\text{extension})$$

Similarly, the range of motion of the radial and ulnar deviation in the frontal plane is determined as:  $S\_rad\_ulnar = \max(\text{radial}) + \max(\text{ulnar})$

We thus reduce the dimensionality of the problem to 5.

Now, the input features are:

Age is in range {11,76}

$S\_flex\_ext$  is in range {131,313}

$S\_rad\_ulnar$  is in range {70, 170}

Dominant\_hand is in [0,1]

Gender is in [0,1]

The disproportionate values of the range of features could lead to a slower convergence and affect the stability of the model. To counter these, the input features are normalized.

$$\hat{X}[:, i] = \frac{X[:, i] - \min(X[:, i])}{\max(X[:, i]) - \min(X[:, i])}$$

(Min-Max normalization)

$$\hat{X}[:, i] = \frac{X[:, i] - \mu_i}{\sigma_i}$$

(Z-normalization)

### 6.3 Logistic regression

The logistic regression takes an input in the form of independent variables and calculates the probability of the input lying in a particular class.

It uses the logistic function to predict the output binary variable:

$$\phi(z) = \frac{1}{1 + e^{-z}}$$

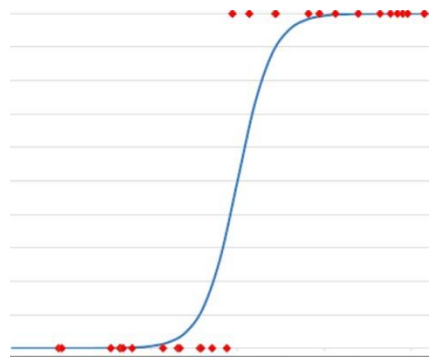


**Fig 6.3 Logistic regression curve**

The Fig 6.3 represents the logistic regression curve in blue. The data points it aims to fit are shown in red. Here, the x-axis is the input value, and the y-axis are their respective classes (here 0 or 1). The curve has a steep slope in the middle portion which gives the probability of an input (x-axis value) lying in class 0 or class 1 (y-axis value).

Model-fitting:

The model is parameterized with the function

$$h_{\theta}(x) = g(\theta^T x)$$

where

$$z = \theta^T x$$

The evaluation of the model parameter  $\theta$  is often done by solving an optimization problem. The cost of a linear regression model is given by:

$$J(\theta) = -\frac{1}{m} \sum_{i=1}^m [y^{(i)} \log(h_{\theta}(x^{(i)})) + (1 - y^{(i)}) \log(1 - h_{\theta}(x^{(i)}))]$$

Where  $y(I)$ 's represents actual output of training set, and  $x(I)$ 's the training input.

Optimization can be done using a gradient descent algorithm. Minimizing the cost function gives

$$\begin{array}{l} \text{Iterate until convergence} \\ \{ \\ \theta_j = \theta_j - \alpha(h_{\theta}(x) - y) x \\ \} \end{array}$$

Visualizing the decision boundary:

A threshold is utilized to assign discrete values in the output. This threshold is suitably adjusted to achieve desired accuracy. If we assume a threshold of 0.5, then the decision hyperplane can be plotted as

$$\begin{array}{l} \theta^T x \geq 0 \Rightarrow y = 1 \\ \theta^T x < 0 \Rightarrow y = 0 \end{array}$$

When the training and testing data was provided using a 6-fold cross validation, the accuracy of the model varied as follows:

```
1st fold:
predicted: [0. 1. 1. 0. 0. 1. 0. 0. 1. 1. 0.]
actual:    [1. 1. 1. 0. 0. 1. 0. 0. 1. 1. 0.]
Errors: 1
Accuracy: 90.9090909090909%

2nd fold:
predicted: [0. 1. 1. 0. 0. 1. 1. 0. 1. 0. 0.]
actual:    [0. 0. 0. 0. 1. 0. 1. 0. 1. 0. 0.]
Errors: 4
Accuracy: 63.6363636363636%

3rd fold:
predicted: [0. 0. 0. 0. 1. 0. 1. 0. 0. 1. 0.]
actual:    [0. 0. 0. 0. 1. 0. 1. 0. 0. 1. 0.]
Errors: 0
Accuracy: 100.0%

4th fold:
predicted: [0. 0. 0. 0. 0. 0. 1. 0. 0. 0. 1.]
actual:    [0. 0. 0. 0. 0. 0. 1. 0. 0. 1. 1.]
Errors: 1
Accuracy: 90.9090909090909%

5th fold:
predicted: [0. 0. 1. 0. 0. 0. 1. 0. 0. 1. 1.]
actual:    [0. 0. 1. 0. 0. 0. 1. 0. 0. 1. 1.]
Errors: 0
Accuracy: 100.0%

6th fold:
predicted: [0. 1. 1. 1. 0. 0. 1. 1. 0. 1. 0.]
actual:    [1. 1. 1. 1. 0. 1. 1. 1. 0. 1. 0.]
Errors: 2
Accuracy: 81.8181818181818%
>>>
```

---

**Fig 6.4 Output of MATLAB implementation of Logistic regression in 6 fold**

Fig 6.4 is the output when logistic regression was implemented in MATLAB. Due to shortage of data, a 6-fold cross validation is applied on the data set. Prediction accuracy ranges from 63% to 100%, which is a significant interval. Confusion matrix along with various other metrics are calculated in Chapter 8.

$$\begin{aligned}\text{Average accuracy} &= (90.9 + 63.63 + 100 + 90.9 + 100 + 81.81) / 6 \\ &= 87.87 \%\end{aligned}$$



## 6.4 Support Vector Machine

In logistic regression, binary classification takes place by the decision hyperplane in the  $n$ -dimensional (here,  $n=6$ ) feature space. This classification is tested for accuracy using only the existing data set. Inputs with features very close to the decision hyperplane might still be classified, but these kinds of inputs might pose a risk of misclassification as there lies a possibility of the decision hyperplane being generated such that it passes very close to training sets. This is shown in Fig 6.5, with the purple and green being different classes.

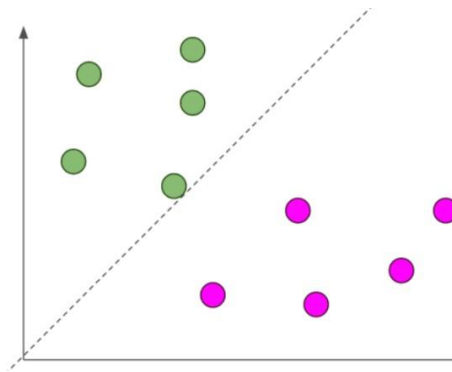


**Fig 6.5 Problems in logistic regression, decision**

Since patient\_input feature space has 6-features and 66 samples, plotting the decision plane situations like these is not as effective. The decision hyperplane might not space well enough from the classes, posing a risk of a generalization error for inputs lying close to the decision boundary.

Thus, the problem is, how do we choose a decision boundary among the many options that can be plotted separating the two classes, or simply put, the best segregating boundary.

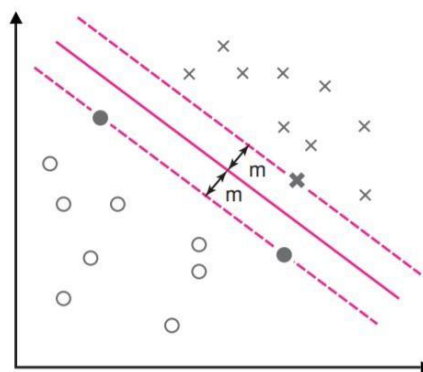


**Fig 6.6 SVM boundary shown with support**

Support Vector Machines separates the classes using a decision boundary with maximum margin. Fig 6.6 represents the decision boundary which can most accurately classify the two classes. It uses support vectors, that are the samples nearest to the boundary, from either class and finds the maximum distance between them, called the margin. This does work well for a linearly separable data. However, SVMs work well with nonlinear data as well using the 'kernel-trick'. The kernel trick basically maps the data into another higher dimension space where the data is linearly separable.

Commonly used kernel functions are:

Radial Basis Function (RBF) Kernel:

$$k(\mathbf{x}, \mathbf{z}) = \exp[-\gamma \|\mathbf{x} - \mathbf{z}\|^2]$$

Polynomial Kernel (of degree  $d$ ):

$$k(\mathbf{x}, \mathbf{z}) = (\mathbf{x}^\top \mathbf{z})^d \quad \text{or} \quad (1 + \mathbf{x}^\top \mathbf{z})^d$$

Training samples in the data set= 66

Number of features= 6

In implementing SVM, the following are parameters that are varied and results compared:

1. Kernel type: RBF, Linear, Polynomial, sigmoid kernels are used.
2. Gamma: this value denotes the spread of the given kernel. A low value denotes a low-curvature boundary. A high gamma value might cause the decision boundary to form 'islands' around the input class, effectively overfitting the data.
3. Random\_state: this is the seed to a random generating function so that data is reproducible.
4. Max\_iters: it is the maximum iterations for converging, optional.

Implementation of the model was done on Python and validation was done using 6-fold validation. Results are as follows:

```
1st fold:
predicted: [0. 0. 0. 0. 0. 1. 0. 0. 1. 1. 0.]
actual:    [1. 1. 1. 0. 0. 1. 0. 0. 1. 1. 0.]
Errors: 3
Accuracy: 72.72727272727273%

2nd fold:
predicted: [1. 0. 1. 0. 1. 1. 1. 0. 1. 0. 0.]
actual:    [0. 0. 0. 0. 1. 0. 1. 0. 1. 0. 0.]
Errors: 3
Accuracy: 72.72727272727273%

3rd fold:
predicted: [0. 0. 0. 0. 1. 0. 1. 0. 0. 1. 0.]
actual:    [0. 0. 0. 0. 1. 0. 1. 0. 0. 1. 0.]
Errors: 0
Accuracy: 100.0%

4th fold:
predicted: [0. 0. 0. 0. 0. 0. 0. 0. 0. 0. 1.]
actual:    [0. 0. 0. 0. 0. 0. 1. 0. 0. 1. 1.]
Errors: 2
Accuracy: 81.81818181818181%

5th fold:
predicted: [0. 0. 1. 0. 0. 0. 1. 0. 0. 1. 0.]
actual:    [0. 0. 1. 0. 0. 0. 1. 0. 0. 1. 1.]
Errors: 1
Accuracy: 90.9090909090909%

6th fold:
predicted: [0. 0. 1. 1. 0. 0. 1. 0. 0. 1. 0.]
actual:    [1. 1. 1. 1. 0. 1. 1. 1. 0. 1. 0.]
Errors: 4
Accuracy: 63.63636363636363%
```

**Fig 6.7: Results of Python implementation of SVM using RBF kernel**

The SVM implementation yields results as shown in Fig 6.7. As the accuracy is varying across the 6 folds due to the unequal numbers of class distribution within each fold, further metrics are evaluated to assess the model using the confusion matrix in Chapter 8.

Average accuracy of model across the 6 folds = 80.29 %

## 6.5 K- Nearest Neighbours

This is a simple yet effective technique of classification and finds application in areas such as data mining and pattern recognition. It is based on the idea that similar classes lie close to each other, i.e. like groups form clusters or are in proximity. Plotting data of a classification, in fact, does corroborate this intuition.

The algorithm is a supervised one and is non-parametric, which means that there are no variables being assumed to be in a certain range or distribution. The factor that has to be selected is 'k'. It is the number of samples the model considers closest to test data for classification.

Implementation of this method is very quick, as it is a query-time calculation. This means the model is fed the training inputs along with the label and it simply stores it by representing them as their respective classes. When unseen, test data is queried, the model looks in the neighbourhood of the test input. It then calculates distance of the test input with samples in its neighbourhood and records their classes in ascending order of their distance from test input. The distance can be quantified according to the problem. In our case we have considered Euclidean Distance. In a classification task, the test input is allotted the same class as the mode of the first 'k' nearest samples in the neighbourhood.

Selection of value of k: A small value for k could lead to mis-classification due to noise present in the data. However, a data set in a higher dimensional feature space increases the complexity for a high value of k, hence increasing computation time. Generally, k values are taken as odd to avoid draw situation. A convention states that  $k = \text{Sqrt}(\text{features})$ .

For our data set, we have 6 features, and thus take  $k=3$ , to avoid situation of draw case.

```

1st fold:
  0   1   1   0   0   1   0   0   1   1   0
  1   1   1   0   0   1   0   0   1   1   0

Number of misclassifications: 1
Accuracy: 90.909091
2nd fold:
  1   0   0   0   1   1   1   0   1   0   0
  0   0   0   0   1   0   1   0   1   0   0

Number of misclassifications: 2
Accuracy: 81.818182
3rd fold:
  0   0   0   0   1   0   1   0   0   1   0
  0   0   0   0   1   0   1   0   0   1   0

Number of misclassifications: 0
Accuracy: 100.000000
4th fold:
  0   0   0   0   0   0   1   0   0   0   1
  0   0   0   0   0   0   1   0   0   1   1

Number of misclassifications: 1
Accuracy: 90.909091
5th fold:
  0   0   1   0   0   0   1   0   0   1   1
  0   0   1   0   0   0   1   0   0   1   1

Number of misclassifications: 0
Accuracy: 100.000000
6th fold:
  0   1   1   1   0   0   1   1   0   1   0
  1   1   1   1   0   1   1   1   0   1   0

Number of misclassifications: 2
Accuracy: 81.818182
>> |

```

**Fig 6.8: Results of MATLAB implementation of KNN with k=3 with 6-fold cross validation**

When the number of nearest neighbours are chosen as 3 for assigning labels, the classification results over 6 folds are shown in Fig 6.8.

Average accuracy over 6 folds = 90.90 %

## 6.6 Decision Trees

Decision trees are models which predict the class of inputs based on the truth of certain conditions in a serial order. The conditions are based on features of the model, evaluated one feature at a time. Because of its ordered structure, it is very easy to interpret the working of the model.

Fig 6.9 shows a simple decision tree structure with two features used for overall classification of inputs. Here, the features x1 and x2 of samples are evaluated one-by-one. Any input is

classified after a complete traversal of the structure top to bottom, hence reaching what is called the leaf node.

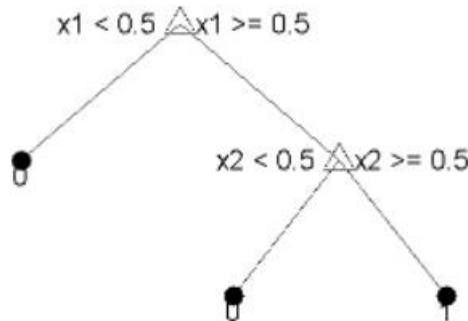


**Fig 6.9: Decision tree with x1,x2 attributes**

The depth of the structure represents the number of checks to be performed for classification. A shallow model might not accurately classify test data due to the lack of specificity because of less condition checks. However, a deeper tree containing both continuous and categorical data might lead to the model getting too specific in the ranges of continuous data, hence overfitting. Setting a maximum depth is an alternative but it might lead to bias.

Generation of the tree structure involves finding the order in which conditions are checked. The algorithm used is the ID3 (Iterative Dichotomiser 3). This algorithm tries to determine the attribute that should be checked at each node to classify the samples usefully.

- A parameter called ‘Information Gain’ helps us give a measure of the best classifying attribute.

Entropy of a sample  $S$  is given by

$\sum_{i=1}^c -p_i \log_2 p_i$ , where  $p_i$  is the fraction of samples in that class,  $i$  denotes the different classes in the sample. As the node is traversed, classification causes the resultant classes to become subsets.

- Information gain is given by:

$$Gain(S, A) \equiv Entropy(S) - \sum_{v \in Values(A)} \frac{|S_v|}{|S|} Entropy(S_v)$$

V represents the different attribute values in the set at hand.

Information gain values are found for all attributes of the data set S.

- The attribute which gives highest information gain is chosen as the classifying attribute.
- Once this is done, the process is repeated for each classified subset till every samples in the subset belongs to same classes, or there are no more samples left.

Categorical data such as Dominant\_hand, Gender can be easily used with ID3. The algorithm also classifies attributes which are continuous like Age and Range\_of\_motions.

Considering the 'Age' attribute, some values are [13, 15,19,21,25,28]

ID3 creates thresholds which partitions the data attribute such that they are transformed into categorical data again. This is done by sorting the attribute values and selecting adjacent values that belong to different classes, and create candidate thresholds lying between them. Selection of best threshold is done so that the information gain is maximum.

In attribute 'Age', if 15 and 19 belong to different classes, then  $(15+19)/2$ , I.e. 17 is a candidate threshold.

```
1st fold:
predicted: [0. 1. 1. 0. 0. 1. 0. 0. 1. 1. 0.]
actual:    [1. 1. 1. 0. 0. 1. 0. 0. 1. 1. 0.]
Errors: 1
Accuracy: 90.9090909090909%

2nd fold:
predicted: [0. 0. 0. 0. 1. 1. 1. 0. 1. 0. 0.]
actual:    [0. 0. 0. 0. 1. 0. 1. 0. 1. 0. 0.]
Errors: 1
Accuracy: 90.9090909090909%

3rd fold:
predicted: [0. 0. 0. 0. 1. 0. 1. 0. 0. 1. 0.]
actual:    [0. 0. 0. 0. 1. 0. 1. 0. 0. 1. 0.]
Errors: 0
Accuracy: 100.0%

4th fold:
predicted: [0. 0. 0. 0. 0. 0. 1. 0. 0. 0. 1.]
actual:    [0. 0. 0. 0. 0. 0. 1. 0. 0. 1. 1.]
Errors: 1
Accuracy: 90.9090909090909%

5th fold:
predicted: [0. 0. 1. 0. 0. 0. 1. 0. 0. 1. 1.]
actual:    [0. 0. 1. 0. 0. 0. 1. 0. 0. 1. 1.]
Errors: 0
Accuracy: 100.0%

6th fold:
predicted: [0. 1. 1. 1. 0. 0. 1. 1. 0. 1. 0.]
actual:    [1. 1. 1. 1. 0. 1. 1. 1. 0. 1. 0.]
Errors: 2
Accuracy: 81.81818181818181%
```

**Fig 6.10 Results of ID3 algorithm  
implementation**

An implementation of decision trees using ID3 algorithm is done on Python and the results are shown as in Fig 6.10.

Average accuracy over the 6 folds = 92.41 %



## ***CHAPTER-7***

### ***FINITE ELEMENT SIMULATION***

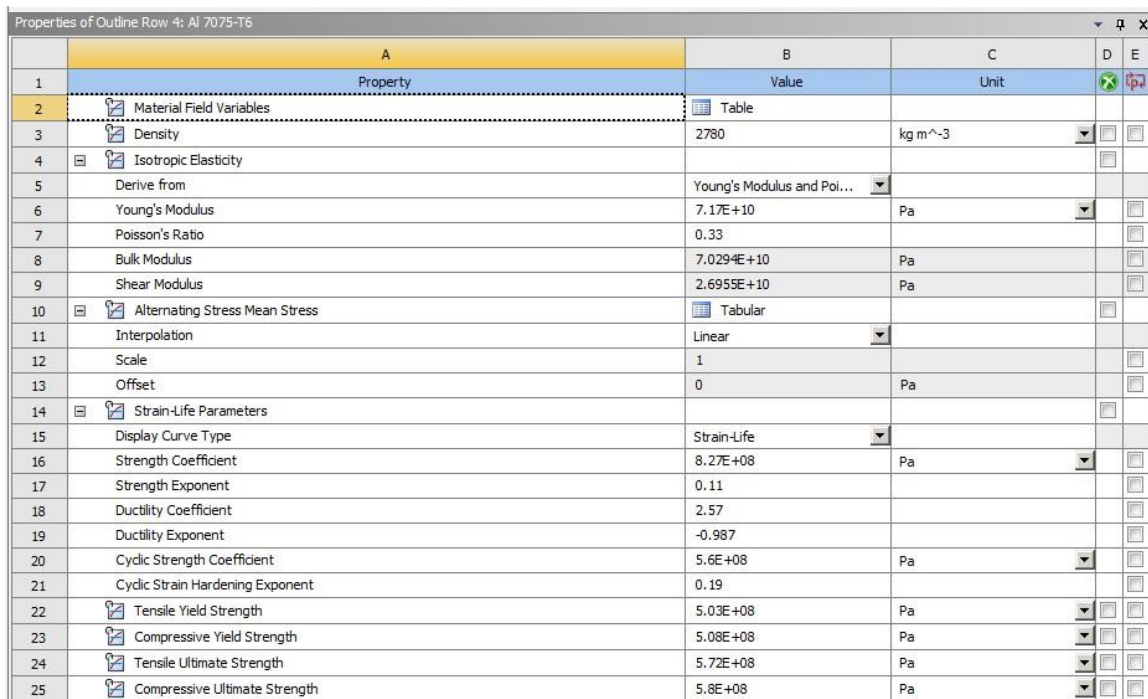
## CHAPTER 7

### FINITE ELEMENT SIMULATION

ANSYS Workbench was chosen to perform the FEA, to create mesh and perform analysis on the component in ANSYS Mechanical because of its easier user interface for simple mesh generation and its unique global acceleration loading option. It is possible to simulate complex materials and material behavior using the built-in models.

#### 7.1 Material Specifications

ANSYS Workbench has a range of material models involving everything from hyperelastics, shape memory alloys, to metallic structures which are accurately modelled. Ansys is also capable of adding a user-defined material model into the problem. For our design, the material used is Aluminium 7075 T6 and Acrylonitrile Butadiene Styrene (ABS). The material data is inputted to material library of ANSYS and a custom material model for each material is created as shown in Fig 7.1 and Fig 7.2 respectively.



	A	B	C	D	E
1	Property	Value	Unit		
2	Material Field Variables	Table			
3	Density	2780	kg m <sup>-3</sup>		
4	Isotropic Elasticity				
5	Derive from	Young's Modulus and Poi...			
6	Young's Modulus	7.17E+10	Pa		
7	Poisson's Ratio	0.33			
8	Bulk Modulus	7.0294E+10	Pa		
9	Shear Modulus	2.6955E+10	Pa		
10	Alternating Stress Mean Stress	Tabular			
11	Interpolation	Linear			
12	Scale	1			
13	Offset	0	Pa		
14	Strain-Life Parameters				
15	Display Curve Type	Strain-Life			
16	Strength Coefficient	8.27E+08	Pa		
17	Strength Exponent	0.11			
18	Ductility Coefficient	2.57			
19	Ductility Exponent	-0.987			
20	Cyclic Strength Coefficient	5.6E+08	Pa		
21	Cyclic Strain Hardening Exponent	0.19			
22	Tensile Yield Strength	5.03E+08	Pa		
23	Compressive Yield Strength	5.08E+08	Pa		
24	Tensile Ultimate Strength	5.72E+08	Pa		
25	Compressive Ultimate Strength	5.8E+08	Pa		

**Fig 7.2 Material data of Aluminium 6061-T6**

Properties of Outline Row 3: ABS				
	A	B	C	D E
1	Property	Value	Unit	
2	Material Field Variables	Table		
3	Density	1040	kg m <sup>-3</sup>	
4	Isotropic Elasticity			
5	Derive from	Young's Modulus and Poi...		
6	Young's Modulus	2.39E+09	Pa	
7	Poisson's Ratio	0.399		
8	Bulk Modulus	3.9439E+09	Pa	
9	Shear Modulus	8.5418E+08	Pa	
10	Tensile Yield Strength	4.14E+07	Pa	
11	Compressive Yield Strength	6.5E+07	Pa	
12	Tensile Ultimate Strength	4.43E+07	Pa	
13	Compressive Ultimate Strength	6.5E+07	Pa	

**Fig 7.1 Material data of Acrylonitrile Butadiene Styrene (ABS)**

## 7.2 Meshing Process

### 7.2.1 Specify global mesh settings

In ANSYS Mechanical interface meshing is done by specifying the global mesh setting, in which element size, sizing function, smoothing, transition, defeature size is defined using minimal inputs as specified in Fig 7.3. This meshing automatically calculates global element sizes based on the smallest geometric entity. For regions involving curvatures and proximity of surfaces advanced size functions are use.

Defaults	
Physics Preference	Mechanical
Relevance	0
Element Order	Program Controlled
Sizing	
Size Function	Adaptive
Relevance Center	Coarse
Element Size	2.0 mm
Initial Size Seed	Assembly
Transition	Fast
Span Angle Center	Coarse
Automatic Mesh Based Defeaturing	On
Defeature Size	Default
Minimum Edge Length	0.331680 mm

**Fig 7.3 Global Mesh Settings**

### 7.2.2 Insert local mesh settings

Local mesh setting is used to select the type of mesh over a specific part and to refine it further. Using local settings, we were able to generate a HEX-Dominant mesh, and improved the quality of mesh by reducing the number of elements and nodes as specified in Fig 7.4.

Object Name	Face Meshing	Face Meshing 3	Hex Dominant Method	Body Sizing	Hex Dominant Method 2
State	Fully Defined				
Scope					
Scoping Method	Named Selection	Geometry Selection			
Named Selection	Holes				
Geometry		4 Faces	2 Bodies	1 Body	
Definition					
Suppressed	No				
Mapped Mesh	Yes				
Constrain Boundary	No				
Method		Hex Dominant		Hex Dominant	
Element Order		Use Global Setting		Use Global Setting	
Free Face Mesh Type		Quad/Tri		Quad/Tri	
Control Messages		No		No	
Type				Element Size	
Element Size				Default (13.73 mm)	

Fig 7.4 Local Mesh Settings

### 7.2.3 Preview and generate mesh

The mesh is generated and preview is displayed in Fig 7.5. It also displays the mesh quality using different mesh metrics like Element quality, Jacobian, Skewness, Warping factor and Aspect ratio. Once the mesh is generated the number of nodes and elements is displayed as shown in Table 7.1.

Table 7.1 Statistics of the Mesh

Statistics	
Nodes	498520
Elements	134600

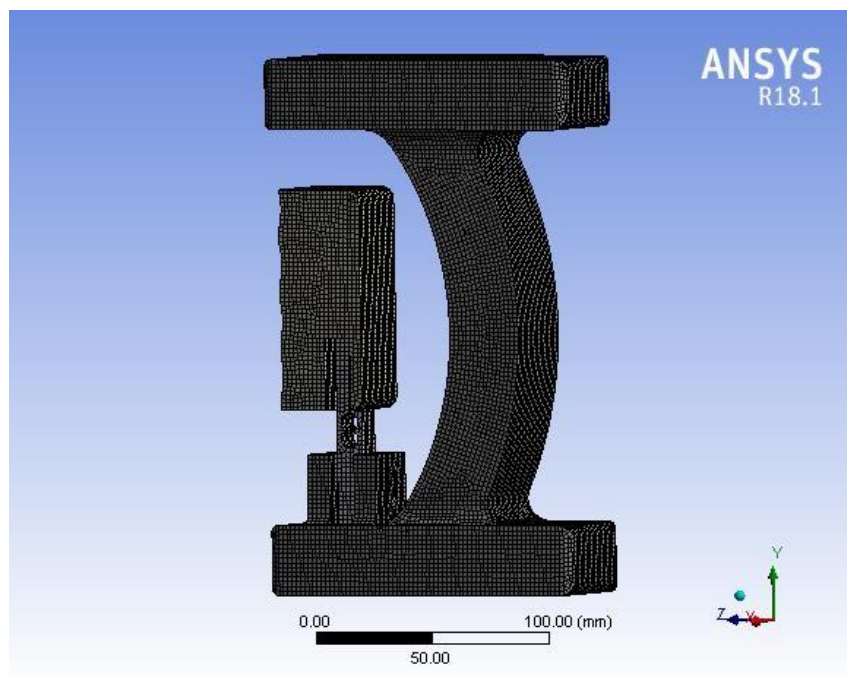


Fig 7.5 Mesh on the assembly

## 7.2.4 Mesh quality

Mesh quality determines the accuracy and stability of the problem, when the mesh metrics are within current range it is said to be good quality mesh. Poor meshes can cause difficulties in convergence, inaccurate results, diffuse solution. Hence it is necessary for the user to check the quality and improve the meshing. The mesh quality displays the minimum, maximum, average, standard deviation of the required metric selected, this should be in the desired range for a good quality mesh.

## 7.3 Mesh metrics

### 7.3.1 Element Quality

**Table 7.2 Element Quality**

Mesh metric	Element Quality
Minimum	6.4938e-003
Maximum	1
Average	0.79942
Standard Deviation	0.26252

The desired value of element quality is 1 and the average is 0.79942 from Table 7.2, implying that the element quality is very good.

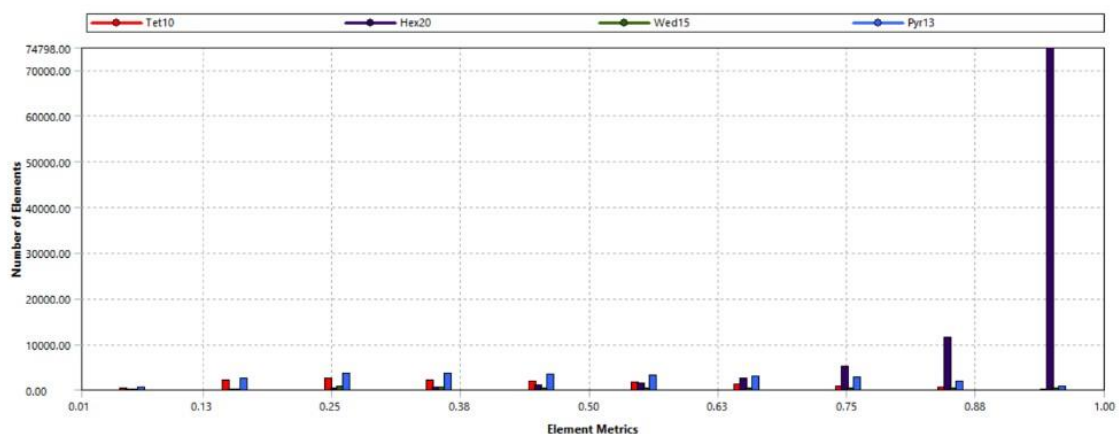
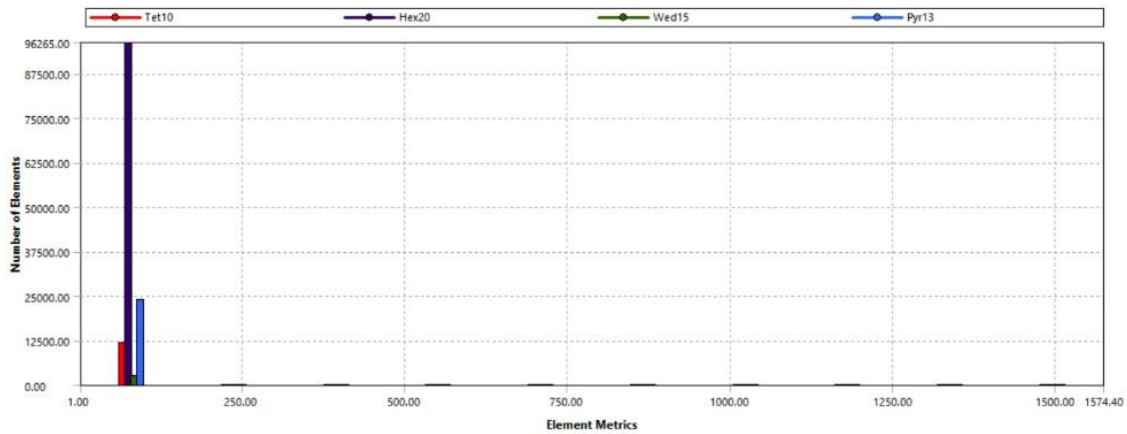


**Fig 7.6 Graph of Element quality Mesh metric vs the number of elements**

### 7.3.2 Aspect Ratio

**Table 7.3 Aspect Ratio**

Mesh metric	Aspect Ratio
Minimum	1.0003
Maximum	1574.4
Average	2.894
Standard Deviation	8.7517

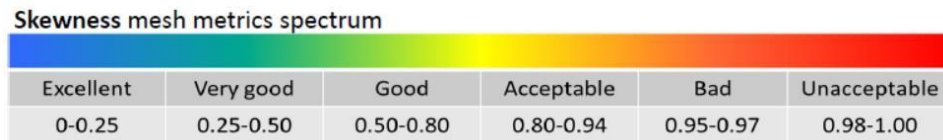


**Fig 7.7 Graph of Aspect ratio Mesh metric vs the number of elements**

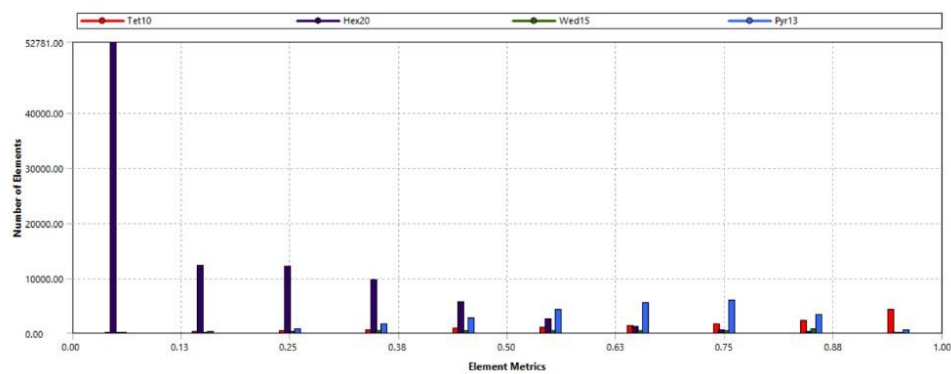
Aspect ratio is defined as the ratio of maximum element size to that of the minimum element size. The ideal value of aspect ratio is 1, but the acceptable value of aspect ratio should be less than 5, and from Table 7.3 the average value is 2.894 and from Fig 7.7 is it clear that most of the elements lie in the range of 1 aspect ratio.

### 7.3.3 Skewness

Skewness is the difference between the shape of the cell and the shape of an equilateral cell of equivalent volume. The desired value of skewness is less than 0.33. Fig 7.8 displays the spectrum of skewness mesh metric. It is evident from Table 7.5 that the average skewness is 0.3 which is termed to be very good, this can also be observed from the graph in Fig 7.9 where most of the elements lie in the range of 0 to 0.3.

**Fig 7.8 Skewness mesh Metric Spectrum****Table 7.5 Skewness Mesh Matrix Table**

Mesh metric	Skewness
Minimum	1.0678e-004
Maximum	1
Average	0.30071
Standard Deviation	0.29174

**Fig 7.9 Graph of Skewness Mesh metric vs the number of elements**

## 7.4 Approximate boundary conditions

An assembly analysis was conducted on the manipulandum, consisting of 3 parts namely the gripper, load cell and the supporting structure. The contacts between load cell and the gripper was bonded and similarly the contacts between the load cell and the supporting structure was kept as bonded.

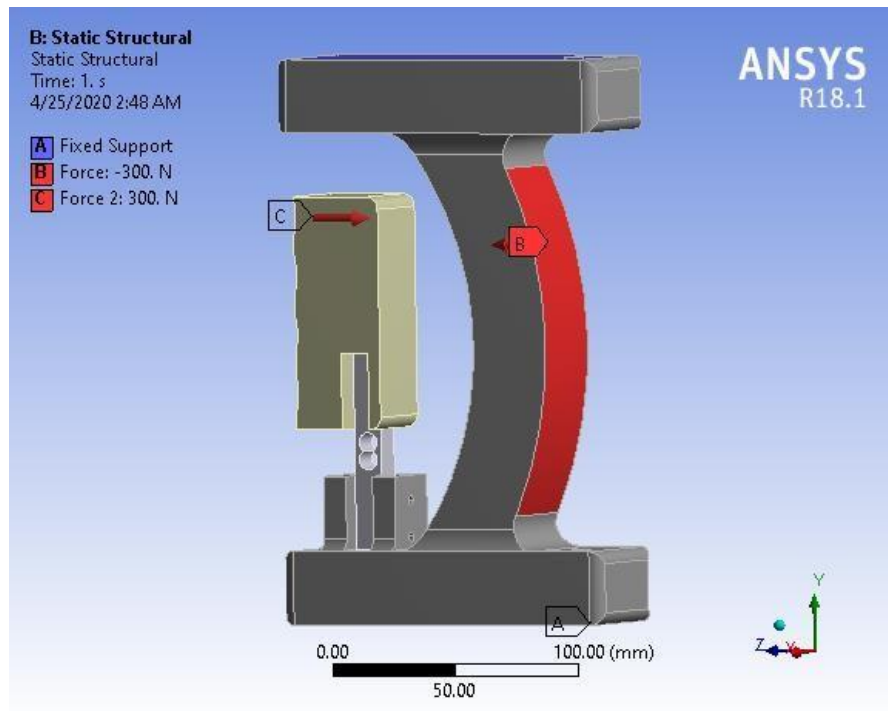


**Fig 7.10 Boundary conditions on the assembly**

According to “The Biomechanics of Kinesiology”, the maximum probable torque and the force that can be applied by a healthy individual is between the range of 150-300N, and the maximum torque that can be applied is 8N-m. Hence, the loading condition was such that 300N was applied on the grip and an equal and opposite reaction was applied on the support structure by fixing the ends of the supporting structure as shown in Figure 7.10.

## 7.5 Estimation of parameters

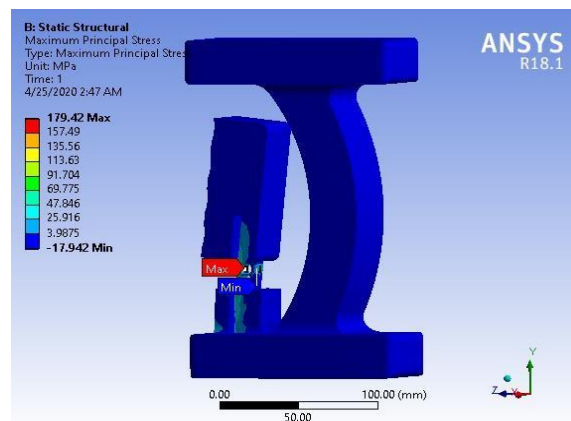


**Fig 7.11 Maximum Principal Stress on the assembly**



The failure criterion considered was Maximum principal stress theory (or Rankine's Theory), this theory was considered because of its applicability on brittle materials. According to the results shown in Fig 7.11, the maximum principal stress was found to be 179.42MPa. The maximum principal stress of 179.42MPa was on the load cell and the FOS of the given assembly was found to be 1.87 as shown in Fig 7.12. The FOS of the structure was determined using Equivalent stress theory, and this assured that the structure won't fail for the given loading conditions while 300N by itself being on the higher side of the applied by a healthy human being.

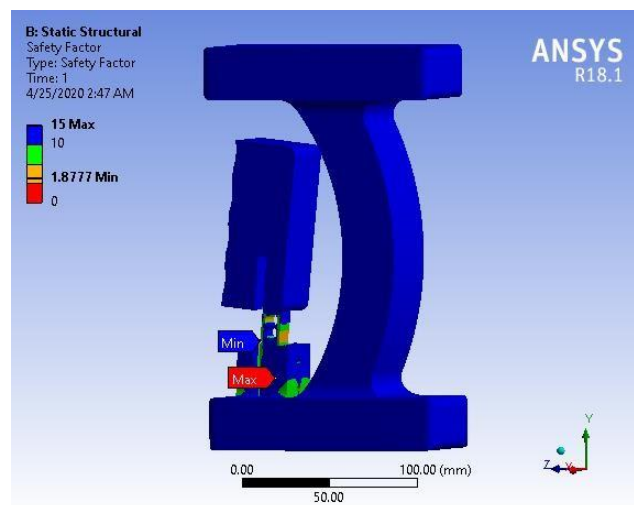


**Fig 7.12 Factor of Safety of the assembly**

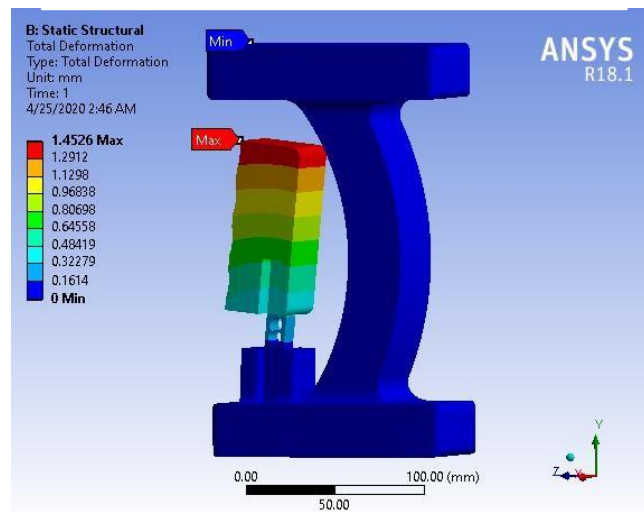


**Fig 7.13 Total Deformation of the structure**

The total deformation for the component for the applied loading conditions was found to be 1.452mm which can be seen in Fig 7.13, a similar value was obtained using theoretical calculations in the earlier chapters and this much deflection is necessary for the load cell to act as a cantilever and measure the gripping force.

## 7.6 Gripper

The assembly analysis gave the results of individual components, for the gripper maximum equivalent stress obtained was 13.25MPa which was well below the safe value and gave 3.12 as the factor of safety as shown in Fig 7.14.

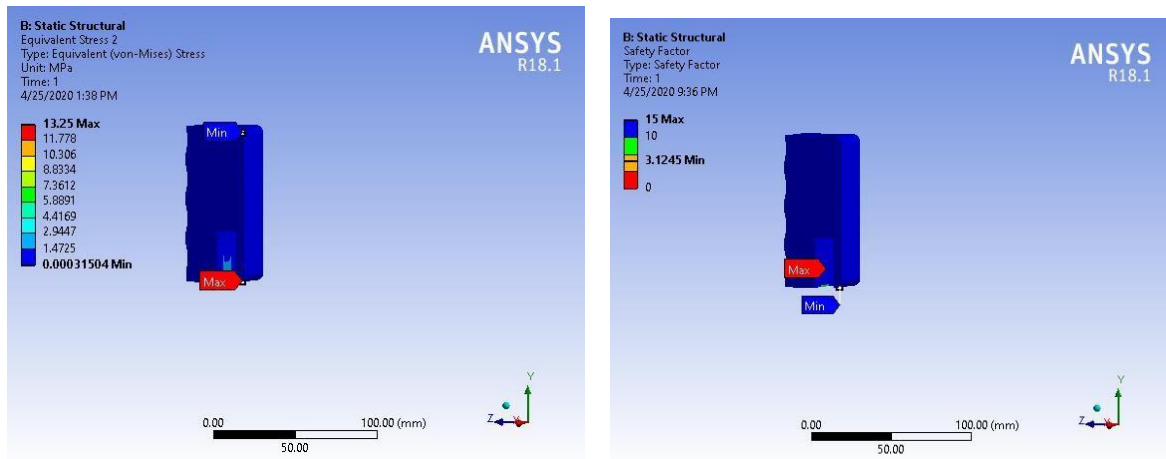


**Fig 7.14 Equivalent Stress on the gripper and Factor of Safety of the gripper**

## 7.7 Support Structure

The equivalent stress on the given structure was 22.048MPa and this value of 20.95MPa was comparable to the theoretical calculations done on the support structure. The factor of safety of the structure was found to be 1.87 as shown in Fig 7.15.

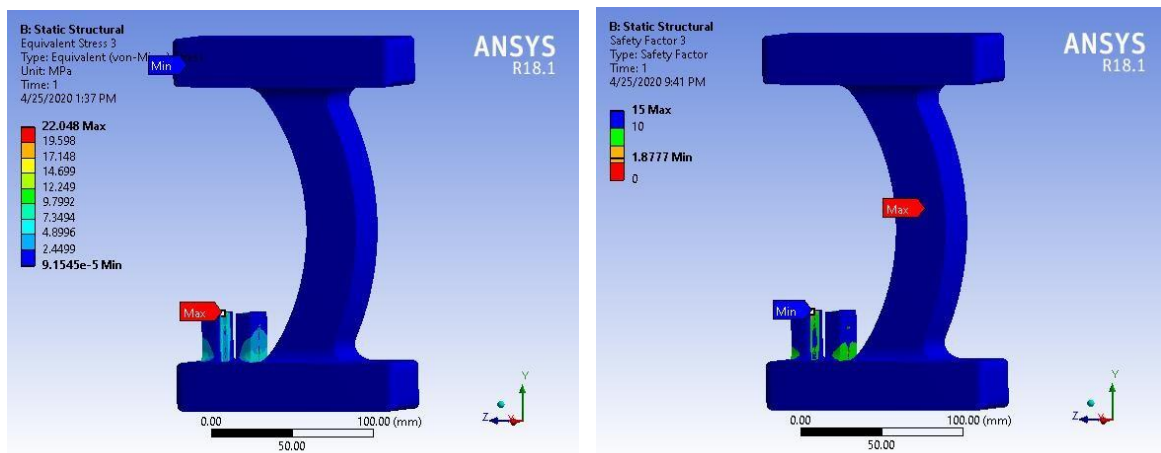


**Fig 7.15 Equivalent Stress on the support structure and Factor of Safety of the support structure**

## ***CHAPTER-8***

### ***RESULTS AND DISCUSSION***

## CHAPTER 8

### Results and Discussion

#### 8.1 Structural Analysis

##### 8.1.1 Comparison of numerical Results and Finite Element Method Results

The structural analysis is to determine the effects of loading it is subjected to during the application. The analysis involves both numerical and analytical calculation. On the other end the model is simulated for the real scenario using FEM packages. A relative comparison between the two results determines whether the design is safe for the given loads it is exposed to.

The analytical assumptions and numerical calculations of the model were made in the chapter 2 and further the FEM simulation was carried out is listed in the chapter 7. This discussion involves the comparison of both the results obtained.

#### Stress Analysis of The Body of the Manipulandum

Assuming the body of the manipulandum to be a curved beam, the stress obtained by numerical method was 20.95MPa and was compressive in nature. The governing equation is the stress on an inner fibre of the curved beam due to loading on a closed curved beam.

The same analysis was carried out in the FEM package Ansys workbench 18.1 and the result obtained is shown below in Table 8.1. The relative comparison is done with numerically calculated value.

**Table 8.1 Results of Equivalent stress**

Property	Numerical Value	FEM Value
Equivalent Stress	20.95MPa	22.048MPa

Fig 8.1 shows the results of the equivalent stress as a result of the loading it is subjected to. The maximum being 22MPa and least being  $9.5 \times 10^{-5}$  MPa. The blue region depicts the least value while red at the mount points of the strain gauge being maximum.

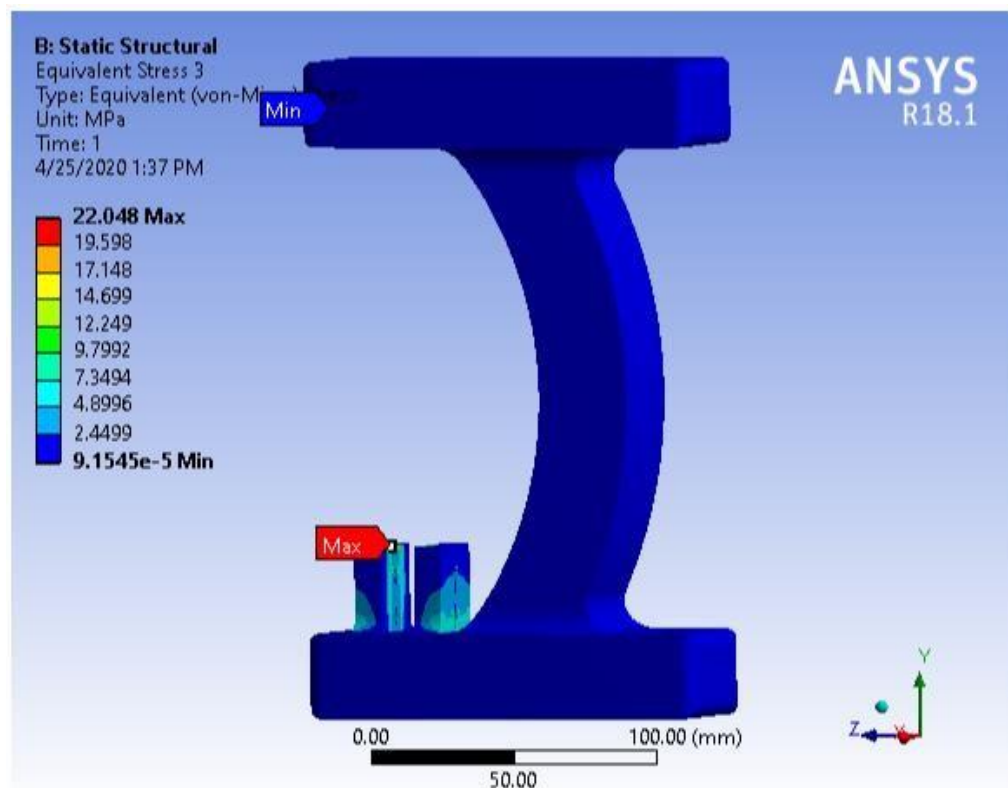


**Fig 8.1 Structural Analysis of the Body of the Manipulandum**

The results prove that the design calculations are coherent with each other. The design is safe and the material properties satisfy the requirement of the design calculations.

### Deformation Analysis of the Manipulandum

The deformation for the compliant revolute joint was carried out in chapter 2. The theoretical result was obtained to be 1.176mm. A comparison of the numerical calculation with that of the finite element method is stated in the Table 8.2.

**Table 8.2 Deformation comparison**

Property	Numerical Value	FEM value
Deformation	1.176mm	1.452mm

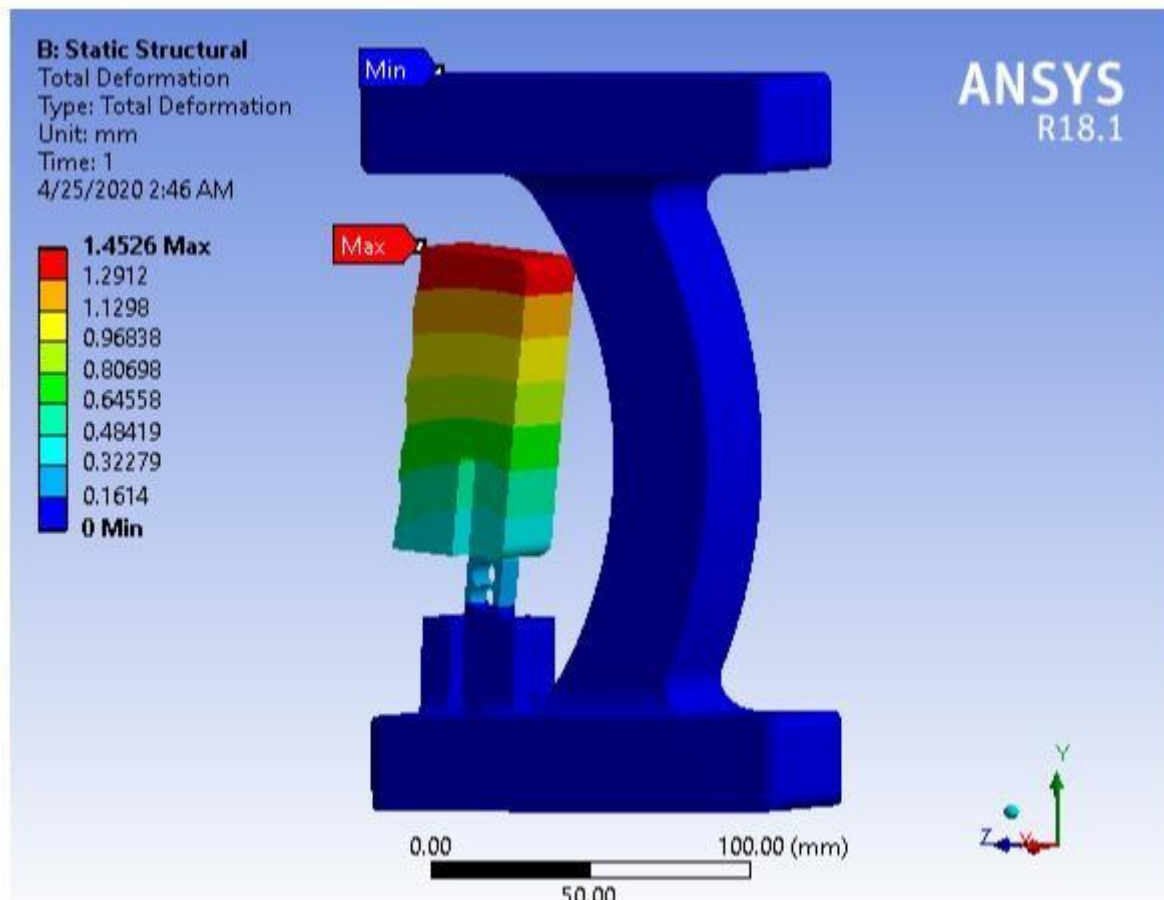


**Fig 8.2 FEM analysis for Deformation**

The deformation values of both results prove that the assumptions made are right for a compliant revolute joint.

Further these two above results prove to be key for the reason for the selection of material. The factor of safety determined from the FEM package is found to be 1.8. This value implies that the material selected is sufficient twice the times of it loading.

Figure 8.2 describes the deformation of the entire manipulandum. The maximum deformation is found to be 1.45mm on the finger grip including the strain gauge. The body of the manipulandum is stable with least deformation. Fig 8.3 gives the value of factor of safety result for the stated above loading conditions. The optimum values being shown in orange colour with a value of 1.877.

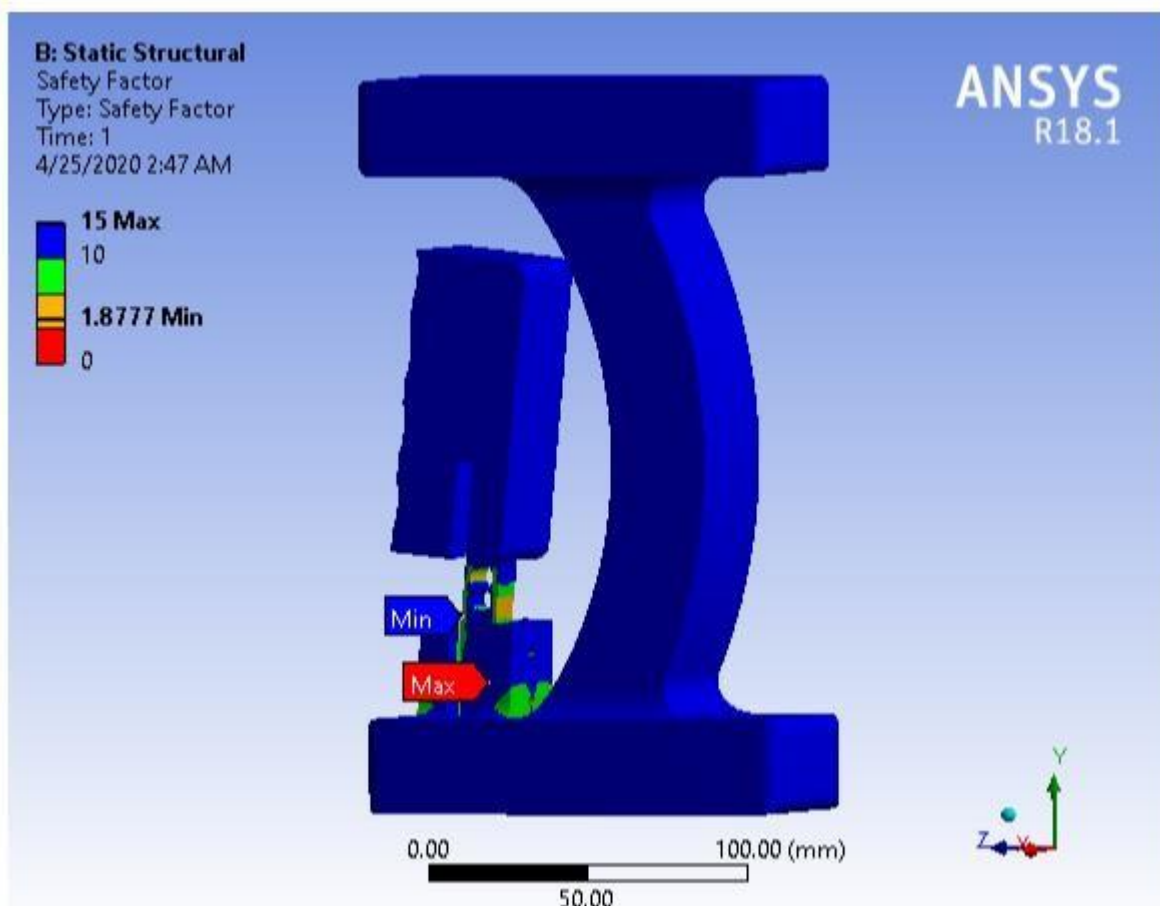


**Fig 8.3 FOS determination from the FEM package**

The load cell used acts as a cantilever beam, whose deflection is a measure of the grip strength. The maximum deflection for the load cell is calculated using the equation, deflection for a cantilever beam under point load.

It is given by

$$\delta = (W \cdot L^3) / (3 \cdot E \cdot I)$$

where W-load acting

L- length of the beam between fixed and free end

E- Modulus Of Elasticity

I- Moment OF Inertia

The above calculation gives a value of 1.37mm. This is I line with the stated above result from the Fig 8.3. The threshold for measurement is just crossed so that on every trial the subject's evaluation parameters are determined.

## 8.2 PID Controller

A PID controller was coupled with the transfer function of the motor, along with a closed feedback, the controller has to be tuned so that the device minimizes the deviation from the set target and responds to the given disturbance within minimal overshoot. In order to tune a PID controller, Zeigler Nichols method was used which is integrated with MATLAB, the PID tuner in MATLAB uses the Zeigler Nichols method to find the gains of the PID controller.

Figure 8.4 gives the description of the transient response of the system and its behavior, starting from without controller to the advanced tuned PID controller. The PID and PD controlled systems are found to more stable with least overshoot, while the system without the controller is highly unstable relative to the one with controlled system.

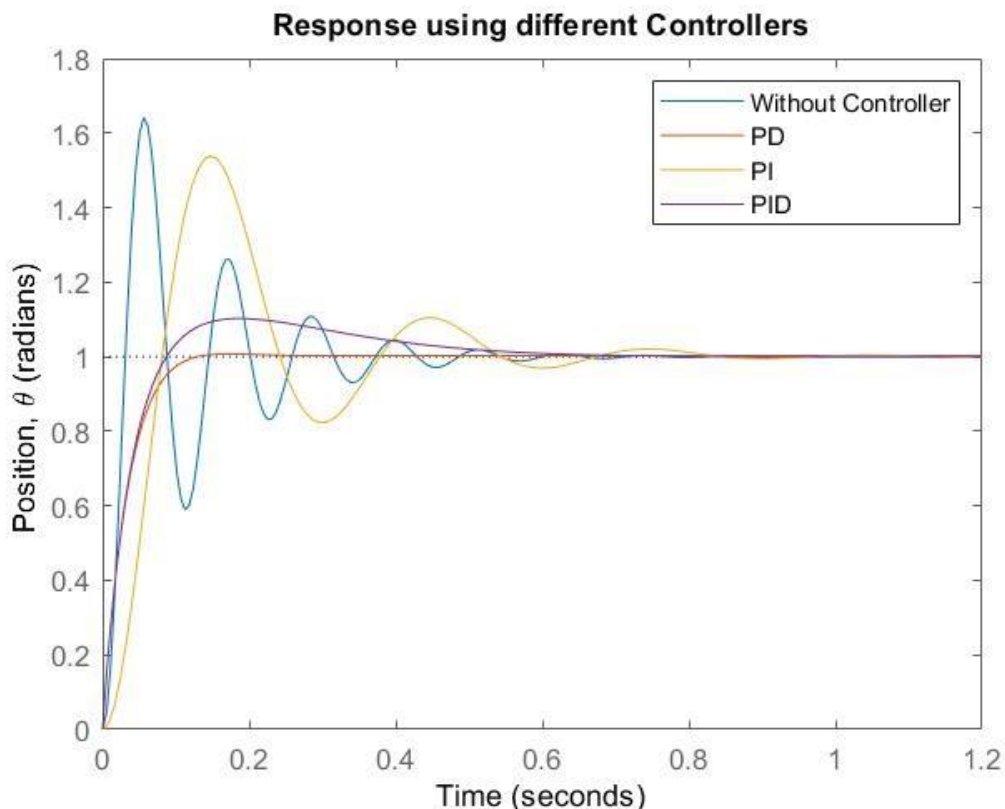


**Fig 8.4 Response of closed loop transfer function without controller, PD, PI, PID**



**Table 8.3 The tuned values of P, PD, PI, PID controller**

Gains	Kp	Ki	Kd
P	0.1681		
PI	0.1681	0.676	
PD	0.1681		0.009296
PID	0.1681	0.676	0.009296

The above table 8.3 has all the co-efficient of the respective controller after fine tuning carried out in Matlab for motor control application.

The design requirements of having a settling time of less than 40milliseconds, overshoot value of less than 16% along with zero steady-state error was obtained using a PD controller.

### 8.3.1 Logistic regression

A confusion matrix is a representation of the distribution of classification results compared with the known labels (outputs).

**Table 8.4 Logistic Regression Confusion Matrix**

	Predicted 1	Predicted 0
Actual 1	22	5
Actual 0	3	36

The above table 8.4 describes the performance of the logistic regression classification carried on the subject test data, having known the true values for the same set of data. Only the accuracy of correct classification does not represent the complete picture of the model. Sensitivity (or true positive rate), specificity (true negative rate) are among some of the other metrics which can be used to assess models.

**Table 8.5 Logistic regression performance metrics**

<b><u>Sensitivity</u></b>	0.8148	$TPR = TP / (TP + FN)$
<b><u>Specificity</u></b>	0.9231	$SPC = TN / (FP + TN)$
<b><u>Precision</u></b>	0.8800	$PPV = TP / (TP + FP)$
<b><u>Negative Predictive Value</u></b>	0.8780	$NPV = TN / (TN + FN)$
<b><u>False Positive Rate</u></b>	0.0769	$FPR = FP / (FP + TN)$
<b><u>False Discovery Rate</u></b>	0.1200	$FDR = FP / (FP + TP)$
<b><u>False Negative Rate</u></b>	0.1852	$FNR = FN / (FN + TP)$
<b><u>Accuracy</u></b>	0.8788	$ACC = (TP + TN) / (P + N)$
<b><u>F1 Score</u></b>	0.8462	$F1 = 2TP / (2TP + FP + FN)$
<b><u>Matthews Correlation Coefficient</u></b>	0.7479	$\frac{TP*TN - FP*FN}{\sqrt{((TP+FP)*(TP+FN)*(TN+FP)*(TN+FN))}}$

Table 8.5 shows the various metrics for the model of logistic regression. The model was able to correctly diagnose 81.48% of the patients who were actually impaired. It also showed a 92.31% rate of correctly diagnosing people as healthy, which meant an exceptionally low rate of misclassification as ‘healthy’ by the model. Moreover, it showed 88% surety in its prediction being true when an individual was classified as ‘impaired’. Thus, we see that there were a few more impaired people who were not able to be diagnosed correctly when compared to the other way round.

### 8.3.2 Decision Tree

**Table 8.6 Decision Tree Confusion Matrix**

	Predicted 1	Predicted 0
Actual 1	23	4
Actual 0	1	38

Table 8.6 describes the classification results, '1' representing 'impaired' and '0' representing 'healthy'. This matrix shows only one incorrect classification by the model when it diagnosed patients as 'impaired'. This is over 95% precision. There were comparatively more incorrect classifications for known impaired condition (denoted by 4). High accuracy of the model is attributed to the complex structure of the model and also the intensive computation required.

**Table 8.7 Decision Tree performance metrics**

<b><u>Sensitivity</u></b>	0.8519	$TPR = TP / (TP + FN)$
<b><u>Specificity</u></b>	0.9744	$SPC = TN / (FP + TN)$
<b><u>Precision</u></b>	0.9583	$PPV = TP / (TP + FP)$
<b><u>Negative Predictive Value</u></b>	0.9048	$NPV = TN / (TN + FN)$
<b><u>False Positive Rate</u></b>	0.0256	$FPR = FP / (FP + TN)$
<b><u>False Discovery Rate</u></b>	0.0417	$FDR = FP / (FP + TP)$
<b><u>False Negative Rate</u></b>	0.1481	$FNR = FN / (FN + TP)$
<b><u>Accuracy</u></b>	0.9242	$ACC = (TP + TN) / (P + N)$
<b><u>F1 Score</u></b>	0.9020	$F1 = 2TP / (2TP + FP + FN)$
<b><u>Matthews Correlation Coefficient</u></b>	0.8445	$TP*TN - FP*FN / \sqrt{((TP+FP)*(TP+FN)*(TN+FP)*(TN+FN))}$

Table 8.7 shows the metrics calculated for the decision tree model created. The decision tree has over 97% accuracy for healthy individuals and 85% for impaired individuals. This information, however is not useful from a prediction standpoint as the patient does not know their condition beforehand. Therefore, more useful metrics are precision and negative predictive rate. This model is correct over 95% of the times when it classified an individual as impaired, and over 90% times correct when it classified someone as healthy. With such high percentage in both these parameters, decision tree model is highly dependable for classification tasks.

### 8.3.3 SVM

**Table 8.8 SVM Confusion Matrix**

	Predicted 1	Predicted 0
Actual 1	17	10
Actual 0	3	36

The above table 8.8 is the confusion matrix for support vector machine (SVM). The matrix shows a relatively high number of misclassifications of known impaired patients, i.e. 10 individuals were classified as healthy even when they were not. However, there were only 3 misclassifications of known healthy individuals. Thus, the model could not accurately capture the features of impaired individuals and was biased in predicting

**Table 8.9 SVM performance metrics**

Measure	Value	Derivations
<b><u>Sensitivity</u></b>	0.6296	$TPR = TP / (TP + FN)$
<b><u>Specificity</u></b>	0.9231	$SPC = TN / (FP + TN)$
<b><u>Precision</u></b>	0.8500	$PPV = TP / (TP + FP)$

Measure	Value	Derivations
<b><u>Negative Predictive Value</u></b>	0.7826	$NPV = TN / (TN + FN)$
<b><u>False Positive Rate</u></b>	0.0769	$FPR = FP / (FP + TN)$
<b><u>False Discovery Rate</u></b>	0.1500	$FDR = FP / (FP + TP)$
<b><u>False Negative Rate</u></b>	0.3704	$FNR = FN / (FN + TP)$
<b><u>Accuracy</u></b>	0.8030	$ACC = (TP + TN) / (P + N)$
<b><u>F1 Score</u></b>	0.7234	$F1 = 2TP / (2TP + FP + FN)$
<b><u>Matthews Correlation Coefficient</u></b>	0.5913	$\frac{TP*TN - FP*FN}{\sqrt{((TP+FP)*(TP+FN)*(TN+FP)*(TN+FN))}}$

Table 8.8 shows the performance on test data using 6-fold validation. The model suffers in sensitivity, as shown by only 62.96% accuracy. Thus there is over 37% probability that a patient might not be diagnosed as one. With 92.31% specificity, it is clear that the model has bias due to the unequal number of distribution of classes. This fact is verified by the Matthews Correlation Coefficient of only 0.59, which shows correctness of the model even with very different class sizes.

### 8.3.4 K-Nearest neighbours

**Table 8.10 K-Nearest neighbour Confusion Matrix**

	Predicted 1	Predicted 0
Actual 1	23	4
Actual 0	2	37

The K nearest neighbor confusion matrix is as shown in the above table 8.9. KNN model also shows a good prediction accuracy, with only 6 misclassifications in total. Various statistical values are determined and are tabulated below in table 8.10

**Table 8.11 KNN performance metrics**

<b><u>Sensitivity</u></b>	0.8519	$TPR = TP / (TP + FN)$
<b><u>Specificity</u></b>	0.9487	$SPC = TN / (FP + TN)$
<b><u>Precision</u></b>	0.9200	$PPV = TP / (TP + FP)$
<b><u>Negative Predictive Value</u></b>	0.9024	$NPV = TN / (TN + FN)$
<b><u>False Positive Rate</u></b>	0.0513	$FPR = FP / (FP + TN)$
<b><u>False Discovery Rate</u></b>	0.0800	$FDR = FP / (FP + TP)$
<b><u>False Negative Rate</u></b>	0.1481	$FNR = FN / (FN + TP)$
<b><u>Accuracy</u></b>	0.9091	$ACC = (TP + TN) / (P + N)$
<b><u>F1 Score</u></b>	0.8846	$F1 = 2TP / (2TP + FP + FN)$
<b><u>Matthews Correlation Coefficient</u></b>	0.8114	$TP*TN - FP*FN / \sqrt{((TP+FP)*(TP+FN)*(TN+FP)*(TN+FN))}$

Specificity of the model is about 95%, which denotes the true negative rate. This model also has 92% precision, meaning that there is 92% chance that a patient classified as impaired is actually impaired. Thus, it is a dependable model for diagnosis.

## 8.4 Comparing the models

There is no single model which is best for any case. In the given classification problem, there are a number of factors one has to consider before choosing one model over another.

**Table 8.12 Comparison of all the ML models**

Measure Model	Accuracy	Time expense	Interpretation	Adaptability with small datasets
Logistic Regression	2	4	4	3
SVM	1	2	2	3
Decision Tree	4	2	4	3
K-NN	3	3	3	4

Here are the models compared, on a scale of 1 to 4 (1 - lowest, 4 - highest).

[Note: Accuracy is based on results of our implementation. These are based on parameters chosen, and might differ on varying them]

- The logistic regression is a simple model which does not take many assumptions (bias). It has given reasonable accuracy. In this model, a linearity is assumed in input data. This model is less likely to overfit in lesser dimensions. The model is easier to train and implement. The interpretability of the model is high. Moreover, the model enables online input of data, that is, data can be readily added later on, unlike other models such as SVM and Decision trees. There are models which have given better accuracy, like decision trees and KNN. However, they have their own limitations.
- A decision tree is a greedy model, that is it takes the best decision for every step, and may not lead to the best model overall. It might also be unstable to minor changes in dataset as the structure of tree might have to change. The levels of trees might become

very complex at times. These models are very prone to overfit. But decision trees are insensitive to outliers, and do not depend on linearity for classification.

- KNN on the other hand, are highly prone to outliers and noise. Also, higher dimensions in input data might become a problem for the model. The memory requirement for KNN is high, as it stores all data. However, it is quick to implement and suitable for small data sets.
- SVM is highly effective in linear and nonlinear data. They are also efficient in higher dimensions. It can perform well even in small data sets. But they are very computationally expensive. They require tedious tuning of parameters and training. An SVM model does not give a probabilistic definition to the classification like logistic regression does. Moreover, it might also be prone to overfitting.

Thus, we see that every model has its own pros and cons, and each problem is unique in the way different models can be utilized to achieve the desired results. Moreover, the parameters (such as accuracy, speed, interpretability, ease of use and application) that are prioritized in an application plays a very important role in selecting a model.

## **8.5 Neurorehabilitation**

The subject test data with selective impairments were mathematically modelled and were treated as input. These data were subjected to repetitive manipulandum model and the expected results were derived. The results of the simulation were checked with the professional physiotherapist and the conclusion was drawn. The range of motion and grip strength proved to be two crucial parameters of evaluation of an impaired subject. The variables were highly dynamic in nature. The evaluation model not only monitors the dynamic data but also refers to the data of healthy individual continuously, making the rehabilitation effective.

The comparison of results data pre and post application of the manipulandum is shown below.



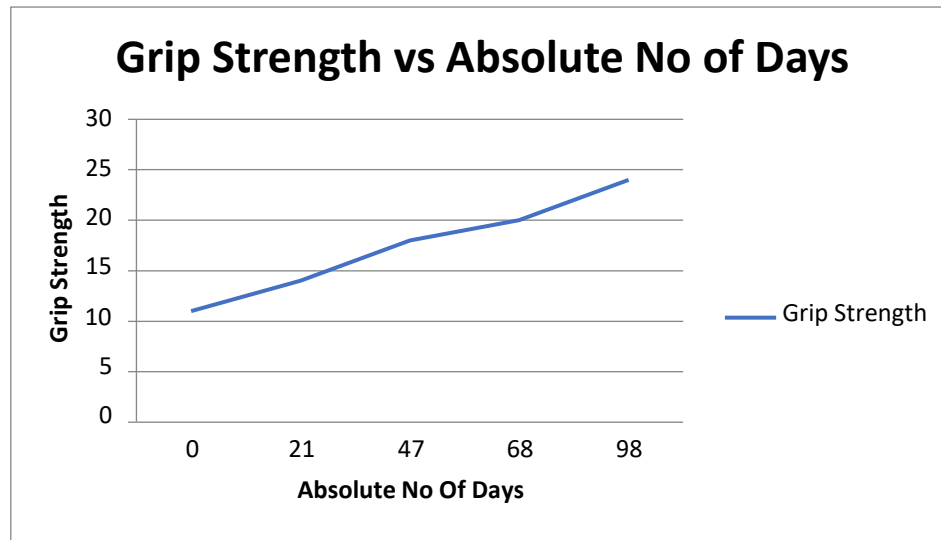


**Figure 8.5 Graph of Grip Strength vs Absolute number of days**

The Figure 8.5 gives a comparison of data recorded of grip strength from day zero to optimal grip strength achieved on day ninety-eight for particular age, BMI, gender and a specific type of impairment. The predicted results say that the rehabilitation to have optimal amount of grip strength is achieved in period of ninety-eight days.

**Table 8.13 Grip Strength of Affected Arm and Unaffected arm of Pre and Post Rehabilitation**

	Affected Arm		Unaffected Arm	
	Pre Application	Post Application	Pre Application	Post Application
Grip Strength	24.3	28.6	27.5	26.9
ROM of Wrist Extension	42.74	45.2	45.1	45.78
ROM of Wrist Flexion	78.4	80.5	83.9	83.7
Precision	88.3		87.5	

The above Table 8.13 is a simulation result of the subjects' both affected and unaffected arm. The comparative results give the improvement in figures after being subjected to manipulandum rehabilitation. A considerable improvement is to be seen in the affected arm. The range of motion for wrist extension post application has improved by 5%, meaning the manipulandum rehabilitation proves to be effective. The precision values suggest that the device was able to record the same value over five set of trials for a given specific position and corresponding such readings can be obtained over various wrist angle positions. The range of motion for wrist flexion has proven to be effective, as the changes in the affected arm is 2.1 degrees. The unaffected arm reading does not vary and is about the same value.

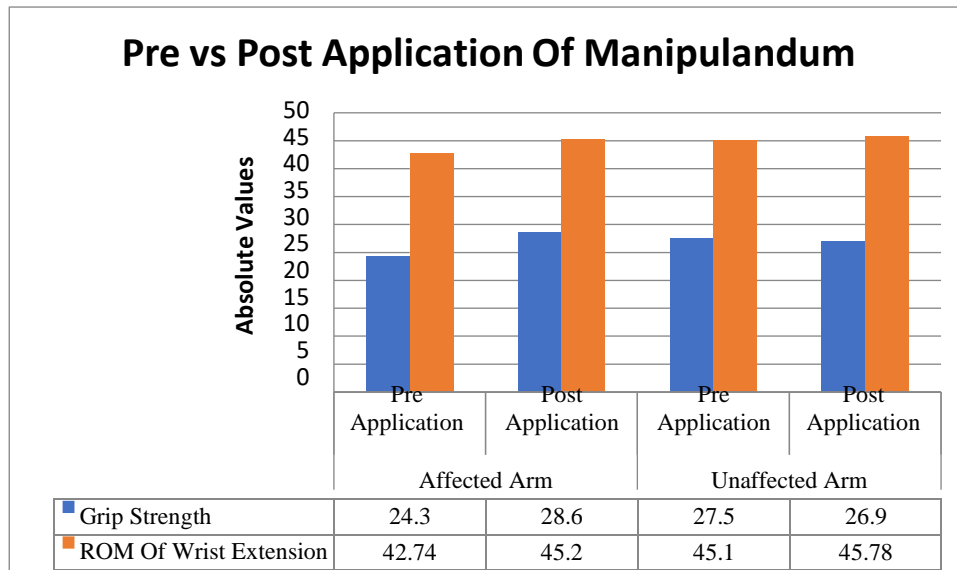


**Figure 8.6 Representation of grip strength and ROM of Pre vs Post Rehabilitation**

The above graph in Figure 8.6 is a comparison of the result data simulated for rehabilitation. The evaluation parameters are grip strength and range of motion of wrist extension. The values are mean about various wrist positions, which imply the various angles of wrist. While there is hairline improvement in the unaffected arm, significant number improvement is for the unaffected arm.

## ***CHAPTER-9***

### ***CONCLUSIONS & FUTURE SCOPE***

## CHAPTER 9

### Conclusions & Future Scope

#### 9.1 Conclusion

Neurorehabilitation plays an important role in gaining control of motor skills for any given human joints. This project introduces neurorehabilitation technique using manipulandum to measure the competency of the impaired patient and inhibit adaptive strategies for an effective rehabilitation, thus comparing the evaluation parameters pre and post application of the manipulandum. Initially the subject test data were subjected to manipulandum model to determine the evaluation parameters and then the adaptive or passive exercises were simulated. A relative comparison is drawn on the evaluation parameters with reference to the pre and post application of model. The following were arrived at

- Findings of this pilot study proves that evaluation parameters such as grip strength and range of motion to be a rate dependant property as the it was observed that post application of the manipulandum therapy the grip strength was increased with decrease in the level of impairment making a better competency.
- The competency classification algorithm was successful in differentiation the test data from that of the healthy individuals.
- The PID motor control configuration was proved to be efficient in driving to the desired place with the adaptive torques of 6Nm, 8Nm and 10 Nm.
- The trials postulate that the device is capable of dual modalities which are therapeutic and assistive device.
- The therapeutic group had only the grip strength improving, while the assistive had both the evaluation parameters convincingly improved.
- Range of motion was slower to improve than the grip strength in the case of affected arm. The range of motion increased at the rate of 0.024deg/day, while the grip strength improved at a rate of .04387N/day.
- The results secured are beneficial in overcoming the demerits of the conventional therapy such as professional intervention, intensive treatment and lacking patients' co-operation. Further it provides a new intuition to the method of rehabilitation technique, integrate error free computation with an unique way of interactive simulation.

## 9.2 Scope for Future Work

The study was concentrated using pilot study of test data to analyze the effect of application of manipulandum rehabilitation technique on subjects. However the study could be extended in the following areas:

- Extension of one DOF motion to multi DOF.
- To make an adaptable type of grips, widening to pinch, snap type of wrist grips.
- To target all age groups and inculcate forearm circumference as one of the evaluation parameters.
- To develop an adaptive interface between the subject and the manipulandum
- The number of subjects and the training groups selected were few in number and add to the demerit of the study. A larger study involving focus groups, enhanced target groups, varied cases of impairment are suggested to be undertaken.

## References

- [1]. Huang, V.S., Krakauer, J.W. Robotic neurorehabilitation: a computational motor learning perspective, *Journal of NeuroEngineering Rehabilitation*, Vol. 6, 2009.
- [2]. Krebs, H., Palazzolo, J., Dipietro, L. et al. Rehabilitation Robotics: Performance-Based Progressive Robot-Assisted Therapy. *Autonomous Robots* 15, 7–20 (2003).
- [3]. JUHANI SIVENIUS, KALEVI PYORALA, OLLI P. HEINONEN, JUKKA T. SALONEN, AND PAAVO RIEKKINEN, The Significance of Intensity of Rehabilitation of Stroke — A Controlled Trial, *Stroke: A Journal of Cerebral Circulation* Stroke Vol 16, No 6, 1985.
- [4]. Robert Teasell, Norine Foley, Norhayati Hussein, Joshua Wiener, Mark Speechley, The Elements of Stroke Rehabilitation, EBRSR [Evidence-Based Review of Stroke Rehabilitation].
- [5]. AMANDA M. CH'NG, DAVINA FRENCH, & NEIL MCLEAN, Coping with the Challenges of Recovery from Stroke Long Term Perspectives of Stroke Support Group Members , *Journal of Health Psychology*, SAGE Publications Vol 13(8) 1136–1146.
- [6] Tomoko Kitago, John W.Krakauer, Motor learning principles for neurorehabilitation, *Handbook of Clinical Neurology*, Chapter 8, Elsevier, Vol. 110, 2013, pp. 93-13
- [7] Lee, Y., Hsieh, Y., Wu, C., Lin, K., & Chen, C. Proximal Fugl-Meyer Assessment Scores Predict Clinically Important Upper Limb Improvement After 3 Stroke Rehabilitative Interventions. *Archives of Physical Medicine and Rehabilitation*, Elsevier, Vol. 96, 2015, pp. 2137-2144.
- [8] Lang, C. E., Bland, M. D., Bailey, R. R., Schaefer, S. Y., & Birkenmeier, R. L. (2013). Assessment of upper extremity impairment, function, and activity after stroke: foundations for clinical decision making. *Journal of Hand Therapy*, Elsevier, Vol. 26, 2013, pp. 104-115.
- [9] Faria-Fortini, Michaelsen, Cassiano, Teixeira-Salmela, Upper Extremity Function in Stroke Subjects: Relationships between the International Classification of Functioning, Disability, and Health Domains. *Journal of Hand Therapy*, Elsevier, Vol. 24, 2011, pp.257-265.

- [10] Kuki Bordoloi , Rup Sekhar Deka, Scientific Reconciliation of the Concepts and Principles of Rood Approach, Journal of Health Science and Research, Vol. 8, 2018.
- [11] Sukanta K. Sabut, Chanda Sikdar, Ramkrishna Mondal, Ratnesh Kumar, Manjunatha Mahadevappa, Restoration of gait and motor recovery by functional electrical stimulation therapy in persons with stroke, Journal of Disability and Rehabilitation, Taylor & Francis, Vol. 32, 2010, pp. 1594-1603.
- [12] Yang A, Wu HM, Tang JL, Xu L, Yang M, Liu GJ. Acupuncture for stroke rehabilitation. Cochrane Database of Systematic Reviews, Issue 8, 2016.
- [13] Lin J., Zheng HP., Xu YQ., Zhang TH. (2018) Methods and Significance of Hand Rehabilitation for Finger Replantation. Springer, 2018, pp. 103-108.
- [14]. Giergiel M., Budziński A., Piątek G., Wacławski M. (2015) Personal Lower Limb Rehabilitation Robot for Children. In: Awrejcewicz J., Szewczyk R., Trojnecki M., Kaliczyńska M. (eds) Mechatronics - Ideas for Industrial Application. Advances in Intelligent Systems and Computing, vol 317. Springer,
- [15] L. Brewer, F. Horgan, A. Hickey, D. Williams, Stroke rehabilitation: recent advances and future therapies, *QJM: An International Journal of Medicine*, Volume 106, 2013, pp. 11–25.
- [16] Riener, Robert, et al. Patient-cooperative strategies for robot-aided treadmill training: first experimental results. IEEE transactions on neural systems and rehabilitation engineering, 2005, vol. 13, no 3, p. 380-394.
- [17] REINKENSMEYER, David J., et al. Computational neurorehabilitation: modeling plasticity and learning to predict recovery. Journal of neuroengineering and rehabilitation, 2016, vol. 13, no 1, p. 42.
- [18] MACIEJASZ, Paweł, et al. A survey on robotic devices for upper limb rehabilitation. Journal of neuroengineering and rehabilitation, 2014, vol. 11, no 1, p. 3.
- [19] WEBER, Lynne M.; STEIN, Joel. The use of robots in stroke rehabilitation: a narrative review. NeuroRehabilitation, 2018, vol. 43, no 1, p. 99-110.
- [20] LAVER, Kate, et al. Virtual reality for stroke rehabilitation. Stroke, 2012, vol. 43, no 2, p. e20-e21.

- [21] CLARK, Elizabeth, et al. Brain-Computer Interface for Motor Rehabilitation. En International Conference on Human-Computer Interaction. Springer, Cham, 2019. p. 243-254.
- [22] KIM, Aram; SCHWEIGHOFER, Nicolas; FINLEY, James M. Locomotor skill acquisition in virtual reality shows sustained transfer to the real world. Journal of neuroengineering and rehabilitation, 2019, vol. 16, no 1, p. 1-10.
- [23] BAI, Jing; SONG, Aiguo. Development of a novel home based multi-scene upper limb rehabilitation training and evaluation system for post-stroke patients. IEEE Access, 2019, vol. 7, p. 9667-9677.
- [24] SONG, Aiguo, et al. One-therapist to three-patient telerehabilitation robot system for the upper limb after stroke. International Journal of Social Robotics, 2016, vol. 8, no 2, p. 319-329.
- [25].Sherd, Kelcey R., Duthie, Matthew H., Langenderfer, Joseph E., Development of a wrist manipulandum for assessment of motor control and biomechanics, Proceedings of the 2014 ASEE North Central Section Conference, 2014 American Society for Engineering Education.
- [26] Ian C Faye, Thesis on An impedance controlled Manipulandum for human movement studies, 1983
- [27].Werner Popp L, Oliver Lambercy, Christian Muller, Roger Gassert, Effect of handle design on movement dynamics and muscle co activation in a wrist flexion task, International journal of Industrial Ergonomics, 56, 2016, p. 170-180.
- [28] Elaine M. Bochniewicz, Geoff Emmer, Adam McLeod, Jessica Barth, Alexander W. Dromerick, Peter Lum, Measuring Functional Arm Movement after Stroke Using a Single Wrist-Worn Sensor and Machine Learning, Journal of Stroke and Cerebrovascular Diseases, Elsevier, Vol. 26, 2017, pp. 2880-2887.
- [29] Lei Yu, Daxi Xiong, Liquan Guo, Jiping Wang, A remote quantitative Fugl-Meyer assessment framework for stroke patients based on wearable sensor networks, Computer Methods and Programs in Biomedicine, Elsevier, Vol 128, 2016, pp. 100-110.
- [30] Kathrin Allgöwer, Joachim Hermsdörfer, Fine motor skills predict performance in the Jebsen Taylor Hand Function Test after stroke, Clinical Neurophysiology, Elsevier, Vol. 128, 2017, pp. 1858-1871



## Appendix -1

### Motor Drawing and MATLAB Code for PID tuning

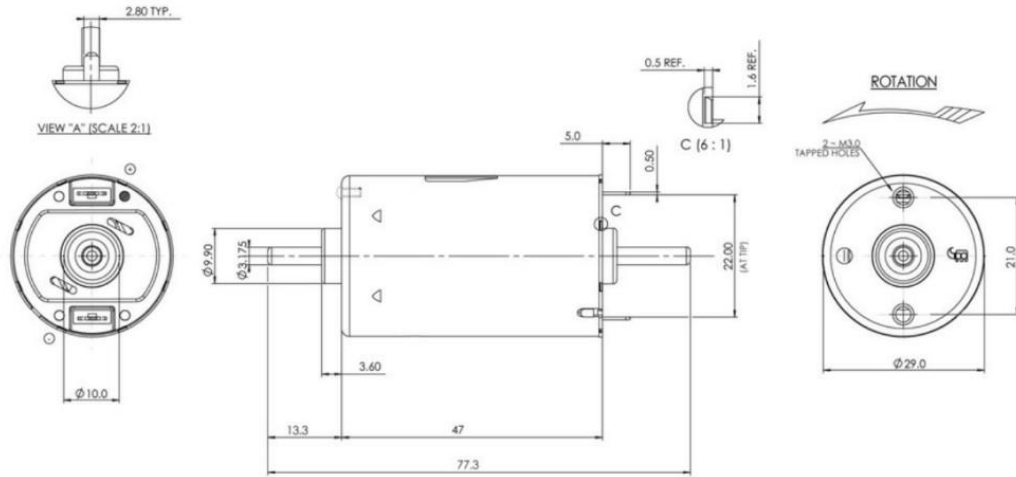


Figure A1.1 Motor Drawing

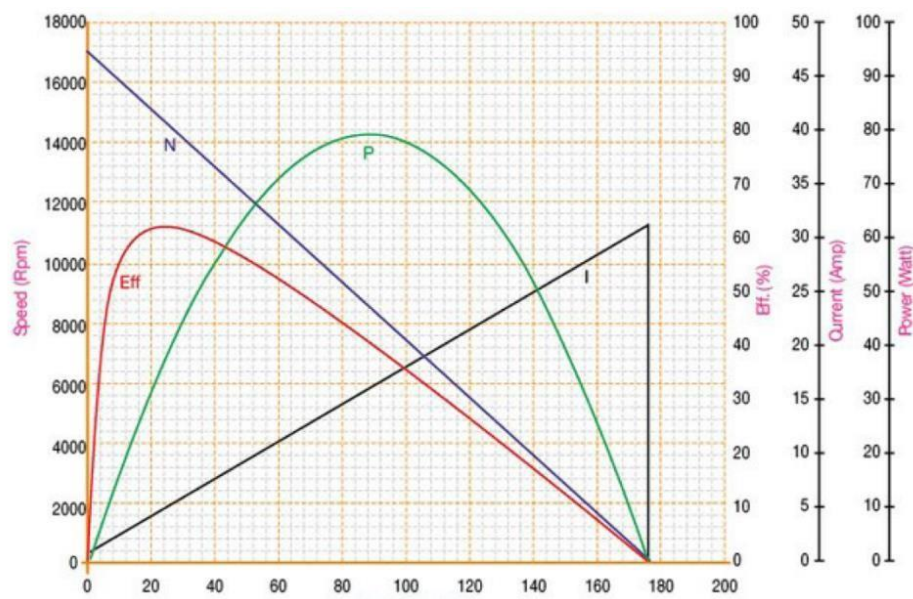


Figure A1.2 Motor Performance Curves

```
J = 2.2917E-5; %Moment of inertia of the rotor
b = 1.5836E-5; %Motor viscous friction constant
K = 0.004831; %Electromotive force constant
R = 0.0678; %Electric resistance
L = 2.75E-6; %Electric Inductance
s = tf('s');
P_motor = K/(s*((J*s+b)*(L*s+R)+K^2)) %Transfer Function of DC motor
```

```
t = 0:0.001:2;
step(P_motor,t) %step input respons for P_motor
sys_cl = feedback(P_motor,1) %closed loop system
%pidTuner(P_motor,'pid')
step(sys_cl,t) %step input respons for closed loop system
damp(sys_cl)
[Wn,zeta,poles] = damp(sys_cl);
%Peak overshoot and 2% settling time
Mp = exp((-zeta(1)*pi)/sqrt(1-zeta(1)^2))
Ts = 4/(zeta(1)*Wn(1))
pidTuner(P_motor,'pid')
Kp = 0.1681;
C = pid(Kp)
T = feedback(C*P_motor,1)
t = 0:0.01:2;
step(T,t)
Kp = 0.1681;
Kd = 0.009296;
C = pid(Kp,0,Kd)
T = feedback(C*P_motor,1);
a=stepinfo(T)
t = 0:0.01:2;
step(T,t)
Kp = 0.1681;
Ki = 0.676;
C = pid(Kp,Ki)
T = feedback(C*P_motor,1)
t = 0:0.01:2;
step(T,t)
Kp = 0.1681;
Ki = 0.676;
Kd = 0.009296;
C = pid(Kp,Ki,Kd)
T = feedback(C*P_motor,1)
t = 0:0.01:2;
step(T,t)
stepinfo(sys_cl)
stepinfo(T)
damp(T)
```

## APPENDIX-II

### Arduino Code for Load Cell Calibration

```
#include "HX711.h"
#define OUT 3
#define CLK 2
HX711 scale;
float calibration_factor = 5000; //Assuming a random value
void setup() {
    Serial.begin(9600);
    Serial.println("HX711 calibration is beginning");
    Serial.println("Enter + or A to increase calibration factor by
10");
    Serial.println("Enter - or Z to decrease calibration factor by
10");
    scale.begin(OUT, CLK);
    scale.set_scale();
    scale.tare(); //Reset scale to 0
    long zero_fact = scale.read_average(); //Obtain baseline reading
    Serial.print("Zero factor: ");
    Serial.println(zero_factor);
}
void loop() {
    scale.set_scale(calibration_factor); //Set this calibration factor
    Serial.print("Reading: ");
    Serial.print(scale.get_units(), 1);
    Serial.print(" kg");
    Serial.print(" using the calibration_factor: ");
    Serial.print(calibration_factor);
    Serial.println();
    if(Serial.available())
    {
        char temp = Serial.read();
        if(temp == '+' || temp == 'A')
            calibration_factor += 10;
        else if(temp == '-' || temp == 'Z')
            calibration_factor -= 10;
    }
}
```

## APPENDIX- III

### Logistic Regression

```
input_raw=readtable('coverged_data_physiotherapist.csv');
input_final=table2array(input_raw);
output_raw=readtable('physio_output_final.csv');
output_final=table2array(output_raw);
m=length(input_final);
x_train=[ones(m,1),input_final(:,1:5)];
ytrain=output_final(:,2);
xtrain=zscore(x_train(:,1:end));% Normalizing the input features
using z-standardization
x_test=xtrain;
y_test=ytrain;

%Finding Cost of logistic function and applying gradient descent
iter=1000; % No. of iterations for weight updation

theta=zeros(size(xtrain,2),1); % Initializing all weights as zero
alpha=0.1 % Learning rate
[J grad h th]=cost(theta,xtrain,ytrain,alpha,iter) % Cost of
logistic function
ypred=x_test*th; % prediction of target variables
% Sigmoid application followed by thresholding to 0.5
[hp]=sigmoid(ypred); % Hypothesis Function
ypred(hp>=0.5)=1;
ypred(hp<0.5)=0;
%%cost function%%
function [J grad h th] = cost(theta, xtrain,ytrain,alpha,iter)
th=theta
m=size(xtrain,1);
for j=1:iter
h=sigmoid(xtrain*th);
J=-(1/m)*sum(ytrain.*log(h)+(1-ytrain).*log(1-h));
th=th+(alpha/length(xtrain))*xtrain'*(ytrain-h)
end
grad=zeros(size(theta,1),1);
for i=1:size(grad)
grad(i)=(1/m)*sum((h-ytrain)'*xtrain(:,i));
end
end
```

## APPENDIX-IV

### Support Vector Machine Implementation

```
import pandas as pd
import numpy as np
from sklearn import svm
data=pd.read_csv('covergred_data_physiotherapist.csv') #input file
output=pd.read_csv('physio_output_final.csv') #output file
input_vals=[]
#Files have stored DataFrames in them.
#This is done to extract the Serials first and then values from the
serials
for i in range(66):
    a=data.loc[i].values.astype('float64')#serializing #data frame
    and subsequent
    input_vals.append(a) #extraction of values from series
op=output['Condition_disabled'].values.astype('float64')
#For the function SVC, kernel used is RBF function. Other #values
are 'linear','poly',etc.
#Gamma denotes the curve of the seperating boundary.
classifier=svm.SVC(kernel='rbf', gamma=0.01,random_state=1)
#Fitting the classifier in the input values and training #labels.
Here the testing set is a manually chosen part of #the available
data
#This can be modifier for cross validation
y=classifier.fit(input_vals[0:45],op[0:45])
prediction=classifier.predict(input_vals[46:66])
#compare prediction and actual outputs
print(prediction)
print(op[46:66])
```

## APPENDIX- V

### K-nearest neighbour

```
K-nearest neighbour
input_raw=readtable('covergred_data_physiotherapist.csv');
input_final=table2array(input_raw);
output_raw=readtable('physio_output_final.csv');
output_final=table2array(output_raw);
m=length(input_final);
X_train=[ones(m,1),input_final(:,2:5)];
Y_train=output_final(:,2);
```

```
[prediction, nn_index,
accuracy]=KNN(3,X_train,Y_train,X_train,Y_train);

function [pred_lab,n_ind,acc] =
KNN(k,train_dat,train_lab,test_dat,test_lab)
pred_label=zeros(size(t_data,1),1);
ed=zeros(size(t_data,1),size(data,1)); %ed is the euclidean
distances
ind=zeros(size(t_data,1),size(data,1)); %corresponding indices
k_nn=zeros(size(t_data,1),k); %k-nearest neighbors for testing
sample (Mxk)

%calc euclidean distances between each testing data point and the
training
%data samples
for test_p=1:size(t_data,1)
    for train_p=1:size(data,1)

        %calc and store sorted euclidean distances with corresponding
indices
        ed(test_p,train_p)=sqrt(sum((t_data(test_p,:)-
data(train_p,:)).^2));
        end
        [ed(test_p,:),ind(test_p,:)]=sort(ed(test_p,:));
    end
    %find the nearest k for each data point of the testing data
    k_nn=ind(:,1:k);
    n_ind=k_nn(:,1);
    %get the majority vote
    for i=1:size(k_nn,1)
        opt=unique(labels(k_nn(i,:)'));
        max_c=0;
        max_l=0;
        for j=1:length(opt)
            L=length(find(labels(k_nn(i,:)')==opt(j)));
            if L>max_c
                max_l=opt(j);
                max_c=L;
            end
        end
        pred_label(i)=max_l;
    end
end
```

## APPENDIX- VI

### Decision Tree Using ID3

#### Decision Tree using ID3

```
import pandas as pd
import numpy as np
from id3 import Id3Estimator
data=pd.read_csv('covergred_data_physiotherapist.csv') #input file
output=pd.read_csv('physio_output_final.csv') #output
file
input_vals=[]
#input_scale=preprocessing.scale(input_vals)
for i in range(66):
    a=data.loc[i].values.astype('float64')
#serializing data frame and subsequent
    input_vals.append(a)
#extraction of values from series
op=output['Condition_disabled'].values.astype('float64')
estimate= Id3Estimator()
#fit input features with the classification labels
estimate.fit(input_vals[0:45],op[0:45])
#Testing on subset of data available. Ranges are modified #in case
of cross-validation
prediction=estimate.predict(input_vals[46:66])
print(prediction)
print(op[46:66])
```



# Neurorehabilitation of Wrist Using Manipulandum<sup>☆</sup>

Amith R Achari<sup>a</sup>, Nitesh Jha<sup>a</sup>, Badrinath Nayak<sup>a</sup>, Ramesh S Sharma<sup>b</sup>,

<sup>a</sup> Undergraduate Students, Department of Mechanical Engineering, RV College of Engineering, INDIA

<sup>b</sup> Professor, Department of Mechanical Engineering, RV College of Engineering, INDIA

## ARTICLE INFO

### Keywords:

Manipulandum

Grip Strength

Rehabilitation

Competency Level

Hand exoskeleton

## ABSTRACT

Approximately 20,00,000 people suffer from Stroke each year, 50-70% of stroke survivors get back their functionalities post stroke while 30% are permanently disabled. In order to regain their functionalities neurological rehabilitation can be done to improve their motor skills using different exercises. In this context, the research mainly focuses on neurorehabilitation of wrist using a manipulandum, but very few devices which are patient centric and hence receiving an optimum therapy for recovery. The objectives of the work was to measure grip strength at various wrist positions and determine the competency level to devise suitable rehabilitation exercises and implementing resistance and assist as needed control

## I. Introduction

Greater than 11 lakh adults reported restraints in their day to day activities caused due to stroke. 50-70% of stroke survivors get back their functionalities post stroke. Still 30% are disabled permanently, in which 20% require professional care for 3 months post stroke [1]. The chances of stroke doubles after every decade after the age of 55 years, this group is specifically prone to suffer from cerebrovascular accident. It was found out that the estimated stroke cost around 3% of the total national health expenditure which is approximately \$30 billion in the US [2]. Recovery from stroke imposes both physical and psychological challenges, so to cope up with the challenges faced post stroke neurorehabilitation becomes critical. The physical and psychological consequences of stroke may lead to difficulties like anxiety and depression; there are a limited number of studies which discuss the types of problems faced by those who have experienced a stroke. Wood-Dauphinee et al examined the performance of traditional care versus a disciplinary team in a randomized controlled trial for male and female patients and compared the performance measures; this was tested for motor performance and functional abilities [3]. Total time spent on rehabilitation varies significantly between institutions, countries and units. Lincoln et al. (1996) stated that only 25% of the total time was engaged for rehabilitation purpose. De Weerd et al. (2000) quantified the duration of time spent on therapeutic or remedial activities using behavioural mapping for two units, one in Switzerland and the other in Belgium. There was a direct relationship between activity and stroke severity, however only 11% of their active day walking was performed by mild stroke patients [4].

## II. Problem Definition

As the pace and extent of recovery after cerebrovascular accidents such as stroke is contingent upon the engagement in the rehabilitation process, the exercises must be made accessible to patients more often to cater to their needs. Moreover, there is a need for continuous assessment to monitor their progress in the rehabilitation programs which can accurately give them feedback as to how their programs are to be modified for fastest recovery.

## III. Literature Survey

Fugl-Meyer Assessment [7], is a popular clinical assessment procedure which gives an index based on performance of a stroke patient. However, due to only three levels of scoring, most patients get intermediate scoring and thus, does not accurately distinguish the intermediate performers. Motricity index [8] is another measure where scores are given for manual muscle test for shoulder abduction, elbow and pinch grip, and a cumulative UE score is generated. Grip strength and pinch strength [9] is also proven to indicate the motor performance. Action Research Arm Test (ARAT) [8] is a test used to evaluate functional performance. It assesses gross motor skill, grip, grasp, and pinch on a 4-point scale. Margaret Rood provided the origin of the exercises to enhance the neuromuscular function and achieve motor control [10]. She also provided maneuvers such as stretching, joint positioning, and resistance which could help in the rehabilitation of the affected. These methods have shown only modest, and sometimes delayed effects, and are best used as a complimentary procedure in addition to other rehabilitation methods. Functional Electrical Stimulation (FES) is an alternative

<sup>☆</sup> Corresponding author.

E-mail address: [badrinathnayakk.im16@rvce.edu.in](mailto:badrinathnayakk.im16@rvce.edu.in) (Badrinath)

Received 4 June 2020;



# BADRINATH NAYAK K REPORT

## ORIGINALITY REPORT

12%

SIMILARITY INDEX

5%

INTERNET SOURCES

4%

PUBLICATIONS

10%

STUDENT PAPERS

## PRIMARY SOURCES

1

Submitted to Visvesvaraya Technological University

Student Paper

3%

2

Submitted to University of Keele

Student Paper

2%

3

Submitted to Coventry University

Student Paper

<1%

4

[www.active-robots.com](http://www.active-robots.com)

Internet Source

<1%

5

Submitted to New University of Astana

Student Paper

<1%

6

[www.slideshare.net](http://www.slideshare.net)

Internet Source

<1%

7

Dan B. Marghitu. "Mechanisms and Robots Analysis with MATLAB®", Springer Science and Business Media LLC, 2009

Publication

<1%

8

Submitted to Deakin University

Student Paper

<1%

9	Submitted to Engineers Australia Student Paper	<1 %
10	Submitted to University of New South Wales Student Paper	<1 %
11	Submitted to University of Newcastle upon Tyne Student Paper	<1 %
12	<a href="http://www.3dprototyping.com.au">www.3dprototyping.com.au</a> Internet Source	<1 %
13	<a href="http://docslide.us">docslide.us</a> Internet Source	<1 %
14	Submitted to Central Queensland University Student Paper	<1 %
15	Submitted to Indian School of Business Student Paper	<1 %
16	<a href="http://nevonprojects.com">nevonprojects.com</a> Internet Source	<1 %
17	<a href="http://www.contact-evolution.ch">www.contact-evolution.ch</a> Internet Source	<1 %
18	<a href="http://download.ni.com">download.ni.com</a> Internet Source	<1 %
19	Submitted to Higher Education Commission Pakistan Student Paper	<1 %

20	W BOLTON. "System parameters", Control Systems, 2002 Publication	<1 %
21	docplayer.net Internet Source	<1 %
22	"Communications, Signal Processing, and Systems", Springer Science and Business Media LLC, 2020 Publication	<1 %
23	Submitted to Datta Meghe College of Engineering Student Paper	<1 %
24	Submitted to University of Wollongong Student Paper	<1 %
25	Submitted to Mt. St. Charles Academy High School Student Paper	<1 %
26	Submitted to Nottingham Trent University Student Paper	<1 %
27	Submitted to Institute of Technology Carlow Student Paper	<1 %
28	Submitted to Universiti Teknologi MARA Student Paper	<1 %
29	Submitted to Nanyang Technological University, Singapore	<1 %

- 
- |    |  |      |
|----|--|------|
| 30 | <a href="http://www.acmanet.org">www.acmanet.org</a> | <1 % |
|    | Internet Source                                      |      |
- 
- |    |   |      |
|----|---|------|
| 31 | Submitted to Siddaganga Institute of Technology | <1 % |
|    | Student Paper                                   |      |
- 
- |    |   |      |
|----|---|------|
| 32 | <a href="https://pi19404.github.io">pi19404.github.io</a> | <1 % |
|    | Internet Source   |      |
- 
- |    |                                       |      |
|----|---------------------------------------|------|
| 33 | Submitted to Taylor's Education Group | <1 % |
|    | Student Paper                         |      |
- 
- |    |  |      |
|----|--|------|
| 34 | K. Elis Norden. "Handbook of Electronic Weighing", Wiley, 1998 | <1 % |
|    | Publication  |      |
- 
- |    |                                      |      |
|----|--------------------------------------|------|
| 35 | Submitted to University of Glamorgan | <1 % |
|    | Student Paper                        |      |
- 
- |    |                                     |      |
|----|-------------------------------------|------|
| 36 | Submitted to North South University | <1 % |
|    | Student Paper                       |      |
- 
- |    |  |      |
|----|--|------|
| 37 | <a href="http://www.brayebrookobservatory.org">www.brayebrookobservatory.org</a> | <1 % |
|    | Internet Source  |      |
- 
- |    |                              |      |
|----|------------------------------|------|
| 38 | Submitted to RMIT University | <1 % |
|    | Student Paper                |      |
- 
- |    |  |      |
|----|--|------|
| 39 | <a href="http://lup.lub.lu.se">lup.lub.lu.se</a> | <1 % |
|    | Internet Source                                  |      |
- 
- |    |                                  |  |
|----|----------------------------------|--|
| 40 | Submitted to University of Duhok |  |
|----|----------------------------------|--|

<1 %

41

[www.coursehero.com](http://www.coursehero.com)

Internet Source

<1 %

42

Submitted to Institute of Technology, Tallaght

Student Paper

<1 %

43

Submitted to Kingston University

Student Paper

<1 %

44

Kenneth G. Holt, Elliot Saltzman, Chia-Ling Ho, Masayoshi Kubo, Beverly D. Ulrich. "Discovery of the Pendulum and Spring Dynamics in the Early Stages of Walking", Journal of Motor Behavior, 2006

Publication

<1 %

45

[instruzengg.blogspot.com](http://instruzengg.blogspot.com)

Internet Source

<1 %

46

Submitted to Cranfield University

Student Paper

<1 %

47

[www.mechhead.com](http://www.mechhead.com)

Internet Source

<1 %

48

Submitted to Texas A & M University, Kingville

Student Paper

<1 %

49

[dspace.mit.edu](http://dspace.mit.edu)

Internet Source

<1 %

50	<a href="https://hdl.handle.net">hdl.handle.net</a> Internet Source	<1 %
51	<a href="http://www.ijert.org">www.ijert.org</a> Internet Source	<1 %
52	<a href="http://www.tandfonline.com">www.tandfonline.com</a> Internet Source	<1 %
53	<a href="https://academic.oup.com">academic.oup.com</a> Internet Source	<1 %
54	<a href="http://topclues.in">topclues.in</a> Internet Source	<1 %
55	Submitted to Australian National University Student Paper	<1 %
56	<a href="http://bioinformation.net">bioinformation.net</a> Internet Source	<1 %
57	Submitted to University of Derby Student Paper	<1 %
58	Submitted to MCI Management Centre Innsbruck Student Paper	<1 %
59	Submitted to University of Birmingham Student Paper	<1 %
60	Submitted to University of Johannesburg Student Paper	<1 %

61	Submitted to University of Southern California Student Paper	<1 %
62	Submitted to Dr. Pillai Global Academy Student Paper	<1 %
63	Submitted to University of Edinburgh Student Paper	<1 %
64	Submitted to University of Strathclyde Student Paper	<1 %
65	Submitted to Jawaharlal Nehru Technological University Student Paper	<1 %
66	Marc Leman. "Music and Schema Theory", Springer Science and Business Media LLC, 1995 Publication	<1 %
67	Submitted to University of Hull Student Paper	<1 %
68	robokits.download Internet Source	<1 %
69	www.arvihitech.com Internet Source	<1 %
70	Submitted to University of Portsmouth Student Paper	<1 %
71	Submitted to Universiti Malaysia Pahang	

<1 %

72

A. T. N. A. Miza, Z. Shayfull, S. M. Nasir, M. Fathullah, M. M. Rashidi. "Optimisation of warpage on plastic injection moulding part using response surface methodology (RSM)", AIP Publishing, 2017

Publication

<1 %

73

Submitted to Oxford Brookes University

Student Paper

<1 %

74

Submitted to University of South Alabama

Student Paper

<1 %

75

Submitted to Queensland University of Technology

Student Paper

<1 %

76

Submitted to University of Bradford

Student Paper

<1 %

77

[mafiadoc.com](http://mafiadoc.com)

Internet Source

<1 %

78

Submitted to Multimedia University

Student Paper

<1 %

79

Norden. "Load cell designs and installation principles", Handbook of Electronic Weighing, 04/04/1998

Publication

<1 %

---



80	Submitted to Turun yliopisto Student Paper	<1 %
81	Submitted to Heriot-Watt University Student Paper	<1 %
82	Submitted to University College London Student Paper	<1 %
83	Submitted to Vels University Student Paper	<1 %
84	Submitted to University of Lincoln Student Paper	<1 %
85	Submitted to University of Witwatersrand Student Paper	<1 %
86	Li Liu, Jyhwen Wang. "Modeling Springback of Metal-Polymer-Metal Laminates", Journal of Manufacturing Science and Engineering, 2004 Publication	<1 %

Exclude quotes  
Off

Exclude matches

Off

Exclude bibliography  
Off